DISSERTATION

OBESITY ACCELERATES MAMMARY CARCINOGENESIS IN A RAT MODEL OF POLYGENIC OBESITY SUSCEPTIBILITY

Submitted by

Shawna Beth Matthews

Graduate Degree Program in Cell and Molecular Biology

In partial fulfillment of the requirements

For the Degree of Doctor of Philosophy

Colorado State University

Fort Collins, Colorado

Fall 2015

Doctoral Committee:

Advisor: Henry J. Thompson

Charles Henry
Matthew Hickey
Christopher Melby

ABSTRACT

OBESITY ACCELERATES MAMMARY CARCINOGENESIS IN A RAT MODEL OF POLYGENIC OBESITY SUSCEPTIBILITY

Given the ongoing obesity epidemic, in which more women in the US are overweight or obese than are lean, the impact of obesity on the development of breast cancer is an important public health concern. Obese women with breast cancer generally have larger tumors and poorer prognosis than lean women with breast cancer. In an effort to deconstruct the biological mechanisms that link obesity and breast cancer, we have developed a novel rat model with high relevance to the polygenic development of obesity and breast cancer in humans. These rats have differing susceptibility to obesity when fed a diet of similar macronutrient composition as that consumed by the average American woman. Diet susceptible (DS) rats rapidly accumulate excess body fat and display metabolic perturbations, including resistance to insulin and leptin, which normally provide “stop eating” anorexigenic cues. In contrast, diet resistant (DR) rats remain lean despite being fed the same diet.

Findings from experiments conducted in our novel rat model have provided several critical pieces of information. When DR and DS rats were treated with a chemical carcinogen, DS rats displayed markedly accelerated mammary cancer formation compared to DR rats, including higher cancer incidence, multiplicity, and tumor burden, in conjunction with reduced cancer latency. The larger tumor mass in DS rats was found to be attributable to higher growth rates in DS vs. DR tumors, due to a combination of accelerated cell cycle progression and reduced apoptotic efficiency.

Importantly, DS rats tended to develop more tumors that were negative for sex hormone receptor expression, a subtype of breast cancer with high rates of breast cancer mortality. This observation was

corroborated by an endocrine ablation experiment, i.e., bilateral ovariectomy. Removal of the ovaries puts a strong selection pressure on expansion of cell populations that can grow in the absence of high circulating levels of sex hormones. In addition to removal of the primary source of circulating sex hormones, several experiments failed to provide evidence in support of peripheral production of estrogen by adipose tissue. In spite of the lack of estrogen at the host systemic and local (mammary gland) level, ovariectomized DS rats displayed elevated cancer multiplicity and sum tumor weight compared to ovariectomized DR rats, indicating that obesity in DS rats promotes the growth of cancer cells in an estrogen-independent manner.

Clinically, chronic inflammation in adipose tissue as a consequence of obesity has been shown to create a permissive environment for the development of breast cancer. While DS rats display evidence of heightened fat storage in the form of adipocyte hypertrophy, there was no evidence of inflammation accompanying this hypertrophy in the rat mammary gland in the current studies. Thus, peripheral production of estrogen by fat tissue and chronic inflammation in fat tissue—two of the mainstream mechanisms proposed to link excess fat and breast cancer—do not appear to be obligatory biological processes for the effect of obesity on the increased cancer response in DS rats in our model.

These findings suggest that our novel rat model represents a preclinical tool that facilitates investigation of mechanisms beyond those currently considered to link obesity to carcinogenesis of the breast. Breast cancer is a highly heterogeneous disease, and the integrated rat model reported herein is a tool that complements monogenic models of obesity and breast cancer in an effort to deconstruct the complex problem of breast cancer in clinical subpopulations whose disease is not explained via traditional mechanisms.

ACKNOWLEDGMENTS

A million thanks are owed:

To the Cancer Prevention Lab members: for your technical expertise and perpetual willingness to answer questions.

To Henry Thompson: for teaching me that science is a language, but that communicating science is an art.

To my husband: for your love, patience, support, and firm belief that I'll get a real job someday.

To my family: for your support and pride throughout this "not the helpful kind of doctor" journey.

To my friends: for keeping me sane and laughing.

To my dogs: for your daily affirmations that everything is awesome.

I couldn't have done it without all of you.

TABLE OF CONTENTS

LIST OF TABLES

LIST OF FIGURES

CHAPTER 1. INTRODUCTION[1]

1.A. Breast cancer: a global disease with local impact

In 2012, 1.7 million new cases of breast cancer were diagnosed globally, and breast cancer was responsible for nearly 700,000 deaths. Worldwide, cumulative lifetime risk for women of developing breast cancer between the ages of 0 and 74 currently stands at 4.6%, and lifetime risk of dying from breast cancer is 1.4% (1). In the United States (US) alone, one in eight women (12.5%) will be diagnosed with breast cancer during her lifetime. As the most commonly diagnosed cancer and second leading cause of cancer death among women in the US, breast cancer is diagnosed in a woman every two minutes, and breast cancer kills a woman every eleven minutes (2).

The heritable nature of breast cancer is generally overestimated in terms of contribution to breast cancer burden. Seven breast cancer susceptibility genes or gene sets with high penetrance (relative risk >5) have been identified, in which germline mutations are associated with increased breast cancer risk in an inherited Mendelian fashion. These 7 genes are summarized in **Table 1** (3).

Table 1
Legend. Breast cancer susceptibility genes with high penetrance (3).

Gene/ Gene Set	**Function**
BRCA1, BRCA2	DNA damage repair
CDH1	Cell-cell adhesion
PTEN	Phosphatase
SKT11	Serine-threonine kinase
TP53	Cell cycle checkpoint protein
MLH1, MSH2, MSH6 and *PMS2*	DNA mismatch repair

[1]Chapter 1 is being submitted as a critical review and analysis to the journal *Nutrition and Cancer*. Any changes between the version presented herein and that which is published will be minor. Such changes will likely be due to publishing requirements and tone differences between target audiences.

Awareness of the hereditary aspect of breast cancer, particularly cases driven by *BRCA1/2,* which are responsible for >30% of all hereditary breast cancers, has benefited from multiple public education and marketing campaigns and celebrity advocacy. However, these 7 genes are cumulatively found to be drivers in only 5-10% of all breast cancer cases (3;4), leaving the majority of breast cancer cases attributable to a complex summation of genetic, epigenetic, and environmental exposures.

1.B. Carcinogenesis: a process comprised of initiation, promotion, and progression

The cells in our bodies constantly encounter challenges to DNA integrity from a variety of sources. The endogenous process of mitochondrial oxidative phosphorylation alone results in 10^4 DNA "hits", or adducts formed by the interaction of reactive oxygen species with DNA, per cell, per day. DNA is also subject to damage from exogenous biological and chemical agents (5;6). Moreover, DNA damage accumulates over time due to a gradual decline in antioxidant function and reduced efficiency of repair machinery (7). The accumulation of DNA damage is a fact of aging in multiple species: a 2 year old rat displays nearly 2 million DNA lesions per cell, double that observed in a young rat (6). In humans aged 15-91, serum levels of 8-hydroxy-deoxyguanosine, a metabolite generated in response to oxidative DNA damage, increase in a linear fashion over time (8).

1.B.1. Cancer initiation

Only a small fraction of DNA hits escape detection and removal. These adducts can induce DNA mutations due to proofreading errors or mismatch by replicative machinery. Most mutations are silent and cause no noticeable changes in phenotype. However, a small population of mutations is sufficient to transform a healthy cell into a cell with neoplastic potential. The term neoplasia was originally defined in 1940 by the pathologist James Ewing. By Ewing's definition, neoplasia refers to an initiated cell, also called a transformed cell, which is capable of heritably transmitting alterations to its progeny and

displays relative autonomy from the rules and regulations that govern normal cells and cell-cell interactions within a tissue or organism (9). This event, in which a primary mutation or set of mutations transform a healthy cell to a cell with neoplastic potential, is called initiation (10).

1.B.2. Cancer promotion

The "silent interval" between the initiation of a cell and the detection of cancer is referred to as latency, and is governed by the second stage of carcinogenesis known as promotion. Cancer promotion is achieved by agents or processes that are usually insufficient for initiating the neoplastic transformation. In contrast to the long-lasting, largely irreversible effects of cancer initiating factors, cancer promoting agents require repeated, frequent, or continuous exposure or activation to promote neoplastic growth, and may be reversible (11).

Cancer promoting factors frequently induce alterations in gene expression and regulate cellular processes such as enhanced proliferation and suppression of apoptosis through both direct and indirect mechanisms. An example of direct regulation includes ligands binding to cell surface or nuclear receptors, such as observed with insulin and estrogens (11). As an example of indirect regulation by cancer promoting factors, reactive oxygen species can promote neoplastic growth by changing the redox state of transcription factors. Activator protein (AP)-1 and nuclear factor (NF)-kB are transcription factors that coordinate DNA damage repair and immunological defense processes, respectively, and are both susceptible to the cancer promoting effects of reactive oxygen species (11).

1.B.3. Cancer progression

The terms 'neoplasm' and 'cancer' are often used interchangeably. This is incorrect, as neoplasms can be either benign or malignant. Unlike benign growths, malignant neoplasms are characterized by rapid

growth, invasion of surrounding tissues, poor differentiation, increased metastatic capacity, changes in responsiveness to hormones and other endocrine factors, and karyotype instability (reviewed in (9;12)). At a molecular level, carcinomas of the breast tend to contain cells with increased nuclear: cytoplasmic ratio, prominent nucleoli, and high prevalence of mitoses (13). Cumulatively, these characteristics of malignancy comprise the third and final stage of carcinogenesis known as progression.

Individual neoplasms can progress independently of other neoplasms in the same animal. Likewise, cancer characteristics can progress independently of other characteristics in the same tumor—each tumor becomes a self-contained unit (12). Breast carcinomas frequently display dominance of only one cell type, in contrast to the 3 cell types (ductal luminal, alveolar luminal, and myoepithelial) that comprise the architecture of a normal breast (13). Inflammation or a desmoplastic reaction may be observed at the carcinoma border where cancerous cells invade the stroma. The desmoplastic reaction is a phenomenon that occurs during invasion, when adipocytes are replaced by fibroblasts and immune cells, which form a kind of cap at the invading front (13). For the remainder of this dissertation, the term 'cancer' will refer to malignant neoplasms based on histopathological diagnosis.

1.C. The clockwork nature of cancer: initiated cells as stopwatches

To visualize the process of carcinogenesis, each initiated cell can be thought of as a stopwatch. Before stopwatches can start keeping time, they must be programmed. As the body is generally very good at recognizing and removing stopwatches through a series of tightly controlled processes, most stopwatches will never start ticking. If initiated cells evade detection and sustain mutations via mitosis, these stopwatches can persist within a tissue in an unprogrammed state for long periods of time—potentially decades in clinical populations. With the exception of relatively rare cases of germline mutations, a single initiating event is generally not sufficient to cause cancer. For a stopwatch to start

ticking, additional driver or favorable passenger mutations, epigenetic alterations, and a favorable host environment are required to program the stopwatch.

1.C.1. Stopwatch programming via genetic means

In 2000, Hanahan and Weinberg published their classic report on the 6 primary hallmarks of cancer that are acquired as cancer progresses (14). These 6 initial hallmarks are self-sufficiency to growth signals, insensitivity to anti-growth signals, evasion of apoptosis, sustained angiogenesis, tissue invasion and metastasis, and limitless replicative potential via telomerase expression (14).

In 2011, in recognition of the knowledge acquired from an additional decade of research, Hanahan and Weinberg added deregulation of cellular metabolism and evasion of destruction by the immune system as emerging cancer hallmarks (15). Genetic instability and mutation and tumor-promoting inflammation were added as characteristics that enable the acquisition of the other 8 cancer hallmarks (15). The hallmarks of cancer can be acquired through genetic events, including single base (point) substitutions caused by DNA adducts, frameshift mutations caused by insertions or deletions, chromosomal rearrangements, or copy number alterations.

A recent report by Watson *et al.,* published in Nature Reviews in Genetics in 2013, summarized the patterns of somatic mutations that have been identified by sequencing a variety of solid tumors. The breast tumors sequenced in a total of 5 studies displayed 6-35 somatic mutations that were significantly mutated above background mutation rates, depending on the method of sequencing used and the molecular subtype of the tumor (16). Within those studies evaluated, all 5 listed the tumor suppressor gene *TP53* and the tumor driver *PIK3CA* as frequent sites of somatic mutations in breast tumors (16),

which are key regulators of several of Hanahan and Weinberg's cancer hallmarks. Beyond genetic control, evidence is accumulating on epigenetic control of cancer hallmarks.

1.C.2. Stopwatch programming via epigenetic means

As an example of the power of epigenetic alterations to impact cancer promotion, Elsheikh *et al* recently characterized epigenetic alterations in the Nottingham Tenovus Primary Breast Carcinoma Series, which consists of N=880 breast carcinomas of varying histological tumor type (17). The authors report that distinct patterns of histone lysine acetylation and methylation marks were associated with breast tumor grade, molecular subtype, tumor size, lymph node involvement, vascular invasion, and expression of biological markers including the estrogen receptor (ER) and progesterone receptor (PR) (17). Epigenetic marks were also associated with breast cancer outcomes including prognosis, overall survival (hazard ratio (HR)=2.99 (1.29-6.97)) and disease-free survival (HR= 1.76 (1.08-2.89)) (17).

Holst *et al.* recently reported that 47% (N=7 of 15 assessed) of cancer-free women display hypermethylation-induced silencing of the P16/INK tumor suppressor in histologically normal mammary tissue, suggesting that epigenetic silencing of tumor suppressor genes may be one of the earliest events in breast carcinogenesis (18).

Epigenetic regulation has also been reported in cancer stem cell populations. Cancer stem cells are usually hormone receptor negative, resistant to chemotherapy, and may play a role in breast cancer recurrence. Recent data demonstrates that hypermethylation-induced silencing of pro-differentiation signaling via the Polycomb group of proteins may favor cancer stem cells existing in a state of perpetual self-renewal (19). Using tissue from colorectal, breast, and ovarian cancers, Widschwendter *et al.* demonstrated that cancer-associated genes in stem cells were 12X more likely to be hypermethylated

by the Polycomb repressor complex than non-cancer-associated genes (19). MicroRNAs impact the development of cancer in an epigenetic manner, and the contribution of these factors to the carcinogenic process in the breast has been expertly reviewed (20;21).

1.D. Breast cancer and obesity: what's the connection?

The American Cancer Society divides breast cancer risk factors into two categories: factors unrelated to personal choice and factors related to personal choice. Of the former category, the number one risk factor for breast cancer is being a woman. While men can and do develop breast cancer, risk is 100X higher in women than in men (22). Of the risk factors related to personal choice, chronic positive energy balance, manifested as excess adiposity, has been proposed as a permissive host environment for the development of cancer (23-25). Body mass index (BMI) is frequently used as a proxy to body fatness. BMI is calculated as weight (kg) ÷ height (m^2) (26;27). Ideal BMI ranges from 18.5-24.9 kg/m^2. In contrast, BMI=25-29.9 kg/m^2 is considered overweight, and BMI≥30 kg/m^2 is considered obese.

Breast cancer incidence in westernized countries including the US has risen by over 30% in the past 25 years (2). While attributed in part to changes in reproductive patterns and improved early detection methods, this increased breast cancer incidence may also reflect the rising prevalence of hallmarks of Western culture such as obesity and physical inactivity (2). Importantly, after recently reviewing the literature, Howell *et al.* concluded that lifestyle modifications, including maintaining or returning to BMI <25, engaging in moderate physical activity, and limiting alcohol to <3 drinks per week, can cumulatively reduce breast cancer risk by >30% (28). The World Cancer Research Fund reports that 17% of breast cancer diagnoses in the US could be prevented by maintaining a healthy weight (29). This relationship is of considerable public health importance given the ongoing obesity epidemic, in which two out of three women in the US are overweight or obese with BMI ≥25.

Menopausal status is the fulcrum on which the complex association between obesity and breast cancer hinges. In postmenopausal women, the World Cancer Research Fund reports that the sum of evidence supports a probable link between obesity and postmenopausal breast cancer risk (relative risk (RR)=1.12 (1.09-1.16), $p<0.001$) (25;29;30). Conversely, most studies report a null or inverse association of obesity with breast cancer risk in premenopausal women (RR=0.92 (0.88-0.97), $p=0.001$), though this topic remains controversial (29-33).

1.E. The Cecchini study: outlier or challenging the obesity-breast cancer paradigm?

Despite the majority of evidence showing no effect or a protective effect of obesity on breast cancer risk in premenopausal women, a recent study based on data from the National Surgical Adjuvant Breast and Bowel Project Breast Cancer Prevention (P-1) Trial provided evidence contrary to the mainstream of thinking. In 2012, Cecchini *et al.* evaluated the impact of BMI on breast cancer risk in both pre- and postmenopausal women. All women evaluated in the Cecchini article were considered at high risk of developing breast cancer according to the Gail Model.

The Gail Model was initially developed in 1989 as a tool to model the influence of risk factors on 5-year and lifetime invasive breast cancer risk in Caucasian women (34), African American women (35), and Asian and Pacific Islander women (36). The Gail Model is an online breast cancer risk assessment tool from the National Cancer Institute (37) that utilizes the factors summarized in **Table 2** to calculate 5-year risk of invasive breast cancer:

Table 2

Legend. Factors included in determination of 5-year invasive breast cancer risk according to the Gail Model as reported by the National Cancer Institute (37).

Breast Cancer Risk Factor	Risk Association
Cancer history	History of previous breast carcinoma (including *in situ* cancers)
	Radiation therapy to the chest for treatment of Hodgkin lymphoma
Genetic predisposition	Germline mutations in genes/ gene sets described in Table 1
	Genetic syndrome associated with increased breast cancer risk
Age	Risk increases with age (most breast cancers diagnosed after age 50)
Age at menarche	First menstrual period before age 12 due to higher cumulative exposure of breast tissue to sex hormones
Age at first live birth of a child	If 0/1 first-degree relative with breast cancer, risk increases with age at first live birth If ≥2 first-degree relatives with breast cancer, risk decreases with age at first live birth
Parity	Each live birth decreases relative risk by 7%
Breastfeeding	Each 12-month period of breastfeeding decreases relative risk by 4.3% (38)
First-degree relatives with breast cancer diagnosis	≥1 first-degree relative with breast cancer increases risk
Ever having a breast biopsy	Biopsies are performed due to physical changes in the breast, which may be associated with breast cancer (dimpling, puckering, swelling, lump/knot, nipple discharge (39))

1.E.1. Outcomes of the P-1 and P-2 Breast Cancer Prevention Trials: full model

In the Cecchini article, high-risk women were defined as having ≥1.66% 5-year risk of developing invasive breast cancer according to the Gail Model. Cecchini evaluated women enrolled in two breast cancer prevention trials. The P-1 Trial included both premenopausal women (N=5,864) and postmenopausal women (N=6,379). The Study of Tamoxifen and Raloxifene (STAR) Trial, also known as P-2, included postmenopausal women only (N=19,488). Women enrolled in P-1 and STAR trials were evaluated at three tiers of BMI: <25.0 (normal weight), 25.0-29.9 (overweight), and ≥30.0 kg/m^2 (obese).

In high-risk premenopausal women, risk of invasive breast cancer in the final multivariate model after adjusting for age and treatment was significantly increased in overweight (hazard ratio (HR)=1.59 (1.05-2.42)) and obese (HR=1.70 (1.10-2.63), p_{trend}=0.01) women compared to women of BMI <25 (40). In high-risk postmenopausal women, the final multivariate model adjusted for age and treatment showed a

trend towards increased risk of breast cancer in overweight (HR=1.07 (0.88-1.30)) and obese (HR=1.14 (0.94-1.38) women compared to women of BMI <25. However, this trend was not statistically significant in postmenopausal women (p_{trend}=0.17) (41).

1.E.2. Outcomes of the P-1 and P-2 Trials: placebo-treated women only

High-risk women included in these breast cancer prevention trials were randomized to receive placebo vs. tamoxifen (P-1 Trial) or tamoxifen vs. raloxifene (STAR/P-2 Trials). Tamoxifen and raloxifene are both selective estrogen receptor modulators (SERMs) that reduce risk of hormone receptor-positive breast cancers (28;42;43). While the hazard ratios (HR) for the final multivariate assessment across BMI tiers were adjusted for treatment group, SERM treatment could potentially influence the results due to modulation of estrogen signaling. In premenopausal women, the placebo-treated group within the P-1 Trial displayed similar increased breast cancer risk in overweight (HR=1.51 (0.91-2.50)) and obese (HR=1.41 (0.82-2.43)) women as observed in the full analysis (HR=1.59 and 1.70, respectively).

Interestingly, postmenopausal women in the placebo-treated group of the P-1 Trial displayed higher breast cancer risk in overweight (HR=1.77 (1.05-2.97)) and obese (HR=1.28 (0.72-2.28)) subgroups than was observed in the final multivariate model. Approximately half the postmenopausal women evaluated in P-1 and P-2 Trials had a history of using estrogen as part of hormone replacement therapy, which reportedly eliminates the relationship between obesity and increased risk of breast cancer in postmenopausal women (44). Per Cecchini, this diversity in estrogen exposure may explain why the increased risk of breast cancer in placebo-treated groups failed to reach statistical significance in spite of the magnitude of the elevated risk estimate. These data suggest that subgroups exist within breast cancer populations, and that variability in the timing and duration of exposures to “stopwatch programming” agents can exert effects on breast cancer outcomes.

1.E.3. Experimental design considerations for Cecchini's findings

The clinical data reported by Cecchini suggests that in women with multiple breast cancer risk factors, excess fat further increases breast cancer risk. This effect was particularly evident in premenopausal women, a finding that is contrary to the majority of the literature. While some dismissed Cecchini *et al.*'s findings in premenopausal women as an outlier, Anderson and Neuhouser (45) highlight methodological considerations that may explain the discrepancy between findings of the P-1 Trial and other studies of obesity and breast cancer risk in premenopausal women.

First, whereas height and weight in the P-1 Trial were collected by trained staff at baseline prior to diagnosis, many prospective cohort or retrospective case-control studies rely on self-reporting at baseline or following diagnosis. This is a key point, as the Oxford cohort of the European Prospective Investigation into Cancer and Nutrition (EPIC), reported that on average, 27.4% of overweight and 31.3% of obese women underreported weight compared to measured weight (46). In addition, Anderson and Neuhouser point out the P-1 Trial's requirement for regular mammograms, which could alter risk estimates due to frequency of screenings in the overweight/obese vs. women of normal weight. Therefore the implications of the P-1 Trial on premenopausal women are not easily dismissed as an outlier, and rather highlight the need for additional investigation, particularly in populations at high risk of breast cancer.

1.F. Obesity negatively influences breast cancer outcomes

While the effect of obesity on breast cancer risk varies depending on menopausal status, the effect of obesity on poorer breast cancer outcomes has been well documented. Obese women with breast cancer typically have larger tumors, advanced disease stage at diagnosis, higher rates of metastasis, and higher rates of distant recurrence (HR=1.57 (1.11-2.22)). Obese women with breast cancer have increased

chance of initial or acquired chemotherapy resistance, and obese women have higher all-cause mortality (HR=1.56 (1.01-2.40)) and breast cancer-related mortality (HR=2.54 (1.08-6.00)) at any age compared to normal weight women with breast cancer (47-50). In 2003-2004, obesity was estimated to be responsible for 20,000 breast cancer deaths in high-income countries such as the US (51).

A recent article in Epidemiology describes a cohort of N=462 premenopausal women and N=972 postmenopausal women, in which gaining >5% of pre-diagnosis weight within two years of a breast cancer diagnosis was associated with increased all-cause mortality (HR=5.87 (0.89-47.8)) (52). While all-cause mortality was increased in both premenopausal and postmenopausal groups, breast cancer-specific mortality was influenced by post-diagnosis weight gain in premenopausal women (HR=3.09 (0.99-11.2)) but not postmenopausal women (HR=0.89 (0.24-2.81)). The influence of weight gain on increased breast cancer mortality was more pronounced in women who were already overweight or obese at the time of diagnosis (HR=2.76 (0.94-8.47) compared to women with BMI <25 at diagnosis (HR=1.08 (0.34-3.21)) (52). The effect of post-diagnosis weight gain on all-cause mortality in subjects with breast cancer was blunted if weight was gained more than two years post-diagnosis (HR=1.48 (0.62–3.44)), suggesting that the biological processes that accompany the development of obesity negatively impact breast carcinogenesis in a time-sensitive manner.

1.G. Mechanisms behind the proposed effects of obesity on breast carcinogenesis

A study reported in the Journal of the National Cancer Institute recently indicated that obesity reduces survival among women with ER+ breast tumors (progression-free survival HR=1.95 (1.02-3.75)). Likewise, obesity negatively influences cancer-free survival in mice carrying an activating mutation in transforming growth factor (TGF)α under control of the mouse mammary tumor virus (MMTV) (53). To provide insight into molecular mechanisms which may be associated with the worse breast cancer

outcomes, breast tumors from women and transgenic mice were profiled using microarrays. The data revealed that obesity was associated with altered expression of 85 genes in both mice and humans.

When these 85 genes were ranked by average Z-score, the most common cancer hallmark to which these 85 genes mapped was sustained proliferation (top 5 genes: *DUOX1* (dual oxidase 1), *SURF1* (surfeit 1), *CYCS* (cytochrome c (somatic)), *GNPDA1* (glucosamine-6-phosphate deaminase 1), *PHKA1* (phosphorylase kinase, α1)). The second most common hallmark to which these 85 genes mapped was evasion of apoptosis (top 5 genes: *LEP* (leptin), *PDIA5* (protein disulfide isomerase family A, member 5), *ALDH5A1* (aldehyde dehydrogenase 5 family, member A1), *SDHD* (succinate dehydrogenase complex, subunit D), *PHKG2* (phosphorylase kinase, gamma 2)). These data suggest that the balance between proliferation and apoptosis is an important mechanism whereby the promotional effects of obesity on the carcinogenic process in the breast are mediated.

Several hypotheses have been proposed to explain the link between obesity and breast cancer. In the context of the stopwatch analogy, these hypotheses can be thought of as lines of code that can program stopwatches. Multiple lines of code can be used to run the same stopwatch. In the context of obesity and breast cancer, there are four main mechanistic hypotheses, or "lines of code", that have gained mainstream traction to explain the link between these two diseases. In postmenopausal women, the predominant mechanism (**code line 1**) for the increased risk of breast cancer conferred by obesity centers on peripheral production of sex hormones by fat tissue. This mechanism will be discussed in detail in Chapter 4. The remaining three hypotheses—chronic inflammation (**code line 2**), deregulated insulin signaling (**code line 3**), and altered adipokine expression (**code line 4**)—will be discussed separately in the interest of clarity, with the caveat that these processes are part of a tightly woven web of systems within an organism. Thus, these mechanisms have a high level of cross-talk.

1.H. Code line 2: Chronic inflammation as a permissive environment for breast carcinogenesis

From a physiological perspective, inflammation is a necessary response to tissue injury and wound healing and is generally self-limiting. Expression of pro-inflammatory cytokines, including interleukin (IL)-1 α/β, IL-6, interferon (IFN)-γ, tumor necrosis factor (TNF)-α, and transforming growth factor (TGF)-α/β, is usually closely followed by the production of anti-inflammatory cytokines within the tissue, including IL-10, IL-13, and IL-14, under normal acute conditions (reviewed in (54)). This negative feedback loop is impaired in the pathological states of obesity and cancer, which both demonstrate chronic low-grade inflammation.

1.H.1. Obesity is associated with adipocyte hypertrophy and dysfunction

As a compensatory mechanism for chronic positive energy balance, obesity is characterized by both adipocyte hyperplasia (differentiation of preadipocytes into mature adipocytes) and adipocyte hypertrophy (increased size of existing mature adipocytes). Using primary adipocytes isolated from needle biopsies of human abdominal subcutaneous adipose tissue, Isakson *et al.* demonstrated that the number of preadipocytes which could be induced to differentiate was negatively correlated with BMI (correlation coefficient, r^2=-0.59) and adipocyte size (r^2=-0.69, p<0.05 for both analyses) (55).

Compared to smaller adipocytes, hypertrophic adipocytes display increased rates of lipolysis, increased free fatty acid turnover from adipocytes, and increased risk of adipocyte death (56-59). In a study of healthy men and women undergoing elective abdominal surgery, adipocytes with the largest diameter displayed increased expression of TNF-α, IL-6, colony stimulating factor (CSF)-1, and macrophage chemoattractant protein (MCP)-1, which recruits macrophages to the dysfunctional adipocytes compared to adipocytes with the smallest diameter (60).

1.H.2. Obesity is associated with altered macrophage immunological profile

In addition to the enhanced total infiltration of macrophages into adipose tissue during obesity, an article published in the Journal of Clinical Investigation reported that high fat feeding-induced obesity alters macrophage cytokine expression profiles (61). Specifically, a 5.5-fold increase of M1 (pro-inflammatory) vs. M2 (non-inflammatory) macrophages was demonstrated in the epididymal fat pads of C57Bl/6 (diet-induced obesity susceptible) mice (61). Whereas M1-type pro-inflammatory macrophages are activated by lipopolysaccharide (LPS), TNF-α, and IL-6, M2-type anti-inflammatory macrophages are activated in response to IL-10 and IL-14 (62;63). Within the same study, constitutive knockout of the chemokine receptor gene (*ccr2*) reduced macrophage infiltration into adipose tissue, as well as induced a shift towards M2-type macrophages present within adipose tissue (61).

In addition to the local, tissue-specific effects of obesity on inflammation, obesity influences systemic measures of inflammation. C-reactive protein (CRP) is an inflammation-associated biomarker (64). Circulating CRP levels were positively correlated with BMI (regression coefficient= 1.35 (1.25; 1.44)); fat mass (coefficient=2.52 (2.33; 2.70)); and waist circumference (coefficient=3.27 (3.03; 3.52)) in healthy women (65). As a proxy to immune system activation in obesity, two markers of neutrophil activation (myeloperoxidase, which generates reactive oxygen species, and calprotectin) were significantly elevated in morbidly obese vs. lean individuals (66).

1.H.3. Oxidative stress in obesity

What triggers the chronic inflammation phenotype present in obesity? Evidence is accumulating that the obese state is characterized by increased oxidative stress, which may contribute to the inflammatory response. In a 2004 article in the Journal of Clinical Investigation, Furukawa *et al.* reported that urinary levels of two markers of oxidative stress, thiobarbituric acid reactive substance (TBARS) and 8-epi-

prostaglandin-F2α (8-epi-PGF2α), were positively correlated with BMI in obese vs. lean men and women (Pearson's correlation coefficient: r=0.310, r=0.432, respectively; $p<0.05$ for both) (67). In the same study, genetically obese KKAy mice display increased circulating and adipose tissue expression of TBARS and hydrogen peroxide compared to lean wild-type mice (67). Obese KKAy mice also display reduced expression of antioxidant enzymes including superoxide dismutase (SOD), glutathione peroxidase, and catalase (67). These data suggest that oxidative stress in obesity may perpetuate chronic low-grade inflammation.

1.H.4. Chronic inflammation in breast cancer

Similar to obesity, inflammation is associated with increased breast cancer risk. In women with primary breast cancer diagnosis recruited to the Health, Eating, Activity, and Lifestyle (HEAL) Study, circulating levels of inflammatory biomarkers serum amyloid A (SAA) and CRP were associated with reduced disease-free survival (comparison of highest to lowest tertiles, SAA: HR=2.91 (1.61-5.26); CRP: HR= 2.05 (1.14-3.69)) (68). In a separate study by Sheer-Chen *et al.*, women with primary breast tumors had 1.5-fold elevations in circulating TNF-α compared to cancer-free women, and TNF-α levels were positively correlated with increasing tumor stage and tumor size (69).

Inflammation is manifested at both local and systemic levels. Similarly, mammary epithelial cells can gain paracrine exposure to inflammatory cytokines from local sources, as epithelial cells are in close proximity to adipocytes and macrophages as depicted in **Figure 1**.

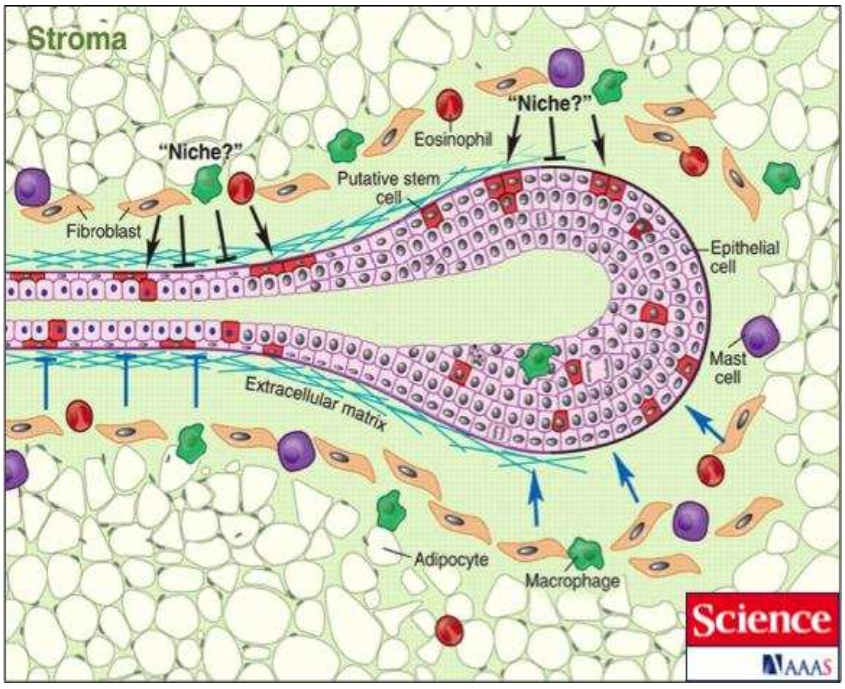

Figure 1
Legend. Previously published as Pengfei Lu and Zena Werb, *Science* (2008) 322(5907): 1506-1509. Reprinted with permission from the American Association for the Advancement of Science. Original caption: "A schematic presentation of the epithelium and stroma during mammary gland development. Stroma, which has a heterogeneous cell population, plays an important role in determining branching patterns (blue arrows and bars indicate stimulatory and inhibitory cues acting on the epithelium). Stroma also regulates biology of stem cells by contributing to a presumptive stem cell "niche.""

Epithelial cells can gain endocrine exposure to cytokines as a result of systemic inflammatory cytokines that are delivered via the vascular system (54;70). Finally, breast tumors may be able to produce their own cytokines. In an article by Jin *et al*., invasive breast carcinomas displayed twice the levels of IL-1β compared to benign breast tissue (71). Also in the Jin article, tumors with high levels of IL-1β displayed elevations in angiogenic factors thrombospontin-1 (2.3X increase) and von Willebrand factor (2X increase) compared to tumors with low expression of IL-1β (71).

However, it is unknown what percentage of tumor-associated cytokines is derived from epithelial vs. stromal production. For example, in a study of 35 primary breast tumors, while 100% of tumors

expressed at least one isoform of the TNF-α receptor (p55 or p75 isoforms), expression of TNF-α was detected only in stromal cells and not in epithelial cells.

1.H.5. Inflammatory cross-talk between adipose tissue and mammary epithelium

At a molecular level, how does adipose tissue inflammation impact breast cell proliferation? Pro-inflammatory cytokines impact cancer hallmarks including proliferation, suppression of apoptosis, and angiogenesis (15;72). For example, IL-6 activates the signal transducer and activator of transcription (STAT)-3, which translocates to the nucleus and stimulates transcription of genes including cyclin D1 and c-myc (73). STAT-3 stimulates expression of Bcl-XL and survivin in orthotopically-induced breast tumors in mice to prevent apoptosis (74). TNF-α activates NF-kB, which in conjunction with STAT3 promotes angiogenesis through upregulation of hypoxia-inducible factor (HIF)-1α and vascular endothelial growth factor (VEGF) (72;73).

Taken together, this literature suggests that inflammation is an important factor in the carcinogenic process in the breast, and that tumor-associated stroma can influence the process as well.

1.I. Code line 3: Dysregulated insulin signaling in obesity

The co-existence of deregulated insulin signaling in conjunction with obesity has been recognized for decades, leading authors Astrup and Finer in 2000 to coin the term 'diabesity' (75). Data from the Nurses' Health Study revealed a strong positive relationship between obesity and risk of type 2 diabetes. Compared to women who maintained their weight, weight gain of 5.0-7.9 kg was associated with a hazard ratio of developing diabetes of 1.9 (1.5-2.3), and weight gain of 8.0-10.9 kg was associated with hazard ratio of developing diabetes of 2.7 (2.1-3.3) (76).

Insulin-like growth factor (IGF)-1 shares 48% amino acid homology with the unprocessed precursor form of insulin (77). Insulin and IGF-1 can bind to the insulin receptor (IR) or the insulin-like growth factor receptor (IGF-R), inducing the formation of homodimers or heterodimers of these two receptors (77). Whereas insulin is released by the pancreas in response to hyperglycemia following a meal, IGF-1 is produced predominantly by the liver in response to stimulation by growth hormone (78). IGF-1 is required for normal mammary gland development. By developing IGF-1 knockout mice, Ruan and Kleinberg demonstrated that IGF-1-null mice displayed significant blunting of mammary gland morphogenesis, including suppression of terminal end bud formation and ductal branching (79). This effect could not be rescued by administration of growth hormone, suggesting that IGF-1 is critical to mammary gland development (79). In contrast, insulin does not appear to be critical for mammary gland development, though insulin may indirectly influence milk production by regulating nutrient flux, such as glucose and fatty acids (reviewed in (80)).

1.I.1. Deregulation of insulin signaling in obesity

BMI is positively correlated with circulating insulin and IGF-1, though the magnitude of the trend is stronger for insulin (insulin, Pearson's coefficient=0.44; IGF-1, Spearman's coefficient=0.20, $p<0.001$). This positive association of insulin and IGF-1 with BMI has important implications to the "stopwatch programming" effect of obesity, as insulin signaling favors cancer promotion. Specifically, binding of insulin or IGF-1 to receptors activates a series of events, including the phosphatidyl inositol 3 kinase (PI3K)/Akt/mammalian target of rapamycin (mTOR) signal transduction cascade. This pathway culminates in the activation of S6 kinase and releasing the inhibition of the eIF4e transcription factor. Cumulatively, these effects induce expression of proteins involved in cell cycle progression, including cyclin D1 and c-Myc (81-87). Insulin signaling also prevents apoptosis via increased expression of anti-apoptotic proteins Bcl-2 and Bcl-XL, with concomitant suppression of pro-apoptotic protein Bax (81-87).

1.I.2. Deregulation of insulin signaling in breast cancer

The mitogenic role of insulin signaling is manifested as increased risk of breast cancer in association with higher circulating levels of insulin and IGF-1. Hyperinsulinemia as a product of insulin resistance is associated with increased breast cancer risk in postmenopausal women (comparison of highest to lowest quartile, HR=1.46 (1.00-2.13)) (84). Similarly, high IGF-1 is associated with increased breast cancer risk in both premenopausal women (comparison of highest to lowest quintile, odds ratio (OR)=1.2 (1.0-1.5)) and postmenopausal women (OR=1.33 (1.1-1.6) (86).

Beyond breast cancer risk, insulin and IGF-1 negatively influence cancer progression and invasion. High levels of insulin signaling promote tumor angiogenesis through upregulation of vascular endothelial growth factor (VEGF) and hypoxia inducible factor (HIF)-1α, stimulation of endothelial cell proliferation, and promotion of vascular tube formation (88). High circulating insulin increases risk of breast cancer recurrence (comparison of highest to lowest quartile, HR=2.0 (1.2-3.3)) (89). Importantly, Calori et al. reported that obese insulin-resistant individuals had elevated risk of cancer mortality (HR=1.52) compared to obese insulin-sensitive individuals (HR=1.04) (90).

In the Cecchini study of pre- and postmenopausal women, a greater percentage of obese (5.9%) and overweight (2.3%) women were diabetic than lean women (1.4%). However, full multivariable adjustment for several variables including diabetes only minimally reduced hazard ratios in premenopausal women from the final multivariable assessment of 1.59 and 1.70 for overweight and obesity to 1.55 and 1.66, respectively (41). As adjustment for diabetes did not substantially influence risk estimates, factors in addition to insulin signaling appear to be influencing breast cancer risk in overweight and obese populations.

1.J. Code line 4: Adipose tissue functions as an endocrine organ with implications on breast cancer

While previously thought of as a passive storage depot for excess energy, fat tissue has gained notoriety as a powerful endocrine organ with far-reaching effects on multiple disease processes. These actions are exerted via adipose-derived cytokines, known as adipokines. Leptin and adiponectin are among the most abundant adipokines in human serum (91). Whereas circulating leptin is positively correlated with adiposity (92;93), adiponectin generally decreases in obese compared to lean individuals (91).

1.J.1. Leptin and breast cancer promotion

An article by Wu *et al.,* published in the British Journal of Cancer in 2009, reported that levels of circulating leptin were associated with increased breast cancer risk in premenopausal women (comparison of highest to lowest tertile, HR=1.40 (0.83–2.38)), though this effect may be mixed in premenopausal populations (i.e., (94)) (95). Leptin was also associated with increased breast cancer risk in postmenopausal women (comparison of highest to lowest tertile, HR=1.69 (0.95–3.06)) (95). When waist circumference was included as a covariate in the Wu article, breast cancer risk associated with circulating leptin was further increased in premenopausal women (comparison for highest to lowest quartile, HR=1.99 (1.06–3.39)) and postmenopausal women (comparison for highest to lowest quartile, HR=3.25 (1.53–6.91)) (95).

In a study of 35 primary breast cancers, 75% of tumors expressed leptin and 80% of tumors expressed the leptin receptor (96). Expression of the leptin receptor was correlated with expression of ER and tumor size (96). Normal breast tissue adjacent to cancerous tissue displayed increased leptin expression in 60% of the cases evaluated; in contrast, leptin was undetectable in the breasts of cancer-free women (97). Breast tumor expression of leptin receptor in conjunction with elevated circulating leptin is associated with poor prognosis (98) and tumor metastasis (99). At a molecular level, leptin displays

considerable cross-talk with estrogen signaling (99). Leptin has been shown to stimulate proliferation of breast cancer cell lines *in vitro* (100), to stimulate tumor growth in nude mice via activation of the extracellular signal-related kinase (ERK) (101), and to stimulate growth of carcinogen-induced rat tumors (102). Leptin also may inhibit apoptosis via upregulation of the anti-apoptotic protein survivin (103;104).

1.J.2. Adiponectin and breast cancer prevention

In contrast to leptin, a recent meta-analysis conducted by Macis *et al.* reported that circulating adiponectin is associated with reduced breast cancer risk in both premenopausal women (summary RR=0.72 (0.30-1.72)) and postmenopausal women (summary RR=0.80 (0.63-1.01)) (105), though findings reported by others are mixed (i.e., (106-108)). Adiponectin exerts systemic insulin-sensitizing effects through increased glucose uptake and increased β-oxidation in muscle (109). Likewise, adiponectin inhibits liver glucogenesis via activation of AMP-activated protein kinase (109). Adiponectin suppresses inflammation, as overexpression of adiponectin in *lep*^{ob}/*lep*^{ob} mice was associated with reduced macrophage infiltration of fat, corresponding to an anti-inflammatory phenotype. Administration of adiponectin induced a switch from M1-type macrophages (pro-inflammatory) to M2-type macrophages (anti-inflammatory) in *lep*^{ob}/*lep*^{ob} obese mice (reviewed in (110)).

Given their opposing impact on breast cancer risk, some have proposed that the adiponectin: leptin ratio, rather than levels of individual adipokines, may be more informative for evaluating breast cancer risk profile (111;112). However, the utility and biological relevance of expressing protein data as ratios in clinical populations has recently been challenged, particularly when the proteins in question are not isoforms (phospho/total protein) or do not directly interact (113).

1.K. Epigenetic effects of obesity on stopwatch programming

Beyond classical genetic regulation, cancer hallmarks are subject to epigenetic regulation by obesity-related mechanisms. Obesity was recently associated with hypermethylation of gene loci involved in inflammation, insulin signaling, and leptin signaling in normal breast tissue from cancer-free women (114). In addition, obesity was recently associated with hypermethylation of gene loci involved in regulation of immune response, proliferation, and DNA repair in breast cancer patients with ER+ tumors (115). MicroRNAs (miR) represent another epigenetic mechanism for the regulation of cancer hallmarks by obesity-related mechanisms. Obese individuals display altered microRNA expression profiles (116). Changes in activity of the miR-processing machinery Dicer have been observed in obesity (116) and in breast cancer (117). MiRs can have tumor suppressing or tumor promoting effects. Tumor promoting effects have been reported to be manifested through regulation of replicative immortality, angiogenesis, inflammation, proliferation, and the epithelial to mesenchymal transition (reviewed in (118;119)).

Collectively, these four schools of thought represent biological processes whereby obesity influences the programming of initiated cells' stopwatches via genetic or epigenetic means, and can be thought of as four lines of code. These code lines are summarized as follows: 1, peripheral production of sex hormones; 2, chronic inflammation; 3, dysregulated insulin signaling; and 4, altered adipokine production.

1.L. Preclinical models of obesity: what tools are available?

As described above, the relationship between obesity and breast cancer is extremely complex. The four lines of code that we know about comprise complex bodies of literature, and there are most certainly other lines of code in addition to these four. Preclinical models are critical tools that can be used to

deconstruct the biology of this problem in a stepwise manner by interrogating specific pieces of the puzzle.

Invertebrate models have provided important information to the field of obesity research, including diet-induced obese and transgenic *Drosophila melanogaster* (120) and *Caenorhabditis elegans* (121). However, the architecture of the mammalian mammary gland is highly complex, with multiple cell types present including epithelial cells, adipocytes, fibroblasts, macrophages, and endothelial cells. As shown in **Figure 1**, stromal cells exist in close proximity to epithelium and are capable of exerting paracrine effects. Thus, mammalian models (including mice and rats) will likely provide the most direct translation of preclinical findings to clinical application towards deconstructing the cross-talk between obesity and breast cancer.

1.M. Rodent models of obesity and breast cancer

The most popular transgenic mice used in obesity research include the *lep*^{ob}/*lep*^{ob} and *lepr*^{db}/*lepr*^{db} transgenic strains, which possess mutations in the genes which encode leptin and the leptin receptor, respectively. These models have provided important mechanistic information relative to obesity. Some obese humans have gene mutations that display Mendelian patterns of inheritance comparable to these transgenic mouse strains. Heritable cases of obesity typically display mutations associated with leptin deficiency, truncated leptin receptor, pro-opiomelanocortin (POMC) deficiency, melanocortin-4 receptor deficiency, and prohormone convertase (PC)1 deficiency (122).

In the case of leptin, as adipose tissue expands, leptin acts to attenuate the positive energy balance and need for expansion of adipose depots by suppressing appetite and increasing energy expenditure (123;124). Interestingly, obesity is often characterized by leptin resistance (124). However, less than 5%

of morbid obesity cases are attributable to single-gene (monogenic) mutations. The majority of obesity cases, as in breast cancer cases, are attributable to multiple factors including polygenic susceptibility (125).

1.M.1. Polygenic mouse models of obesity

To develop preclinical models that are more representative of the polygenic nature of most human obesity, Cleary *et al.* has reported identification of subpopulations of FVB mice with polygenic predisposition to obesity (126-128). However, the application of these models to the clinical obesity-breast cancer puzzle has been limited by several factors.

First, luminal breast cancers are the most commonly observed breast cancer subtype in clinical populations. Luminal breast cancers derive their name from similar protein expression profiles as normal non-neoplastic cells that line the lumen of the breast duct. In the human breast, approximately 10-30% of normal luminal epithelial cells express sex hormone receptors, including the estrogen receptor (ER) and the progesterone receptor (PR) (129;130). Most studies report that obesity increases risk of predominantly luminal (ER/PR+) breast cancer subtypes, though this data is mixed, particularly in premenopausal women (131-133). In contrast, most mammary tumors that arise in mice are hormone receptor negative (ER/PR-) tumors, a molecular subtype of the disease that is less common and associated with poorer prognosis in clinical populations (134;135). Studies have reported conflicting effects of obesity on risk of ER/PR- breast cancer, which may be stratified by menopausal status (reviewed in (136)).

In addition to the molecular subtype of mammary cancers induced in mice, mouse models of diet-induced obesity generally utilize high fat diets containing 45-60% kcal from fat, which is higher than the

30% routinely consumed by most humans (137). As controls for diet-induced obese mice, non-obese control mice are frequently fed a low fat diet containing 10-11% kcal from fat, adding differences in dietary composition as potentially confounding variables in those investigations (138). Finally, whereas the mouse mammary gland is composed almost entirely of adipocytes and epithelium, the human breast has high fibrous and connective tissue content (139).

1.M.2. Rat models of obesity

In contrast to mice, the rat mammary gland is more similar to the human mammary gland in terms of fibrous and connective tissue content (139). Tumors induced in the rat via carcinogen generally have high histological and morphological similarity to human breast cancer (140). Most rat strains are resistant to diet-induced obesity (DIO) in the short term; however, MacLean *et al.* have characterized subpopulations of Wistar rats with sensitivity or resistance to diet-induced excess weight gain (141-144). These studies utilized 45% kcal from fat and have only been performed using the classical model of chemical carcinogenesis, wherein rats are injected around 50 days of age, resulting in long tumor latency. Furthermore, these studies have only been conducted in ovariectomized rats (141-144). Therefore, development of a polygenic rat obesity model with high similarity to the average human's diet and high similarity to manifestation of human breast cancer with rapid preclinical implementation would be a beneficial tool to use in breast cancer research.

1.M.3. The Levin rats: a polygenic model of diet-induced obesity susceptibility

In 1997, a novel model for the study of diet-induced obesity was introduced by Barry Levin of Veterans Affairs Medical Center in East Orange, NJ. This model utilizes two strains of Sprague Dawley rats selectively bred for >20 generations for resistance (DR) or susceptibility (DIO, or DS, as used herein) to

diet-induced obesity when fed diet containing ~32% kcal as fat. This model has been extensively characterized by Levin's group (e.g., (145-147)).

When fed the 32% fat diet, DS rats rapidly gain excess weight and have expanded peripheral and visceral fat depots by 3 months of age. DS rats display multiple metabolic abnormalities, including hyperlipidemia (total cholesterol and triglycerides) by 2 months of age, hyperleptinemia by 3 months of age, and pronounced fat infiltration of the liver by 6 months of age (146). DS rats display prediabetic measures of glucose homeostasis, including hyperinsulinemia and worsened oral glucose tolerance by 2 months of age, insulin resistance by 3 months of age, and eventual reduced pancreatic insulin secretion by 9 months of age, though rats do not fully progress to diabetes up to 2 years of age (146).

The Levin DS rats display many of the same comorbidities as manifested in the human obese condition, and do so when both lean (DR) and obese (DS) strains are fed the same diet. The macronutrient composition of the Levin diet is highly similar to that of the average American woman. Importantly, cancer response in these animals has not yet been reported, suggesting that the Levin rat strains represent novel tools for the study of obesity on carcinogenic processes within the breast.

1.N. Rapid emergence model of MNU-induced mammary carcinogenesis in rats

In 1995, our laboratory developed the rapid emergence model of breast cancer induction, in which sexually immature Sprague Dawley rats are injected with a non-toxic dose of the chemical carcinogen N-methyl-N-nitrosourea (MNU) (148). MNU forms methyl group-DNA adducts *in vivo* predominantly at the N7 position of guanine, though adducts are observed less often at O6 of guanine and N3 of adenine (149). While most DNA adducts are repaired via enzymatic processes, for example via demethylation by alkyl acceptor proteins such as O6-guanine-DNA methyltransferase, or by base/ nucleotide excision

repair, failure to repair these adducts can lead to mutations. For example, alkylation at the N7 position of guanine can result in guanine to adenine (G→A) transition mutations (150).

1.N.1. The rapid emergence model of chemical carcinogenesis

The rapid emergence model of chemical carcinogenesis takes advantage of the developmental timeline of the rat to accelerate the carcinogenic process. During puberty, which begins in rats around 3 weeks of age, terminal end buds proliferate rapidly to populate the mammary fat pad with epithelium. Terminal end buds are highly susceptible to MNU action, as their high proliferation rate results in "fixing" a higher percentage of DNA adducts as mutations than would be observed in a slowly proliferating tissue. Russo *et al.* demonstrated that terminal end buds in the rat mammary epithelium reach peak density of 24.7 terminal end buds/mm^2 at 20 days of age; in contrast, density of terminal end buds at 55 days of age is 5.4 per mm^2 (151). Thus, injecting rats at 21 days of age gives MNU a higher number of targets to accelerate the process of carcinogenesis. Furthermore, new mutations can potentially occur and be "fixed" in the proliferating terminal end buds as a result of DNA repair processes triggered by MNU-induced damage.

1.N.2. Genetic characteristics of MNU-induced tumors

In the 1960s and 70s, Peter Magee from the Courtald Institute of Biochemistry in London demonstrated that the nitrosamides, including MNU, are nonspecific, uniform DNA methylating agents (152-154). Unpublished microarray data from our laboratory reveals that MNU-induced tumors display altered activity of a variety of tumor suppressor and tumor promoting genes as compared to uninvolved mammary gland. While activating mutations in Ha-*ras* and Ki-*ras* are commonly observed in MNU-induced tumors, it is unclear whether *ras* activation is solely sufficient for induction of tumors (reviewed in (150;155)), and MNU-induced tumors are generally considered polygenic in origin.

MNU-induced tumors begin to emerge after sexual maturity, and the incidence (first cancer/rat), multiplicity (total # cancers/rat) and latency (cancer-free survival) of mammary tumors are dependent on carcinogen dose (148;156;157). As illustrated in **Figure 2**, whereas human breast cancer generally develops in

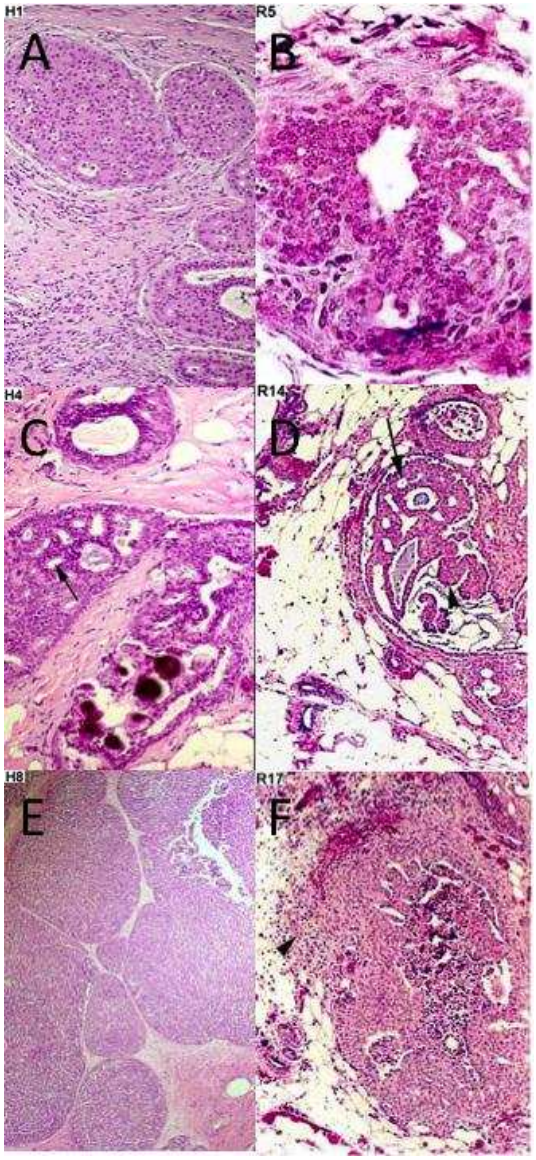

Figure 2
Legend. Adapted from Singh *et al. Lab Invest.* 2000 Feb;80(2):221-31. Histopathological comparison of human (panels A, C, E) and chemically-induced rat (panels B, D, F) mammary lesions. Panels A,B) epithelial hyperplasia. Panels C,D) carcinoma *in situ* of lobular (panel C) or ductal (panel D) origin. Panels E,F) adenocarcinoma of lobular (panel E) or ductal (panel F) origin.

lobules, breast lesions in the rat are predominantly ductal in origin (134). However, the histological characteristics and morphological stages of cancer development induced by MNU closely recapitulate the process of breast carcinogenesis in women (140).

1.N.3. Integration of the Levin rats with the rapid emergence model

Cecchini's report on the clinical outcomes of the P-1 and P-2 Breast Cancer Prevention Trials in high-risk women demonstrated the power of using subgroups within a population to challenge the standard conventions about obesity and breast cancer risk. Similarly, in our laboratory's rapid emergence rat model of breast carcinogenesis, 70-90% of rats develop cancer, demonstrating that not all animals treated with a carcinogen develop cancer. Rather, the process is stochastic in nature. Specifically, the MNU model simulates a population of at-risk individuals. Whereas carcinogen treatment establishes risk (initiates cells), the biology of each animal determines the response (programs the stopwatches). By combining the Levin strains of rats with our laboratory's rapid emergence model of mammary carcinogenesis, we have developed a novel preclinical model with high relevance to clinical populations.

1.O. Conclusion

In conclusion, this dissertation seeks to use a novel preclinical model with potential value to a wide range of researchers, from basic scientists to clinicians, in which to study the impact of excess weight and adiposity on mammary carcinogenesis. This work was envisioned as a starting point to deconstruct a complex clinical problem: how does obesity alter the carcinogenic process in the breast?

The subsequent chapters of this dissertation deconstruct the obesity-breast cancer problem in several directions. Chapter 2 examines the markedly accelerated cancer response in obese ovary intact rats. Chapter 3 elucidates molecular mechanisms responsible for the accelerated cancer response in obese

ovary intact rats observed in Chapter 2. Chapter 4 employs a classical ovarian ablation experiment to evaluate the hypothesis that peripherally produced estrogen is a primary driver of breast cancer in obese populations. Chapter 5 was designed to be a hypothesis-generating intervention in which to assess the evidence in support of the remaining 3 lines of mechanistic code whereby obesity might be involved in the accelerated cancer response. Finally, Chapter 6 summarizes the work accomplished to date and proposes a series of experiments that represent the next logical extension of the current work.

CHAPTER 2. OBESITY ACCELERATES MAMMARY CARCINOGENESIS IN OVARY INTACT RATS[2]

2.A. Rationale

In Chapter 1, we summarized the outcomes of the P-1 and P-2 Breast Cancer Prevention Trials recently published by Cecchini (41). In these trials, obesity was associated with substantially increased breast cancer risk in high-risk women, particularly in premenopausal women. To evaluate Cecchini *et al.*'s hypothesis that obesity accelerates cancer in premenopausal women with increased risk for breast cancer, we integrated the rapid emergence model of mammary carcinogenesis developed by our laboratory with the Levin strains of diet-induced obesity resistant (DR) or susceptible (DS) rats. Similar to the premenopausal women evaluated by Cecchini, who are actively cycling, ovary intact rats have cyclically high levels of sex hormones due to progression through the estrus cycle. Therefore, ovary intact rats allow for the evaluation of the carcinogenic response in the presence of high levels of endogenous sex hormones.

Materials and methods for the experiments reported in Chapter 2 are provided in **Appendix A**.

2.B. Results and Discussion

Figure 3 depicts the study design. This study was comprised of N=101 diet-induced obesity susceptible (DS) and N=103 diet-induced obesity resistant (DR) female ovary intact rats. Purified sucrose and moderate fat (32% kcal) diet (called SUMO32) was fed ad libitum throughout the study. Macronutrient composition of SUMO32 is highly similar to the composition of the average American woman's diet, in terms of kcal contributed by protein, fat, and carbohydrate, as reported in **Table 3**.

[2]Chapter 2 was published as Matthews SB *et al., Cancer Prev Res (Phila).* 2014 Mar;7(3):310-8 (158). Differences between the published version and that which appears herein are minor and serve to provide additional information which is relevant to subsequent dissertation chapters.

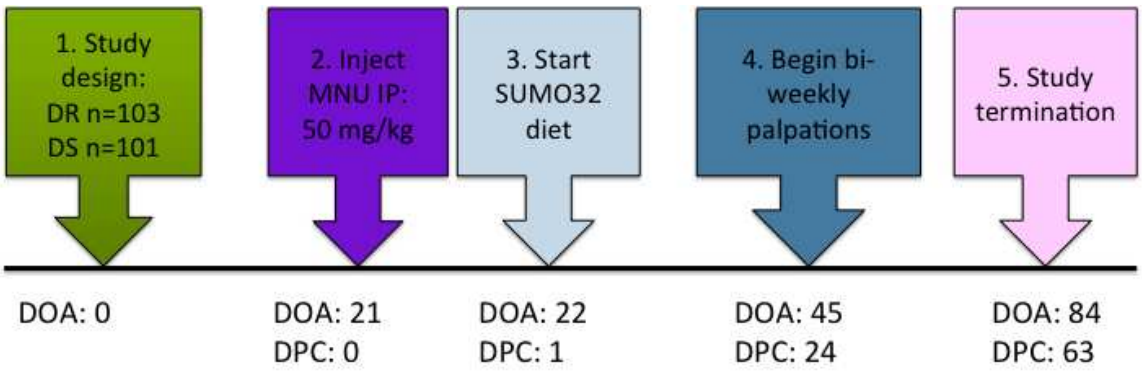

Figure 3
Legend. Study design for assessing the impact of excess weight gain on ovary intact female rats. DOA= days of age; DPC= days post-carcinogen injection.

Table 3
Legend. Composition of average woman's diet in 2007-2008 based on National Health and Nutrition Examination Survey (NHANES) data (159).

Macronutrient	Composition of average US woman's diet (% kcal)	Composition of SUMO32 diet (% kcal)
Protein	15.5	16.7
Carbohydrate	50.5	51.2
Total fat	33.5	32.1
Saturated fat	11.1	9.4

2.B.1. DS rats gain weight at an accelerated rate compared to DR rats

At the study outset, DS rats were not significantly heavier than DR rats (DS 56.7 ± 8.7 g; DR 53.6 ± 6.3 g). However, body weights of DS and DR rats began to diverge immediately with SUMO32 feeding (**Figure 4**). DS rats continued to gain weight at an accelerated rate for the duration of the study (p_{trend}<0.001). At study termination 63 days post carcinogen, DS rats were 15.5% heavier than DR rats (217.0 ± 24.5 vs. 187.9 ± 14.6, respectively, *p*

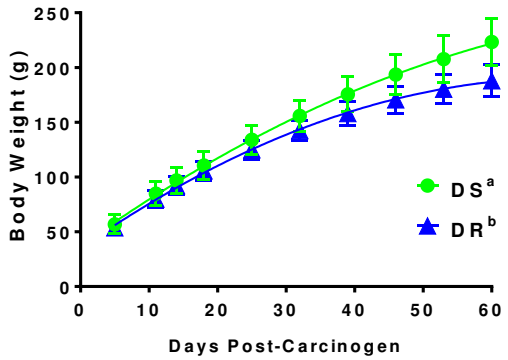

Figure 4
Legend. DS rats gain weight at an accelerated rate compared to DR. Rats were weighed weekly while on study; data, mean ± SD for N=103 DR, N=101 DS rats. Weight gain trend was analyzed with nonlinear regression. DS display significantly more weight gain compared with DR rats, p_{trend}<0.001.

<0.001). Plasma leptin, which is related to fat mass (93;160), was 5.9-fold higher in DS versus DR rats at study termination.

The magnitude of the difference between DR and DS rats is a relevant comparison to the clinical BMI tiers of normal weight (BMI <25 kg/m^2), overweight (25.0-29.9 kg/m^2), and obese (≥30.0 kg/m^2). For example, a 5'4" adult woman weighing 140 lbs with BMI 24.0 kg/m^2 is considered normal weight, while a 5'4" woman weighing 161.7 lbs (15.5% increase) with BMI 27.8 kg/m^2 is considered overweight. Thus, the moderate body weight differences observed between DS and DR rats closely recapitulates clinical populations.

2.B.2. Chemically-induced mammary carcinogenesis is accelerated in DS rats

Mammary carcinogenesis was induced by injecting rats with the carcinogen MNU (50 mg/kg) at 21 days of age. Tumors were harvested at necropsy 63 days post-carcinogen. Following diagnosis, palpable histopathologically confirmed mammary adenocarcinomas were compared between DR and DS rats. Tumor-free survival was evaluated with Kaplan-Meier analysis with tumor-free rats right-hand censored at 60 days post-carcinogen (last palpation day prior to study termination (censored: DS N=9, DR N=39)).

As shown in **Figure 5A,** DS rats displayed significantly reduced cancer-free survival, with 50% incidence of mammary adenocarcinoma achieved in DS rats by 39 days post-carcinogen compared to 49 days post-carcinogen in the DR group (p<0.001). DS rats displayed higher cancer incidence (91%) than observed in DR rats (65%) (**Figure 5B**). DS rats displayed higher cancer multiplicity (total cancers per rat) and cancer burden (sum tumor weight per rat) compared to DR (**Figure 5C and 5D**; p<0.001 for all analyses as summarized in **Figure 5E**). Of particular interest was the 5.4-fold increase in tumor burden in DS

compared to DR rats, given the trend towards larger breast tumor size in obese women compared to normal weight women (161;162).

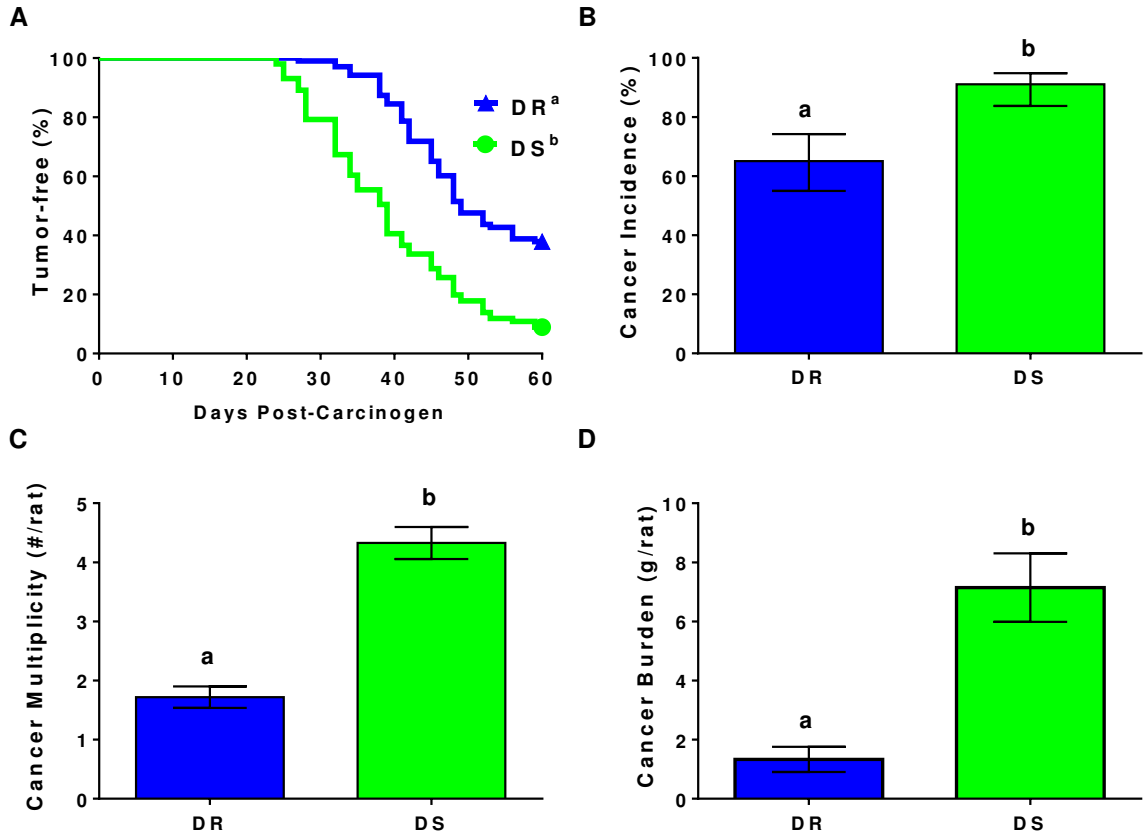

E

Group	N	Latency[1] (days)	Incidence[2] (%)	Multiplicity[3] (#/rat)	Burden[4] (g/rat)
DR	103	49	65.1	1.7	1.33
		(48, 56)	(55.0, 74.2)	(1.4, 2.1)	(0.91, 1.75)
DS	101	39	91.1	4.3	7.15
		(35, 41)	(83.8, 94.8)	(3.8, 5.0)	(5.99, 8.31)

Figure 5

Legend. Obesity accelerates mammary carcinogenesis in DS rats. Mammary carcinogenesis was initiated by injecting rats intraperitoneally with 50 mg/kg MNU at 21 days of age. Study was terminated 63 days (9 weeks) after carcinogen; only palpable confirmed mammary adenocarcinomas were included for analysis. In Panels A-D, groups with different letters significantly differ based on statistical comparisons described in Appendix A. Panel A) Cancer-free survival (survivor function) was reduced in DS compared to DR rats. Cancer incidence (Panel B), cancer multiplicity (Panel C), and cancer burden (Panel D) were elevated in DS compared to DR rats. Panel E) [1]Data corresponds to survival curves in Panel A. Values are point estimates at 50% quartile (95% confidence interval of linear-transformed survivor functions). Censored: DR N=39, DS N=9. [2]Values correspond to incidence in

Panel B and are percentages (95% CI). [3]Values correspond to multiplicity in Panel C and are means (95% CI). [4]Values correspond to burden in Panel D and are means (95% CI).

2.B.3. Hormone receptor expression is not altered in DS compared to DR rats

Several studies report that obesity is associated with increased risk of hormone receptor-positive (estrogen receptor (ER), progesterone receptor (PR) positive) breast cancers, though this data is mixed (131-133). To evaluate hormone responsiveness of tumors induced in the ovary intact DR and DS rats, the carcinomas used to construct **Figure 5A** were assessed for progesterone receptor (PR) status, as PR contains an estrogen response element in its promoter and is frequently used as an indicator of ER signaling (163;164).

When classifying tumors as hormone receptor positive or negative, clinical pathologists seek out tumor hot-spots (areas of intense staining) to identify patients who will likely benefit from endocrine-based chemotherapy. To evaluate whether the hot-spot field approach vs. a random raster-pattern field approach changed the interpretation of the data, DR and DS tumors were evaluated by both methods (**Figure 6A** and **6B**, respectively).

As expected, higher % nuclear immunoreactivity was observed using the hot-spot method compared to the random field method; however, neither method revealed a difference between DR and DS tumors. Independent of DR/DS strains, 65-75% of tumors induced by MNU in ovary intact rats were hormone receptor-positive, corresponding to a luminal breast cancer subtype. This data is in agreement with luminal breast cancer being the predominant molecular subtype of breast cancer observed in both clinical populations and in our laboratory's rapid induction model of mammary carcinogenesis (140;165;166).

Importantly, as shown in **Figure 6C**, percentage of carcinomas classified as PR negative was slightly increased in DS (34.9%) vs. DR tumors (22.8%) (odds ratio by contingency analysis=1.78 (0.83–3.81; *p*=0.117)). This is a difference of 11.7% compared with DR rats, a finding that parallels the 14% increase in hormone receptor-negative breast cancers in premenopausal high-risk women in the P-1 Trial as reported by Cecchini (41). This observation has important clinical implications. Cancers negative for ER and PR are associated with younger age at diagnosis, higher rates of metastasis, and reduced disease free (HR=2.7 (1.3-5.8)) and reduced overall survival (HR=1.7 (1.3-2.2)) (167;168).

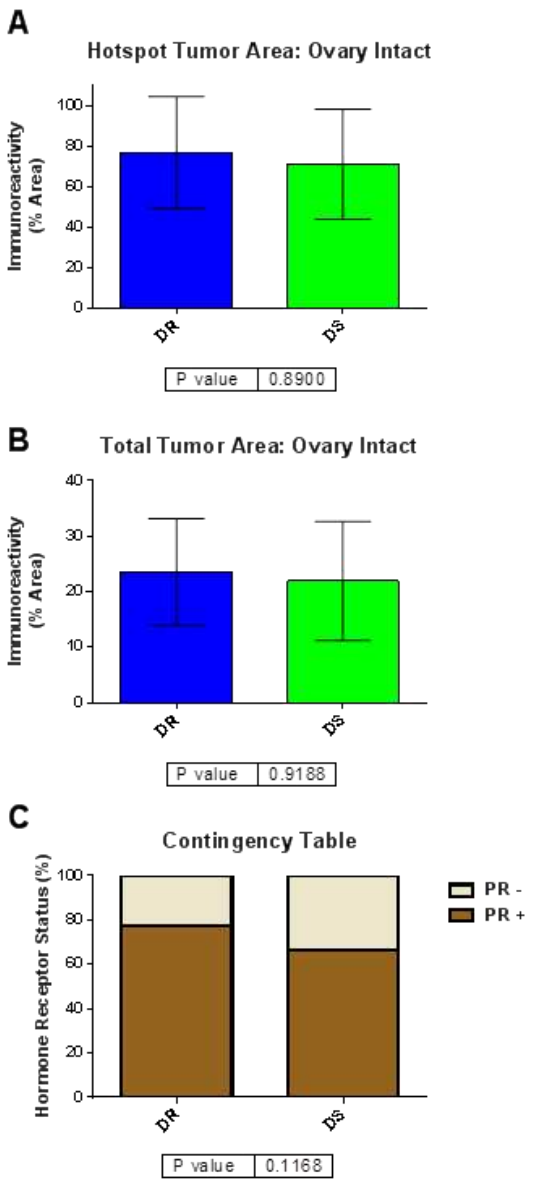

Figure 6
Legend. DS tumors do not display higher PR immunoreactivity than DR tumors. First-palpated tumors (DR N=65; DS N=117) were assessed for PR expression using immunohistochemistry. Panel A) PR immunoreactivity (% nuclear area) of hot-spot (high intensity-stained) tumor fields. Panel B) PR immunoreactivity of random tumor fields. Panel C) Classification of tumor PR status based on visual thresholding.

A recent meta-analysis of 11 case-control and cohort studies found that obesity was associated with increased risk of triple-negative breast cancer (pooled odds ratio=1.20 (1.03-1.40) (136), a subtype of hormone receptor-negative breast cancer that is negative for expression of ER, PR, and the human epidermal growth factor receptor (Her)2. This trend was maintained only in premenopausal women after separating studies by menopausal status (pooled OR for premenopausal women=1.43

(1.23-1.65); pooled OR for postmenopausal women=0.99 (0.74-1.24)) (136). Cecchini *et al.* did not specifically evaluate expression of Her2 in tumors from women in the P-1/P-2 studies; therefore, we cannot be sure as to whether the increased prevalence of hormone receptor-negative tumors was attributable to triple negative breast tumors vs. those that overexpress Her2. However, the general findings of the meta-analysis were consistent with the effect reported by Cecchini, wherein obesity increased risk of hormone receptor-negative breast tumors to a greater extent than observed for hormone receptor-positive breast tumors (HR for ER+ tumors in P-1 premenopausal women= 1.41 (0.82-2.43) overweight, 1.78 (1.03-3.07) obese; HR for ER- tumors in premenopausal women= 2.52 (1.19-5.33) overweight, 1.79 (0.76-4.22) obese).

To determine whether expression of PR was associated with alterations in growth characteristics of tumors, palpation date for each tumor in **Figure 6** was regressed on its corresponding PR % immunoreactivity. While we anticipated tumors with low PR % immunoreactivity would grow faster, and therefore be palpated sooner, there was no correlation between PR % and palpation date for either DR or DS rats. As another way to evaluate growth characteristics of tumors, final tumor mass was divided by days post-carcinogen at which each tumor was palpated to give growth estimates in g/day. There was no correlation between PR % and growth rate for either DR or DS rats. Therefore, these data suggest that tumor growth is not associated with sex hormone receptor expression.

2.C. Conclusions and Future Direction

In Chapter 1, a study was discussed in which breast tumors from obese women and mice display differential expression of 85 common genes, which mapped most often to the cancer hallmark of sustained proliferation followed by mapping of genes to the hallmark of evasion of apoptosis (53). These

data indicate that the role of obesity in programming the stopwatches of initiated cells may be manifested as an imbalance between the processes of cell proliferation and death.

In the current study, tumors developed in both DR and DS rats. To rephrase, both rats had stopwatches that were activated. However, weight gain in DS rats was associated with marked acceleration of mammary carcinogenesis compared with DR rats. Specifically, increased cancer incidence (26% increase), multiplicity (2.5-fold increase), and tumor burden (5.4-fold increase) with a concomitant reduction (16% earlier detection) in cancer latency were observed in DS compared to DR rats. This suggests that the programming of DS stopwatches may be altered by obesity. To determine whether obesity-mediated stopwatch programming impacts molecular mechanisms in DS compared to DR tumors, we interrogated the balance of proliferation and death processes in Chapter 3.

In addition, evaluation of hormone receptor expression in tumors from ovary intact rats in the current study revealed a trend towards higher prevalence of hormone receptor-negative tumors in DS animals, which are clinically associated with poor prognosis. To further interrogate this finding, an ovarian ablation experiment (ovariectomy) was conducted and is reported in Chapter 4. Ovarian ablation creates a selection pressure for expansion of cell populations that can grow in very low levels of estrogen, resulting in development of tumors that are predominantly hormone receptor-negative. The ablation experiment provided an avenue to assess the effect of obesity on the growth of tumors in the absence of significant estrogen signaling.

CHAPTER 3. ACCELERATED CELL CYCLE TRANSIT AND REDUCED APOPTOTIC EFFICIENCY CONTRIBUTES TO NEGATIVE EFFECTS OF OBESITY ON MAMMARY CARCINOGENESIS IN OVARY INTACT RATS[3]

3.A. Rationale

In 1967, when describing growth kinetics of tumors, Gordon Steel determined growth curves of tumors from a variety of clinical and preclinical studies. Steel defined three terms: V_0, tumor volume at time zero; V_T, the tumor volume at a given time; and V_{max}, maximal tumor volume at the asymptote of the growth curve. V_{max} is the point at which the distance between the curve and a fitted line approach zero as the values progress to infinity (169). Growth rate determines how quickly a tumor progresses from V_0 to V_{max}.

Returning to the stopwatch analogy, the carcinogen MNU is a DNA alkylating agent capable of transforming normal cells into cells with neoplastic potential, i.e., deposits the stopwatches. The stopwatches of initiated cells can be characterized by the terms of growth curves defined by Steel: V_0, the point at which the stopwatch button is pressed to start "keeping time"; growth rate, how fast stopwatches are ticking; and V_{max}, the point at which stopwatches reach their target time.

How does this apply to the accelerated cancer response in DS rats reported in Chapter 2? If obesity had no effect on mammary carcinogenesis in the Levin rats, DS and DR rats would have similar MNU-induced cancer outcomes. On the contrary, incidence, multiplicity, burden, and latency of MNU-induced tumors were all significantly affected in DS vs. DR rats. To explain this phenomenon, one of two explanations, or a combination of the two, must be true:

[3]Chapter 3 is being submitted to a special cell cycle issue of the journal *Molecular Cancer Research*. Any changes between the version presented herein and that which is published will be minor. Such changes will likely be due to publishing requirements and tone differences between target audiences.

1) DS stopwatches must be running "longer":
    a. Tumors have a longer period of time to grow in DS. vs. DR.
    b. Earlier V_0?
2) DS stopwatches must be running "faster"
    a. Tumors grow at a faster rate in DS vs. DR.

In our preclinical rat model, measuring V_0 and V_{max} is problematic. In the case of V_0, gene sequencing platforms are theoretically capable of identifying a single mutated cell from amongst millions of normal cells within a mammary gland. However, in 1998, Lu *et al.* reported that MNU-induced tumors within the same animals display discordant genotypes (170). This finding is consistent with reports of MNU as a nonspecific DNA alkylating agent, in which mutations arise from DNA adducts throughout the genome. Lu *et al.*'s findings are also consistent with a model of carcinogenesis in which independently initiated cells undergo clonal expansion to form individual carcinomas (170). To rephrase, there is no single gene mutation that has been identified as the event that triggers V_0 in 100% of MNU-induced tumors.

In our experience, tumors in the rat reach palpability (detection with the fingers in a manner that can be likened to breast self-examination) around 0.1 g. Based on the mass of a single cell as $1e^{-9}$ g as estimated by Steel, to reach palpability, a transformed cell must undergo approximately 27 doublings to generate $1e^{8}$ cells (171), the estimated number of cells in a tumor with a mass of 100 mg. These doublings occur during what Steel refers to as the 'silent interval' between initiation of a single cell and detection (172). V_0 resides within that silent interval. Therefore, tumor palpation occurs post-V_0. Likewise, tumors collected at necropsy correspond to V_T, not V_{max}. V_{max} represents the predicted maximal tumor volume achieved prior to the death of the animal. To rephrase, our window of tumor detection is always after V_0 and before V_{max}.

Therefore, the parameter of tumor kinetics that we are equipped to evaluate is the period between V_0 and V_{max}, which corresponds to tumor growth rate. Evaluation of the tumor growth rate in DS vs. DR tumors will hence be referred to as the "faster" hypothesis.

3.A.1. Cellularity as a balance of opposing processes: how does a tumor grow?

The "faster" hypothesis proposes that DS stopwatches run faster, or accumulate cancerous cells at a faster rate, than DR rats. This can be stated as follows:

H_0 (null hypothesis): DS tumor growth rate = DR tumor growth rate

H_A (alternative "faster" hypothesis): DS tumor growth rate > DR tumor growth rate

Growth rates of non-cancerous tissues are strictly balanced to maintain a constant cell number: one cell replicates to replace one cell that has died. In 1993, Thompson and Strange devised **Equation 1**, which models the size of a tissue as a balance between proliferation and death (173):

Equation 1

$$\Delta S = N(k_P - k_D) = 0$$

in which ΔS is the change in tissue size, N represents cell number, k_P is the rate of cell proliferation, and k_D is the rate of cell death. When ΔS = 0 and rates of proliferation are equivalent to the rate of death, the tissue is in homeostasis and does not increase in size (173).

3.A.2. ΔS is >0 for both DR and DS tumors

As both DR and DS rats developed tumors in Chapter 2, both strains have an imbalance somewhere in the Thompson-Strange equation. To rephrase, stopwatches are ticking in both animals. Are the stopwatches ticking at the same speed? If stopwatches are running at the same speed in DS and DR rats,

tumors palpated on the same day would be expected to have the same mass at study termination (V_T). In **Figure 7**, by regressing V_T on week of palpation, we can approximate ΔS for DR and DS tumors. The magnitude of ΔS in DS tumors is nearly double that of DR tumors (slope: DR 0.533 ± 0.070 g/week; DS 0.968 ± 0.140 g/week; 1.82-fold increase in DS over DR). This suggests a greater imbalance in the k_P and k_D terms of the Thompson-Strange equation for DS tumors, and is the first piece of evidence in favor of rejecting the null hypothesis in favor of the "faster" hypothesis.

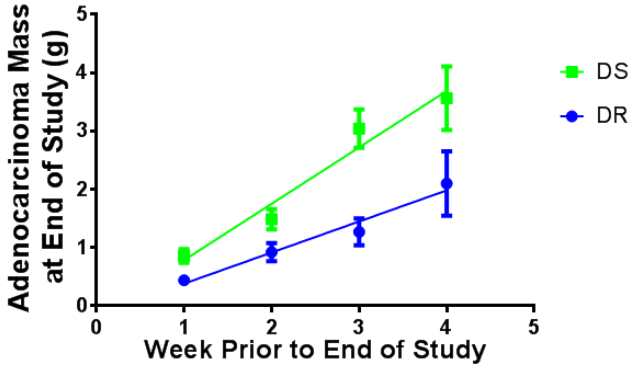

	DR	DS
Best-fit values		
Slope	0.5330 ± 0.07046	0.9678 ± 0.1401

Figure 7
Legend. Tumors from DS rats are larger than tumors form DR rats, regardless of week in which tumors are palpated. Palpable mammary adenocarcinoma mass was regressed on week prior to end of study and slopes are expressed as g tumor mass gained per week prior to end of study. Tumors palpated 1 week prior to the end of study are smaller, as expected, compared to tumors palpated 4 weeks (1 month) prior to the end of study, and slope of growth rate between DR and DS is different. Magnitude of the difference between growth rates = 1.82-fold steeper slope in DS tumors.

As reported in Chapter 1, a recent article in the Journal of the National Cancer Institute suggests that sustained proliferation (k_P) and evasion of apoptosis (k_D) are key mechanisms whereby obesity influences breast carcinogenesis in both obese women and mice (17). These hallmarks can be applied to break the "faster" hypothesis into two sub-hypotheses, which may be synergistic:

1) New cells are produced more quickly in DS tumors.
2) Existing cells die more slowly in DS tumors.

Using MNU-induced carcinomas from DR and DS rats, we evaluated the biological balance of k_P and k_D terms in the Thompson-Strange equation by a combination of histological and molecular biology techniques. Materials and methods for the experiments performed in Chapter 3 are provided in **Appendix B**.

3.B. Results and Discussion

Over 800 histopathologically confirmed mammary adenocarcinomas were obtained from the study reported in Chapter 2. To choose a subset of tumors for analysis, we used ΔS values (slope of the regression line) in **Figure 7** to identify matched pairs of N=20 each DR and DS tumors based on size and palpation date. These N=20 tumor pairs will be referred to as the full tumor set. Based on **Figure 7**, we know that DS tumors palpated on the same day as DR tumors are, on average, 1.82X larger. For DR and DS tumors palpated on the same day that fit within those size criteria, can we detect molecular mechanisms that provide an explanation for how DS tumors become larger than DR tumors?

3.B.1. Balance of proliferation and death: which process is winning?

Using high-powered fields collected from the full set of DR and DS H&E stained tumor sections, apoptotic and mitotic indices (expressed as # apoptotic bodies/ 100 cells and mitotic figures/ 100 cells, respectively) were determined. Under a negative binomial distribution, probability of a given cell undergoing mitosis trended towards being higher in DS tumors than in DR tumors (**Figure 8A**: DR 0.453 ± 0.030; DS 0.581 ± 0.057 mitotic figures per 100 cells; p=0.173).

Similarly, the probability of a given cell from DS tumors undergoing apoptosis was higher than in DR tumors (**Figure 8B**: DR 1.877 ± 0.192, N=20; DS 2.549 ± 0.252 apoptotic cells per 100 cells, N=20, p<0.01). While increased apoptotic index does not inform the larger tumor size observed in DS compared to DR rats, this finding is not wholly unexpected: in the Thompson-Strange equation, increased apoptosis (larger $-k_D$) is required to offset increased proliferation in the maintenance of tissue size homeostasis.

There was no difference in average cell number per field (**Figure 8C**), and by extension no difference in cell size between DR and DS tumors (DR 838.7 ± 19.1, N=20; DS 863.2 ± 15.3 cells per field).
When apoptotic indices, mitotic indices, and cell number per field for the full set of N=20 DR and DS tumors were regressed on the week in which they were first palpated, there was no difference between the slope of the line for DR and DS tumors for any of the 3 comparisons. However, interesting growth trends were revealed independent of DR/DS strain designation. Week 8 corresponds to newer tumors, first palpated only one week prior to the end of study. Week 5 corresponds to older tumors, first palpated a full month prior to the end of study.

As shown in **Figure 8D**, tumors that were palpated later in the study tended to have higher mitotic indices. The slope of the line shows a moderate positive association of mitotic index with time, with week 5 tumors having lower mitotic indices than week 8 tumors. To rephrase, older tumors show lower growth rates (k_P) than newer tumors.

Conversely, as shown in **Figure 8E**, apoptotic index tended to decrease slightly in tumors palpated earlier vs. tumors palpated later in the study. The slope of the line shows a weak inverse association of apoptotic index with time, with week 5 tumors having higher apoptotic indices than week 8 tumors. To rephrase, older tumors show slightly higher death rates (k_D) than newer tumors.
Finally, there was a decrease in cell number per field in tumors palpated later vs. tumors palpated earlier (**Figure 8F**). This suggests that as tumors become larger, cells become smaller, potentially due to the influence of limited space, oxygen, and nutrients (171).

These effects of tumor age on histological indices of apoptosis and mitosis may explain some of the heterogeneity apparent in **Figures 8A-C**, given that the full set of N=20 matched DR and DS tumor pairs

was comprised of tumors across a wide range of 'age'. Within the N=20 tumor pairs, 1 "old" tumor pair was palpated 5 weeks post-carcinogen; 5 tumor pairs were palpated 6 weeks post-carcinogen; 10 tumor pairs were palpated 7 weeks post-carcinogen; and 4 "new" tumor pairs were palpated 8 weeks post-carcinogen. However, if tumor pairs are limited to only those 10 from week 7, there is no difference between DR and DS mitotic index, apoptotic index, or cell number per field (data not shown). This suggests that factors in addition to chronological tumor age are influencing the growth rate of DS and DR tumors. Neither mitotic index nor apoptotic index was solely capable of explaining the "faster" tumor growth rate in DS tumors compared to DR from **Figure 7**. Therefore, we turned to immunohistochemistry as another way to assess tumor proliferation.

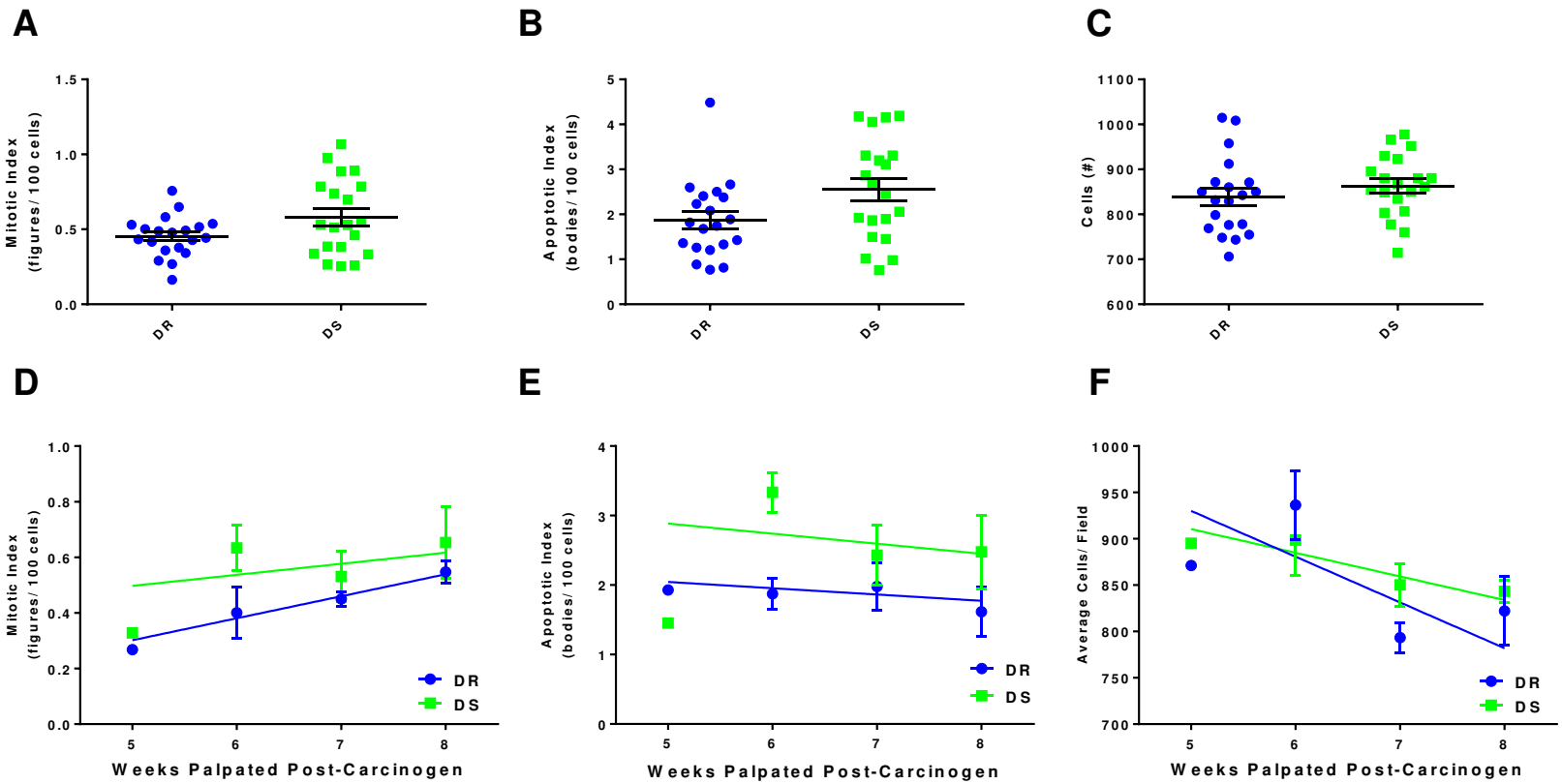

Figure 8

Legend. DS tumors display higher apoptotic and mitotic indices compared to DR tumors. Determination of cellular indices (cells per 100 cells) from N=20 each DR and DS H&E stained tumor sections as calculated under a negative binominal distribution. Mitotic index shown combined (Panel A) and regressed on weeks post carcinogen (WPC) (Panel D). Apoptotic index shown combined (Panel B) and regressed on WPC (Panel E). Combined cell counts (normal + mitotic + apoptotic) per field combined (Panel C) and regressed on WPC (Panel F). Values are means ± SEM.

3.B.2. Determination of proliferative fraction

The protein Ki67 was identified in 1991 by Gerdes *et al.* as a nuclear protein expressed in proliferating cells in all phases of the cell cycle (174). Whereas Ki67 is largely absent from quiescent cells, Ki67 is expressed at low levels in late G1 and S phases, at moderate levels in G2, and displays peak expression in M phase (174). Thus, Ki67 identifies the proliferating fraction of cells within a population. As shown in **Figure 9,** analysis of immunoreactive nuclear area revealed no difference in proliferating fraction of cells in the full subset of DS vs. DR tumors (DR N=20, 9.0% ± 0.7; DS N=20, 9.4% ± 0.9, *p*=0.41). This was unexpected, given the trend towards increased mitotic index in DS tumors. To determine the relationship between mitotic index and proliferative fraction within tumors, we developed a method to estimate cell cycle duration.

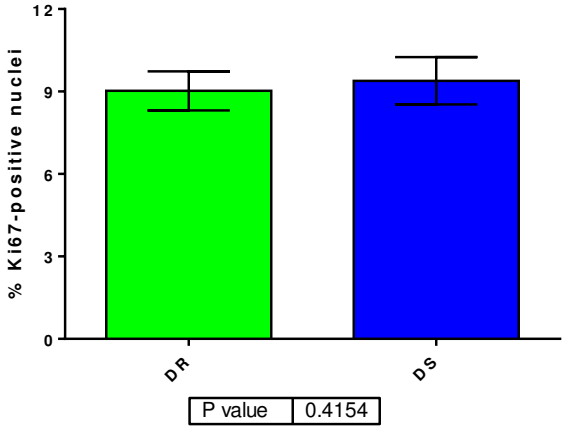

Figure 9
Legend. DS tumors do not display elevated Ki67 proliferative marker compared to DR tumors. Immunohistochemistry of proliferation marker Ki67 in full set of N=20 each DR and DS tumors. Values are means ± SEM expressed as % nuclei which express Ki67 by immunoreactivity.

3.B.3. Cell cycle duration is reduced in DS compared to DR tumors

In the average cell, cell cycle duration is estimated at 24 hours, with mitosis lasting approximately 1 hour (175). Ki67 % nuclear immunoreactivity represents the proliferating fraction of cells. In both DR and DS tumors, the majority of cells were negative for expression of nuclear Ki67, indicating that the proliferative fraction of these tumors corresponds to small percentage of cells. To determine if the observed mitotic index in DS and DR tumors was reasonable given the Ki67 proliferative fraction and an expected cell cycle duration of 24 hours, mitotic index of DR and DS tumors was predicted by dividing proliferative % of cells by expected cell cycle duration (24 hours) (175;176), as shown in **Equation 2**.

Equation 2

$$Predicted\ mitotic\ index\ (\%) = \frac{Proliferative\ fraction\ (\%)}{Cell\ cycle\ duration\ (h)}$$

Predicted mitotic index was then compared with the observed mitotic index, as shown in **Table 4**.

Table 4
Legend. Predicted mitotic index is based on **Equation 2**. Observed mitotic index was reported in **Figure 8A**. Values are means ± SEM.

	Predicted mitotic index: Average Ki67 % immunoreactivity ÷ 24 hours (estimated cell cycle duration)	**Predicted mitotic index**	**Observed mitotic index**
DR tumors (N=20)	9.0 ÷ 24	0.375	0.453 ± 0.030
DS tumors (N=20)	9.4 ÷ 24	0.392	0.581 ± 0.057

For both DR and DS tumors, observed mitotic index was higher than predicted. To rephrase, mitotic cells were observed more frequently than could be explained by the Ki67-expressing proliferative fraction and a 24-hour cell cycle duration. Therefore, cells must be progressing through the cell cycle more rapidly than every 24 hours. The equation can be rearranged as shown in **Equation 3** to solve for cell cycle duration:

Equation 3

$$Cell\ cycle\ duration\ (h) = \frac{Proliferative\ fraction\ (\%)}{Mitotic\ index\ (\%)}$$

As shown in **Figure 10**, cell cycle duration in both DR and DS proliferating tumor cells was less than 24 hours. Interestingly, cell cycle duration in proliferating DS tumor cells was approximately 3.5 hours shorter than in proliferating DR tumor cells (DR 21.2 ± 1.7 hrs; DS 17.7 ± 1.3 hrs; p=0.104). These data

suggest that DS tumor cells may be capable of progressing through the cell cycle at an accelerated rate compared to DR, providing additional support for the “faster” hypothesis.

Returning to the higher apoptotic index observed in DS vs. DR tumors, we performed a series of activity assays to determine whether apoptosis in MNU-induced tumors was due to intrinsic vs. extrinsic caspase activity.

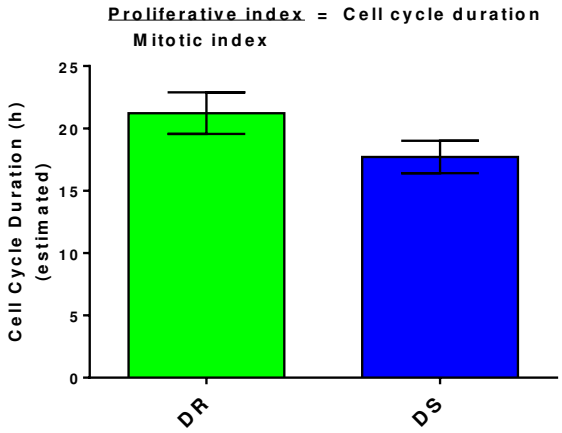

Figure 10
Legend: DS tumors display shortened estimated cell cycle duration compared to DR tumors. Estimated cell cycle duration in hours based on Ki67 proliferative index and mitotic index in full set of N=20 each DR and DS tumors.

3.B.4. Caspase activity does not differ between DR and DS tumors

Apoptosis refers to a morphologically distinct type of programmed cell death in which chromatin condenses and DNA fragments in internucleosomal regions. Apoptotic cells maintain an intact cell membrane that pinches off into “blebs” containing organelles and nuclear material, which are phagocytosed by surrounding cells (177-179).

The morphological changes associated with apoptosis are triggered through intrinsic and extrinsic caspase signaling pathways, which have been well characterized (i.e., (179-181)). The intrinsic pathway of caspase activation is induced via cytochrome c release from the mitochondria, resulting in activation of the initiator enzyme cysteinyl-aspartyl protease (caspase) 9. Caspase 9 cleaves components required for apoptosome formation and activates caspases 3, 6, and 7, known as the executioner caspases (182).

In the extrinsic pathway (also known as the death receptor pathway), apoptosis is induced via FAS ligand, TNF-related apoptosis inducing ligand (TRAIL), or TNF ligands binding to their receptors. This ligand-receptor interaction results in activation of initiator caspases 8 and 10 that activate the executioner caspases. Induction of the apoptotic cascade relies on proteolytic cleavage of caspase target proteins, so caspase activity is a good proxy to apoptotic activity within a tissue.

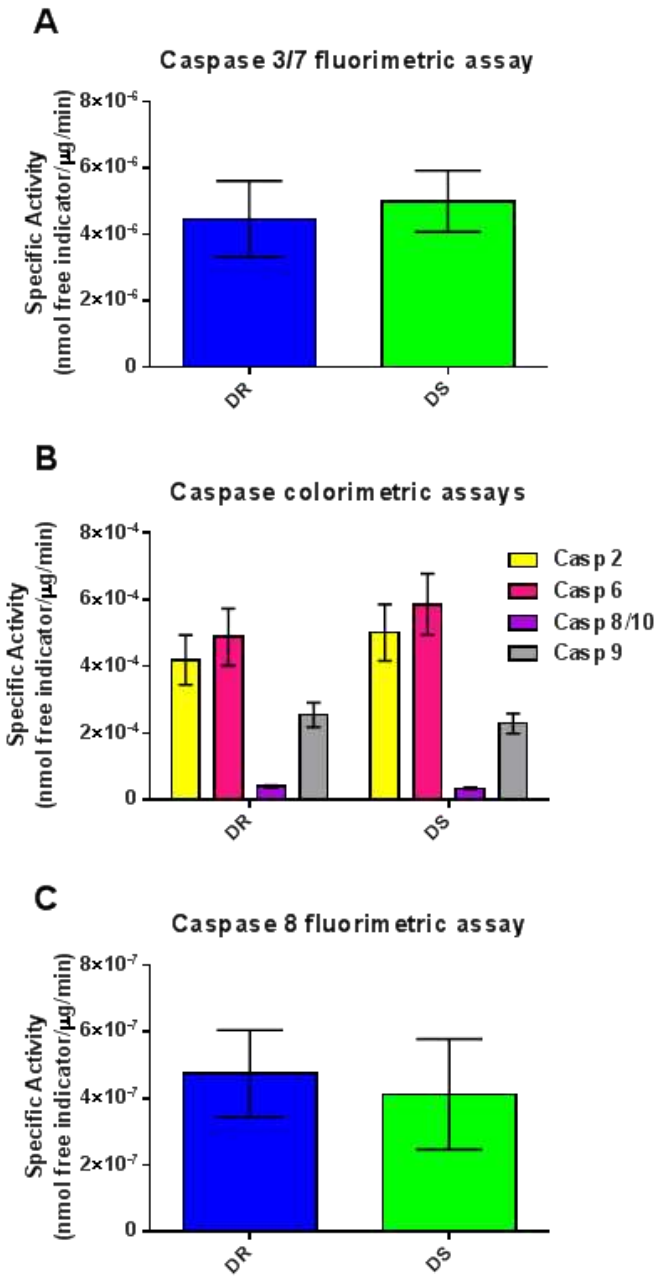

Figure 11
Legend: Caspase activity is similar between DR and DS tumors. Activity of caspases was determined in N=20 each DR and DS tumor lysate by assessing free fluorophore (panels A and C) or chromogen (panel B) release upon cleavage of the linked consensus peptide sequence of each caspase (**Appendix B**). Values are means ± SEM expressed as specific activity, nmol free indicator/µg protein/min.

To evaluate whether intrinsic vs. extrinsic pathways were responsible for initiating apoptosis in MNU-induced tumors, lysates from DR and DS tumors were evaluated for caspase activity using fluorimetric and colorimetric activity assays. As shown in **Figure 11A**, there was no difference in caspase 3/7 specific activity (reported as nmol fluorescent substrate released/µg protein/min) between DR and DS samples (DR 4.46 ± 1.45; DS 5.00 ± 9.19;

p=0.71). Activity of the other caspases was evaluated via colorimetric detection of free chromogen released in response to proteolytic cleavage of the caspase substrate (**Figure 11B**), or in the case of caspases 8/10, via detection of free fluorophore, due to low colorimetric signal production (**Figure 11C**). No differences between caspase activity in DR and DS tumors were detected by any method.

When caspase activity was assessed as a function of time, both DR and DS tumors showed a trend towards reduced caspase 3/7 activity in newer vs. older tumors. Interestingly, there was no trend associated with caspase 8 (extrinsic initiator caspase) or caspase 9 (intrinsic initiator caspase) activity over time (data not shown). To rephrase, apoptosis-initiating factors appear to be remaining relatively constant over time, yet executioner activity is reduced in newer compared to older tumors. Therefore, anti-apoptotic cues may be reduced as tumors continue to grow.

However, before investigating the relative abundance of molecular signals that may facilitate the observed effects on proliferation and apoptosis, we returned to the Thompson-Strange equation to evaluate whether our indices of proliferation and death could predict the faster growth rate observed in DS tumors.

3.B.5. Thompson-Strange equation revisited: *apoptotic duration may be longer in DS compared to DR*

Rates of proliferation (k_p) and death (k_D) can be split into terms of cell number (proliferation number = P_n; dead number = D_n) and process duration (proliferation duration = P_d; death duration = D_d). Rate of proliferation (k_p) was estimated using Ki67% immunoreactivity (P_n) ÷ estimated cell cycle duration (P_d).

To our knowledge, there is no direct relationship between caspase activity and apoptotic duration. Therefore, rate of death (k_D) was estimated using apoptotic index (D_n) ÷ 3h, which is the duration of

visible histological changes associated with apoptosis (D_d) (183;184). Change in tissue size (ΔS) is known, as final tumor mass, hours elapsed between palpation and study termination (weeks prior to end of study * 24 hours), and mass of a single cell ($1e^{-9}$ g as estimated by Steel), can be used to calculate cell gain/hour required to achieve the final tumor mass observed at study termination. N is unknown, so the Thompson-Strange equation can be arranged as shown in **Equation 4**:

Equation 4

$$N = \frac{\Delta S}{\left(\left(\frac{P_n}{P_d}\right) - \left(\frac{D_n}{D_d}\right)\right)}$$

Apoptotic and proliferative indices of each tumor were used to solve for N. Whereas average N (cell number) in DR tumors was negative, indicative of net cell loss, average N in DS tumors was positive, indicative of net cell gain (DR $-6.08e^6 \pm 4.57e^6$ cells/hour; DS $44.19e^6 \pm 11.80e^6$ cells/hour). The negative N value for DR tumors would indicate tumor shrinkage. In comparison, **Figure 7**, representing observed growth rates, indicated a 1.8-fold increase in DS vs. DR tumor growth rates. Using **Equation 4**, values for N indicate an 8.2-fold increase in DS compared to DR. Therefore, the Thompson-Strange approximation to tumor growth rates isn't telling the whole story.

What factors within the equation could be responsible for this disconnect? While 3 hours is a common estimate for apoptotic duration, this process can range from 2-24 hours depending on several factors. These factors can include cell type, method of inducing apoptosis, whether apoptosis was induced via extrinsic vs. intrinsic pathways, whether cells were evaluated *in vivo* vs. *in vitro*, and how apoptotic starting and stopping point are defined (i.e., cleavage of caspases vs. appearance of early morphological changes) (185;186).

To determine whether apoptotic duration may be influencing the disconnect between growth rates observed in **Figure 7** and the rates predicted by **Equation 4**, the Thompson-Strange equation can be rearranged yet again to solve for apoptotic duration (D_d). As an estimate for N in the rearranged equation, slopes from **Figure 7** were converted from g/week to cells gained/hour, resulting in N=3172619 cells gained/hour in DR tumors (slope of 0.5333 g/week) and N=5760714 cells gained/hour in DS tumors (0.9678 g/week):

Equation 5

$$D_d = \frac{D_n}{\left(\left(\frac{P_n}{P_d}\right) - \left(\frac{\Delta S}{N}\right)\right)}$$

Solving for D_d of each tumor, apoptotic duration ranged from 1 hour to 15 hours, and trended towards being longer for DS vs. DR apoptotic cells (DR 4.7 ± 0.6 hrs; DS 5.9 ± 1.0 hrs; *p*=0.306), though this did not reach statistical significance. To state this in another way, if 1% of cells in a DR tumor undergo apoptosis in 4.7 hours, 5.1% of DR cells will undergo apoptosis within a 24-hour period. Contrary to what the apoptotic index suggests, it appears that fewer cells in DS tumors may actually be undergoing apoptosis compared to DR tumors. DS cells display a trend towards taking longer to complete the apoptotic process, so the morphological changes associated with apoptosis may persist longer than in DR, causing the apoptotic index to be artificially inflated in DS vs. DR tumors.

When the revised apoptotic duration (D_d) values were entered into the Thompson-Strange equation to solve for N, both DR and DS tumors display positive values for N, indicating net cell gain (DR $6.30e^{12}$ ± $3.77e^{12}$ cells/hour; DS $19.94e^{13}$ ± $12.85e^{13}$). The magnitude of these values still indicate a disconnect in the model, as $1e^{13}$ cells/hour corresponds to about 10 kg per hour gain in tumor mass. However, these estimates come much closer to modeling the observed relationship between DR and DS tumor growth

rates. Growth rates for DS compared to DR tumors by the Thompson-Strange equation was a 3.2-fold increase, compared to the 1.8-fold increase in slopes of DR and DS tumor growth as reported in **Figure 7**. These data suggest that DS tumors have faster growth rates than DR tumors.

3.B.6. Unmasking effects by considering tumor heterogeneity

Within the full set of N=20 each DR and DS tumors, there is considerable heterogeneity in the indices of proliferation and apoptosis and the estimated duration of these events. By using growth kinetics to model tumor growth curves, Steel concluded that most tumors do not have a single growth rate, and rather that growth rate varies continuously with tumor age (171). In particular, experimental tumors have been demonstrated to grow more slowly as they approach V_{max}, due to limitations in blood supply, nutrient availability and accessibility, and accumulated cytotoxic products of necrosis (171). Steel reports that it is not uncommon for the volume doubling time of a tumor to increase 10-fold (i.e. slow down by a factor of 10) during the period of macroscopic growth. Steel's postulates are supported by the apoptotic and mitotic index data shown in **Figure 8**. Specifically, older tumors tend to have higher apoptosis and lower mitosis than newer tumors.

We propose going one step further, and suggest that biological tumor age, in addition to chronological tumor age, should be considered when evaluating the balance of proliferation and apoptosis. The other side of that coin, however, is that because DS stopwatches "tick" faster than DR stopwatches, DS tumors are theoretically always closer to V_{max} at study termination than DR tumors palpated on the same day.

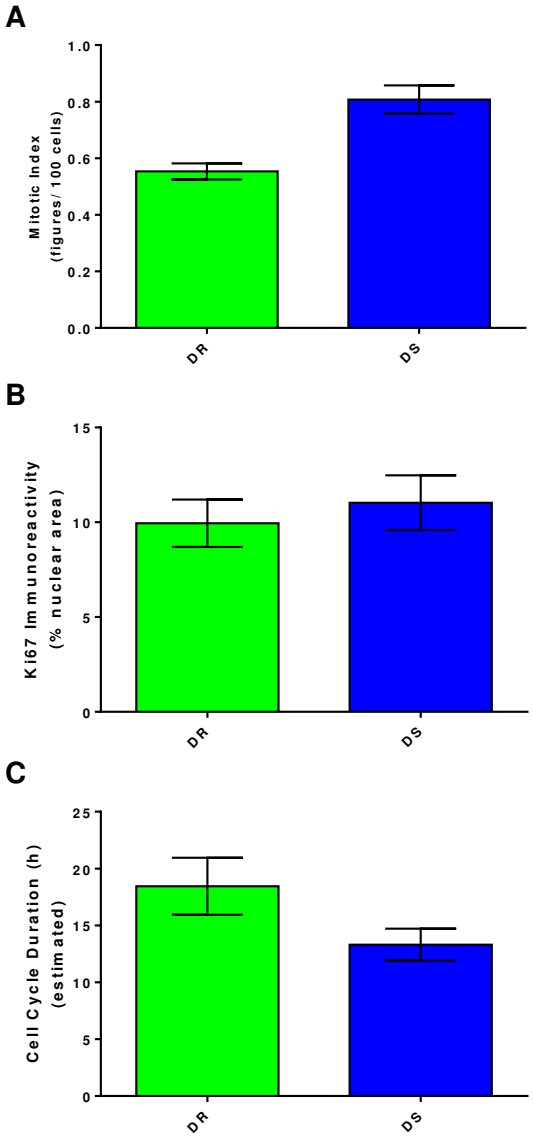

Figure 12
Legend. DS tumors within the high mitotic index subset of display evidence of accelerated growth characteristics compared to DR tumors. High mitotic index: N=9 each DR and DS tumors. Panel A) mitotic index based on H&E stained tumor sections. Panel B) Ki67% nuclear immunoreactivity via immunohistochemistry. Panel C) estimated cell cycle duration based on mitotic index and Ki67% reactivity.

In an effort to match tumors more closely by biological age, the full set of N=20 each DR and DS tumors were separately ranked by mitotic index. Nine tumors each DR and DS with highest mitotic index, called the high mitotic index tumor subset, were then used for further analysis. As shown in **Figure 12A**, mitotic index was higher in DS vs. DR tumors within the high mitotic index tumor subset (DR 0.553 ± 0.029; DS 0.807 ± 0.050; p<0.001). Ki67 % nuclear reactivity was increased, though this did not reach statistical significance (**Figure 12B:** DR 9.9 ± 1.2%; DS 11.0 ± 1.4%; p=0.578). Estimated cell cycle duration was shorter for both DR and DS tumors in the high mitotic index tumor subset (**Figure 12C)** (DR 18.4 ± 2.5 hrs; DS 13.3 ± 1.4 hrs; p=0.093). Apoptotic index was not different between DR and DS tumors from the high mitotic index subset (DR 2.0 ± 1.1; DS 1.3 ± 0.4 apoptotic cells/100 cells;

p=0.338). Together, these data suggest that within the high mitotic index tumor subset, there is evidence of DS tumors growing at a faster rate than DR tumors.

The growth characteristics of tumors reported in sections 3.B.1-3.B.5 revealed that the full set of N=20 each DR and DS tumors had a high degree of heterogeneity, which frequently translated into failure to reach statistical significance at the level of α=.05. While this heterogeneity was improved by use of the high mitotic index tumor subset, significant heterogeneity remained within groups of DR and DS tumors. Many interesting trends were observed between DR and DS tumors; however, the high *p*-values associated with several of these findings indicate that the potential for drawing a false conclusion is substantial. Therefore, we set out to validate these trends by identifying molecular machinery that could elicit the observed effects.

3.B.7. DS rats display hyperphosphorylation of the retinoblastoma restriction checkpoint protein

Most variability in cell cycle duration is due to varying lengths of G0 and G1 phases, whereas duration of S, G2, and mitosis are all relatively constant (175;187). The G1/S restriction checkpoint machinery is the gateway to S-phase. Upon hyperphosphorylation of the retinoblastoma (Rb) protein at serines 807 and 811 by cyclin dependent kinases (cdks) 2 and 4, pRb changes conformation and dissociates from the E2F1 transcription factor, which is then free to stimulate transcription of factors required for DNA synthesis in S phase (175).

Given the shorter cell cycle duration observed in proliferating DS tumor cells, we evaluated expression of proteins that regulate the transition from G1 into S phase. Expression levels of the majority of G1/S restriction checkpoint proteins, including p27, cdk2, cdk4, and cyclin D1 did not differ (**Figure 13A**). In DS tumors compared to DR tumors, a trend towards reduced expression of the anti-proliferation protein p21 with concomitant trends towards increased expression of pro-proliferation proteins cyclin E and E2F1 was observed.

While DS tumors displayed little to no evidence of increased cyclin/cdk expression, DS tumors displayed evidence of increased cyclin/cdk complex activity based on their physiological role in the G1/S checkpoint, which is to phosphorylate Rb. Tumors from DS rats displayed a significantly higher ratio of phosphorylated Rb to total Rb compared to DR rats (**Figure 13B**). In support of the hyperphosphorylated state of Rb, immunoprecipitation of lysate with antibodies against E2F1 revealed a

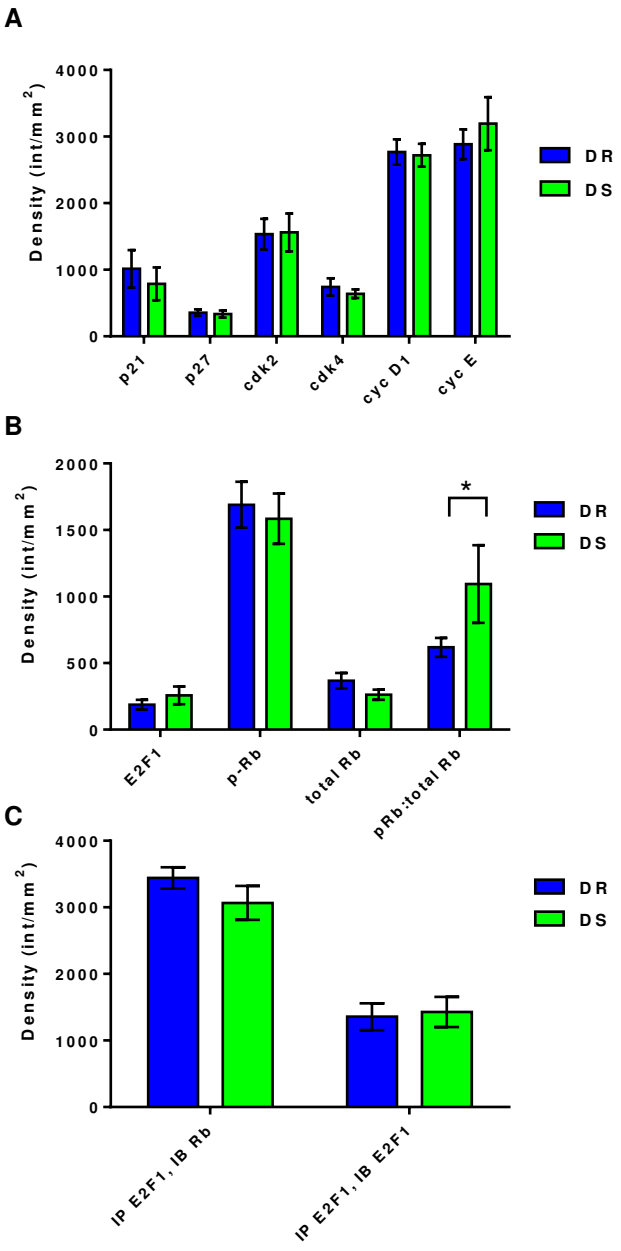

Figure 13
Legend. DS rats display hyperphosphorylation of the Rb protein. Lysate from N=9 each high mitotic subset DR and DS tumors were evaluated for expression of G1/S restriction checkpoint proteins. Panels A and B) Densitometry of proteins separated by SDS-PAGE and detected via Western blot. Panel C) lysate was immunoprecipitated with E2F1 then assessed for expression of Rb or E2F1. Values are mean density ÷ mm^2 ± SEM, normalized to GAPDH expression.

trend towards reduced Rb in the complex (**Figure 13C**), which is expected, as inactivated Rb is incapable of forming a complex with E2F1. These data support a role for reduced Rb function in DS tumors.

Protein expression data in **Figure 13** suggests that cyclin/cdk complexes in DS tumors maintain hyperphosphorylation of Rb. In this scenario, E2F1 is free to exert transcriptional control over a number of proteins. The classical role for E2F1 is to induce transcription of genes involved in the progression to S phase. As an indicator of E2F1 activity, expression of the S phase protein cdc6, whose promoter contains an E2F-binding site (188), was increased in DS tumors compared to DR tumors (**Figure 14**). These data suggest that proliferating cells in DS tumors have fewer obstacles (such as bound/inactive E2F1) at the transition from G1 to S phase and so demonstrate faster cell cycle transit. This protein expression data provides a biologically plausible mechanism behind the reduced cell cycle duration in DS tumors.

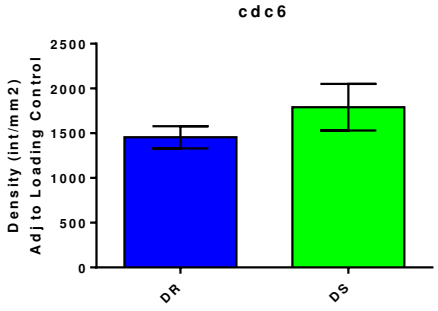

Figure 14
Legend. DS rats display increased expression of E2F1 target protein cdc6. Lysate from N=9 each high mitotic subset DR and DS tumors were evaluated for expression of cdc6 via Western blot. Values are mean density ÷ mm^2 ± SEM, normalized to GAPDH expression.

Interestingly, E2F1 can stimulate proliferation as well as apoptosis, depending on energy state. In a 2008 study published in Cancer Cell, Hallstrom *et al.* reported that E2F1 can induce distinct gene expression programs that correspond to proliferation or apoptosis in rat fibroblasts (189). When fibroblasts are serum-starved ("fasted"), the apoptotic gene expression program dominates. In contrast, when fibroblasts are provided with serum ("fed"), the proliferative gene expression program dominates at the expense of apoptotic signaling (189). This effect of serum on E2F1-induced gene expression programs was found to be dependent on activation of the PI3K/Akt signaling pathway.

Moreover, the apoptotic and proliferative gene expression programs induced by E2F1 appear to be mutually exclusive. Within the Hallstrom study, breast and ovarian tumors with high PI3K activity display the E2F1-induced proliferative gene expression signature. Conversely, tumors with low PI3K activity display the E2F1-induced apoptotic gene expression signature. The E2F1-induced proliferative gene expression signature was associated with advanced tumor stage at diagnosis, reduced survival, and increased risk of recurrence (189). This finding of Hallstrom *et al.* has important implications for obesity, as the PI3K/Akt pathway is downstream of insulin signaling, which is commonly found to be deregulated in obesity.

In the current study, this finding can be interpreted to suggest that in the chronic positive energy balance state of DS rats, the proliferative gene expression program is being induced by E2F1, due to the lack of repression of E2F1 by Rb hyperphosphorylation.

3.B.8. DS rats display increased expression of pro-apoptotic markers

To evaluate whether the E2F1-induced apoptotic gene expression program was active in DS tumors, we evaluated expression of several pro- and anti-apoptotic proteins via capillary electrophoresis as an alternative to traditional Western blot. Pro-apoptotic effects of E2F1 are exerted by binding to promoters of pro-apoptotic proteins,

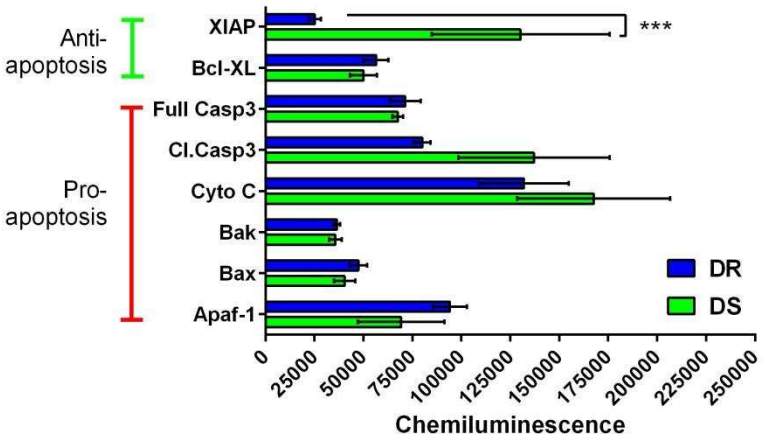

Figure 15
Legend. DS tumors display increased expression of X-linked inducer of apoptosis protein (XIAP) and trend towards increased cleaved caspase 3 and cytochrome c. Expression of apoptotic proteins was evaluated in N=9 tumors each DR and DS from the high mitotic tumor subset. Expression was detection using capillary electrophoresis-based Western blot technology. Values are mean chemiluminescence ± SEM, normalized to GAPDH. ***=p<0.001.

including Apaf-1 and Bak (reviewed in (190)). DR and DS tumors displayed similar expression levels of Apaf-1 and Bak, suggesting that the pro-apoptotic gene expression program of E2F1 was not activated. These data are in agreement with the clinical data reported by Hallstrom *et al.*, which reported that activation of proliferative and apoptotic gene expression programs of E2F1 in breast and ovarian tumors are mutually exclusive (189).

DS tumors displayed a trend towards higher cleaved caspase 3 (executioner caspase) and higher cytochrome c expression levels, though these data did not reach statistical significance. However, DS tumors displayed more than 5X the expression level of anti-apoptotic protein X-linked inhibitor of apoptosis (XIAP) compared to DR tumors. This markedly increased expression of XIAP may facilitate the longer estimated apoptotic duration in DS tumors, as XIAP has been found to bind to cleaved caspase fragments and interfere with downstream induction of the morphological changes associated with apoptosis (195). Therefore, higher levels of pro-apoptotic stimuli, such as cytochrome c and cleaved caspase 3, are required to induce apoptosis in DS tumors.

This data can be considered in terms of the stopwatch analogy. If DS stopwatches are ticking faster than DR stopwatches, DS tumors will always be closer to V_{max} than DR tumors despite being palpated on the same day. To rephrase, DS tumors evaluated in these experiments are biologically older and closer to V_{max} than DR tumors, despite tumor pairs being matched for chronological age. This phenomenon of biological differences in age, despite similar chronological age, may explain why apoptotic duration is longer in DS tumors. Recently, Ueno *et al.* reported that serum levels of pro-apoptotic proteins soluble Fas ligand (FasL) and cytochrome c decrease as a function of patient age and breast cancer stage (191). Thus, higher pro-apoptotic signals may be required to initiate apoptosis in DS tumors.

All the growth characteristics of DR and DS tumors, while presented individually, are interrelated at a cellular level. In order to simultaneously evaluate the relationship between characteristics of proliferation and death on tumor mass and cell cycle duration, all variables were imported into the Simca-P+ multivariate data analysis program.

3.B.9. Multivariate analysis of tumor growth characteristics

In multiple regression analysis, co-linearity between X variables can lead to poor prediction of Y response variables (192). Partial least squares projections to latent structures (PLS) analysis is a method used to visualize the effect of noisy, interrelated X predictor variables on Y response variables (reviewed in (193)). PLS analysis takes a set of X predictor variables and creates new X variables, called components, as linear representations of the old X variables, based on their distribution in the model space and weights of the X variables (194). In the current study, N=33 X variables (including count data, immunohistochemistry data, and protein expression data) were used to separately model N=2 Y variables (tumor mass and cell cycle duration).

One component was fit for each PLS model. Principal components in well-fitted models ideally explain the majority of the variance in X and Y. For the PLS model constructed wherein Y=tumor mass, this component explained 49.0% of the variance in X (tumor growth characteristics), 19.7% of the variance in Y (tumor mass), and is estimated to correctly predict tumor mass of 4.8% samples based on 7-fold cross validation using the leave-one-out approach. Coefficients of the X variables represent the strength of their correlation with Y variables. Specifically, whereas large negative values have strong inverse associations with Y, large positive values have strong positive associations with Y. Coefficients for the interaction of each X variable in the first (only) component is shown for tumor mass (**Figure 16A**) and cell cycle duration (**Figure 16B**).

The three X variables with strongest positive correlation with tumor mass (i.e., increased in larger tumors) were cleaved caspase 3, cytochrome c, and anti-apoptotic protein XIAP (**Figure 16A**). This data informs the confusion reported in previous sections. By rearranging the Thompson Strange equation, we demonstrated that DS tumors have a trend towards longer apoptotic duration; however, there was no difference in caspase activity between DR and DS. This co-association of XIAP and cleaved caspase 3 with larger tumor mass suggests that XIAP may interfere with caspase activity in larger tumors.

Cdc6 and immunoprecipitated E2F1 were positively correlated with tumor mass (**Figure 16A**). However, the magnitude of this correlation was much smaller than that observed with apoptotic proteins. Conversely, the three X variables with strongest inverse correlation with tumor mass (i.e., decrease in larger tumors) were pro-apoptotic proteins Apaf-1, Bax, and cdk2. Cdk2 and cyclin E were inversely correlated with tumor mass, as was immunoprecipitated Rb. This suggests that whereas expression levels of cdk2 and cyclin E do not increase with tumor mass, activity of this cdk/cyclin complex (which phosphorylates and inactivates Rb) may increase in larger tumors, as evidenced by the pro-proliferative alterations in the Rb/E2F1 restriction machinery.

For the PLS model constructed wherein Y=estimated cell cycle duration, the first (only) component explained 48.8% of the variance in X (tumor growth characteristics), 5.4% of the variance in Y (tumor mass), and is estimated to predict estimated cell cycle duration for 0% of samples based on 7-fold cross validation using the leave-one-out approach. The coefficients for the PLS for cell cycle duration, shown in **Figure 16B**, revealed that the same X variables correlated with tumor mass were also most inversely correlated with cell cycle duration. Specifically, the three variables with strongest positive correlation with cell cycle duration (i.e., increased with longer cell cycle duration) were Bax, total caspase 3, and

Apaf-1. The three variables with strongest inverse correlation with cell cycle duration (i.e., decrease with longer cell cycle duration) were cleaved caspase 3, cytochrome c, and XIAP.

These data demonstrate the benefit of using multivariate analysis to look at interrelationships of biologically related variables. Whereas apoptosis markers on their own seemed fairly uninformative in explaining the larger tumor size observed in DS rats, PLS analysis paints a picture wherein changes in apoptosis may enable the changes in proliferative processes. Changes in frequency and duration of apoptosis in DS tumors are correlated with tumor characteristics including tumor mass and cell cycle duration. However, there was no correlation between proliferative markers and tumor mass or cell cycle duration. This suggests that changes in apoptosis may represent the early events in DS tumors that enable the faster growth rate, reduced cell cycle duration, and ultimately larger tumor size.

Tumor mass represents the functional outcome of the balance achieved between proliferative and apoptotic processes. This may explain why tumor growth characteristics are more strongly correlated with tumor mass at end of study than with estimated cell cycle duration—accelerated cell cycle transit may indeed be occurring in DS tumors, but proliferation represents only one side of the Thompson-Strange equation. These data suggest that the balance between pro-apoptotic and anti-apoptotic signals, particularly those mediated via XIAP and other inhibitor of apoptosis (IAP) family members, may be important factors to consider during future investigations of mechanisms that drive DS tumor growth.

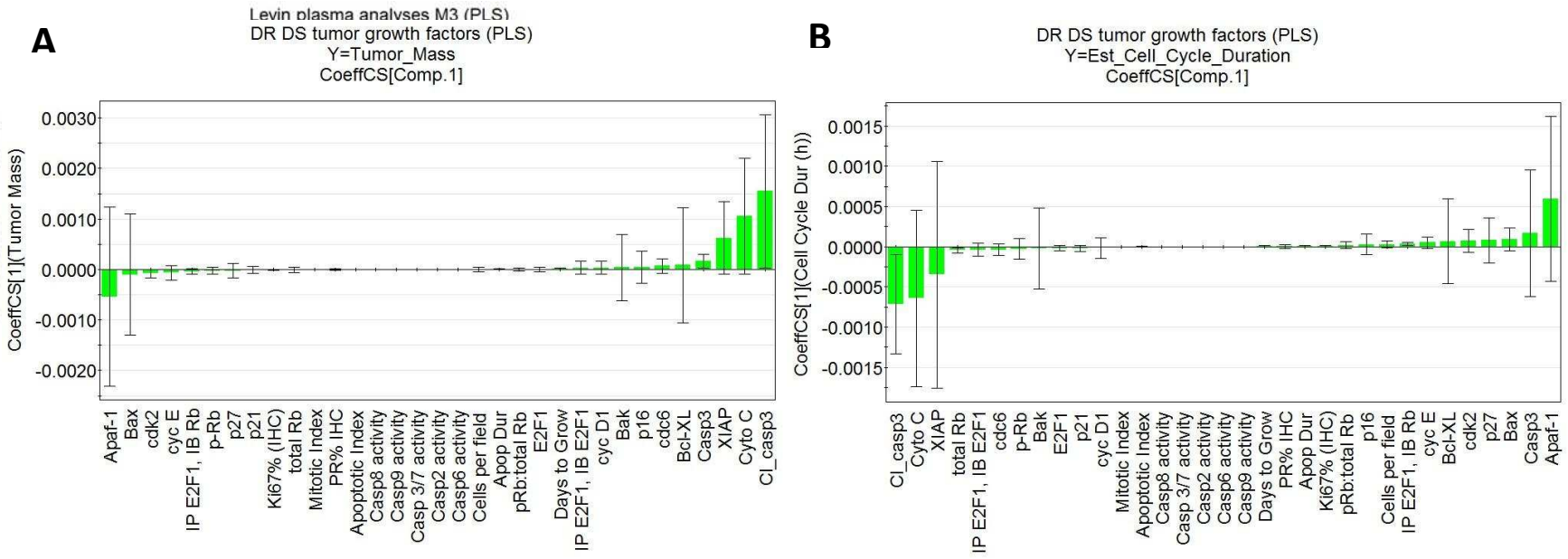

Figure 16

Legend. Apoptotic markers display stronger correlation with tumor growth characteristics than do proliferative markers. Partial least squares projections to latest structures (PLS) analysis of DR and DS tumor growth characteristics. Coefficients for the interaction of DR X variables in the first component are shown for tumor mass (Panel A) and cell cycle duration (Panel B). Coefficients are shown with jack-knifed 95% confidence intervals.

3.C. Conclusions and Future Direction

In Chapter 2, an accelerated cancer response to a chemical carcinogen was detected in obese DS vs. lean DR rats. This accelerated cancer response was particularly evident in the 5.4-fold increase in tumor burden observed in DS compared to DR rats. Given a previous report suggesting that obesity disrupts the balance of proliferation and apoptotic processes in breast tumors from obese women and mice, we set out in the current chapter to evaluate the balance between these processes.

Relative to proliferation, DS tumors displayed a trend towards increased mitotic index, which was found to be attributable to reduced estimated cell cycle duration. Relative to molecular machinery that enables this accelerated cell cycle transit, DS tumors displayed hyperphosphorylation of the Rb protein, reduced interaction of Rb with E2F1, and loss of repression of E2F1. This cumulative effect of increased E2F1 transcriptional activity was manifested as increased expression of the S phase protein cdc6 in DS tumors. As most variability in cell cycle duration is due to length of G0 and G1, our findings of alterations in G1/S restriction checkpoint machinery are consist with cells in DS tumors being able to transition through the cell cycle more rapidly.

Increased apoptotic index was found in DS compared to DR tumors, a biological process that seemed to be a counter-measure to the accelerated proliferation in DS tumors. However, no difference in caspase activity was observed between DR and DS tumors, leaving us unable to explain how the increased apoptotic index was accomplished. A trend towards increased cytochrome c and cleaved caspase 3 was found in DS compared to DR tumors, which again appeared consistent with the increased apoptotic index. However, DS tumors displayed a 5-fold increase in expression of anti-apoptotic protein XIAP. Furthermore, when all tumor data were evaluated using multivariate analysis, the evidence was consistent with a dominant effect of apoptosis with XIAP being implicated as playing a dominant role in

the balance between proliferation and death. Together, this data suggests that reduced apoptotic efficiency, wherein XIAP binds and sequesters caspase fragments, may be early events in DS rat carcinogenesis, which create a permissive environment for the observed alterations in G1/S restriction checkpoint machinery. In summary, these experiments provided several pieces of evidence that suggest the faster tumor growth rate (1.8 fold) of DS tumors may be attributable to accelerated cell cycle transit and reduced apoptotic efficiency.

Whereas the current chapter (Chapter 3) sought to identify mechanisms behind the accelerated cancer burden in DS compared to DR rats reported in Chapter 2, Chapter 3 did not address an important finding of Chapter 2. In Chapter 2, DS rats displayed a trend towards reduced hormone receptor expression in tumors compared to DR rats. This is a molecular subtype of breast cancer associated with poor prognosis. To further examine this finding, we next performed a classical endocrine ablation experiment. Ovariectomy removes ovarian-derived sex hormones from circulation and elicits strong selection pressure on expansion of cancerous cells that can grow under low estrogen conditions. The effect of obesity on the growth of these largely hormone-receptor independent tumors, as well as whether obesity increases peripheral production of estrogens, is reported in Chapter 4.

CHAPTER 4: PERIPHERAL PRODUCTION OF ESTROGEN IS AN UNLIKELY MECHANISM WHEREBY OBESITY IMPACTS MAMMARY CARCINOGENESIS[4]

4.A. Rationale

In 1896, Beatson provided the first definitive evidence for a role of estrogen signaling in breast carcinogenesis, when ovarian removal (known as ovariectomy or oophorectomy) was used to successfully treat advanced breast cancer in young women (reviewed in (196)). In 1966, the Nobel Prize in Physiology and Medicine was awarded to Charles Huggins as a result of his ground-breaking research on the induction of regression in breast and prostate cancers following sex hormone withdrawal (197). These events mark the beginning of a long history of targeting estrogen signaling in breast cancer.

4.A.1. Targeting estrogen in breast cancer

Given estrogen's mitogenic function in stimulating cell proliferation, targeting estrogen signaling is one of the most commonly employed therapeutic strategies against breast cancer. This targeting can include disruption of estrogen signal transduction, such as with tamoxifen, which is a selective estrogen receptor modulator (SERM). Targeting estrogen signaling can also be accomplished by disrupting production of estrogen. The gene *cyp19a1* encodes the protein aromatase, which catalyzes the rate limiting step in the synthesis of estradiol (E2), the most bioactive estrogen compound, from testosterone (198). Aromatase inhibitors are often used in cancer treatment regimens for hormone-receptor positive breast cancers.

[4]Chapters 4 and 5 are being combined in a manuscript to be submitted to the journal *Cancer Prevention Research*. Any changes between the version presented herein and that which is published will be minor. Such changes will likely be due to publishing requirements and tone differences between target audiences.

4.A.2. Mitogenic effects of estrogen signaling

Estrogen and its metabolites influence the programming of initiated cells' stopwatches via classical receptor-mediated and non-classical mechanisms. ER is comprised of two isoforms with high structural similarity. Whereas the role of ERα is well characterized, ERβ may have opposing roles to ERα, including suppression of proliferation, and more studies are needed to elucidate the role of ERβ on breast cancer risk (199).

To summarize several excellent reviews (i.e., (200-209)), in the canonical estrogen signaling pathway, estrogen or its metabolites bind to and activate ERs at the nuclear membrane, the plasma membrane, or the mitochondrial membrane. Activated ERs dimerize and bind DNA at estrogen response element (ERE) sites to influence transcription. Genomic targets of estrogen signaling with EREs include the progesterone receptor, pro-angiogenic protein vascular endothelial growth factor (VEGF), transforming growth factor (TGF)-α, and receptor binding cancer antigen (RCAS)-1, which is expressed by most breast cancers, and is associated with poor prognosis.

ER exerts transcriptional control on genes lacking full EREs via interaction with coactivators including SP-1, activation transcription factor (ATF)-2, cyclic AMP response element binding protein (CREB), and activator protein (AP)-1 (203). These ER/coactivator complexes stimulate transcription in a number of genes with implications in breast cancer, including the protooncogenes c-*jun* and c-*fos*; pro-proliferation genes including c-*myc*, cyclin D1 and E2F1 with repression of cdk inhibitor p21; and anti-apoptosis genes including Bcl-2 and Bcl-XL. Mitochondrial estrogen signaling induces transcription of mitochondrial DNA-encoded genes with EREs, including components of the electron transport chain such as cytochrome c oxidase subunits I and III, and TCA cycle enzymes including aconitase, pyruvate dehydrogenase, and

malate dehydrogenase. Activated ER can also exert non-canonical effects including induction of second messenger signaling such as cyclic adenosine monophosphate (cAMP).

4.A.3. Targeting estrogen signaling in preclinical models

Whereas hormone expression in mice can be controlled by knocking in or out a gene of interest, this technology is premature in rat models. Rather, rat models employ ablation studies, in which ablation of hormone production is achieved through surgery, chemical agents, or with targeted radiation. In the case of breast cancer, removing the ovaries through bilateral ovariectomy eliminates the primary source of sex hormones, including estrogen and progesterone.

Ovarian ablation creates a negative selection pressure environment, which selects for expansion of a population of cells that can grow in very low levels of estrogen. Tumors eventually develop in ovariectomized animals, albeit with delayed latency compared to ovary intact animals. Importantly, tumors that develop in ovariectomized rats are predominantly ER/PR-, allowing researchers to study a molecular subtype of breast cancer with poor clinical prognosis.

4.A.4. Study goals

We used a classical ovarian ablation approach to create an environment in which to evaluate two specific questions. First, does obesity in DS rats stimulate growth of hormone receptor negative mammary carcinomas in the absence of ovarian function, when estrogen signaling is substantially reduced? To rephrase, does the cancer-promoting effect of obesity in DS rats, which was reported in Chapter 2, persist in the absence of high circulating levels of estrogen?

Secondly, do DS rats display evidence of elevated peripheral (mammary gland) production of E2 in the rat mammary gland? One of the primary hypotheses proposed to explain how obesity may increase risk of postmenopausal breast cancer centers on extragonadal production of estrogen by fat tissue. Fat tissue can express aromatase, and extragonadal production of estrogen as a result of aromatase activity within fat tissue is one of the four major proposed mechanisms whereby obesity increases breast cancer risk. However, it is unknown whether this mechanism exists in rats to the extent that could exert biological effects on mammary carcinogenesis.

Materials and methods for the experiments described in Chapter 4 are provided in **Appendix C**.

4.B. Results and Discussion

Design of the ovariectomy manipulation experiment is depicted in **Figure 17**, and was comprised of N=74 ovariectomized diet-induced obesity susceptible (DS-OVX) and N=36 ovariectomized diet-induced obesity resistant (DR-OVX) rats. Female rats were fed the purified SUMO32 diet ad libitum throughout the study, and bilateral ovariectomy was performed on all rats at 49 days of age.

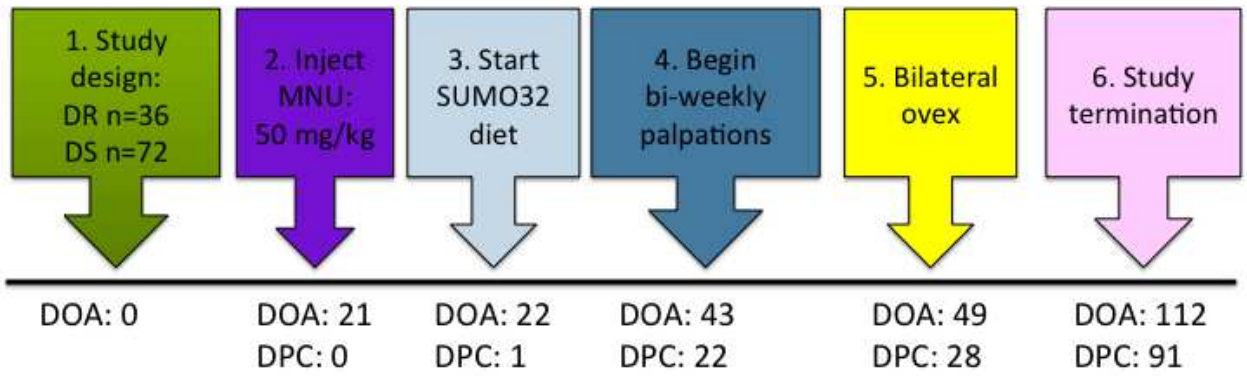

Figure 17
Legend. Study design for assessing the impact of ovarian ablation on mammary carcinogenesis. DOA= days of age; DPC= days post-carcinogen injection.

4.B.1. DS-OVX rats gain significantly more weight than DR-OVX rats within collective ovariectomy-induced stimulation of weight gain

Final average body weight was significantly different between DR and DS (**Figure 18A:** DR-OVX 294.2 ± 24.7 g, DS-OVX 333.5 ± 30.3 g, $p<0.001$), a difference of approximately 13% across the study duration. This 13% difference in final body weights at 4 months of age (study termination in current ovariectomy study) was similar to the 15% difference observed between DR and DS rats at 3 months of age (ovary intact study reported in Chapter 2).

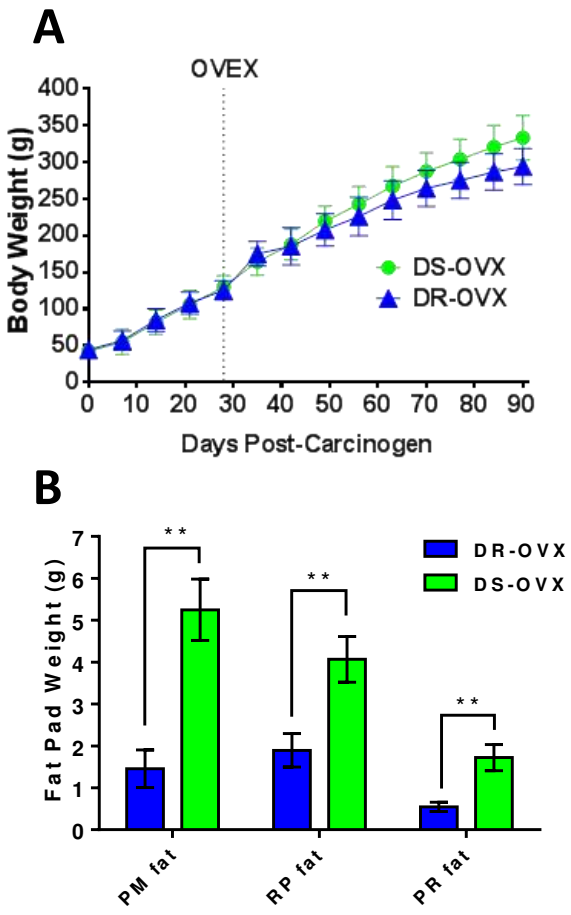

Figure 18
Legend. DS-OVX rats are obese compared to DR-OVX rats. Panel A) DS-OVX rats gain weight at an accelerated rate compared to DR-OVX. Rats (DR-OVX N=36, DS-OVX N=74), were weighed weekly while on study; data, mean ± SD. Weight gain trend was analyzed with nonlinear regression, $p<0.001$. Panel B) DS-OVX rats have larger perimesenteric (PM), retroperitoneal (RP), and perirenal (PR) fat pad stores at end of study. Values are mean ± SEM. **= $p<0.01$ by two-sided Student's t-test with false discovery rate=1%.

Whereas we might have expected a larger difference between DR and DS body weights in older rats, multiple studies describe the phenomenon wherein animals are predisposed to weight gain in the first 3-5 weeks post-ovariectomy due to a combination of hyperphagia and increased energy efficiency (210;211). Therefore, all rats, including DR, gain weight post-ovariectomy, resulting in narrowing of the gap between DR and DS weights.

The initial cancer study in this rat model, which was reported in Chapter 2, used body weight and leptin levels as indirect proxies to rat obesity. To confirm Levin's reports that the DS-OVX were in fact obese,

and not just larger, compared to DR-OVX rats, we excised fat pads from perimesenteric (PM), retroperitoneal (RP), and perirenal (PR) adipose tissue depots from N=6 each DR-OVX and DR-OVX rats. As depicted in **Figure 18B**, all fat pads were significantly heavier in DS-OVX compared to DR-OVX (p<0.01 for all analyses).

4.B.2. DS-OVX rats maintain increased cancer response in the absence of high circulating estrogen

Cancer was initiated in rats using the rapid emergence model of mammary carcinogenesis developed by our laboratory. Cancer outcomes are depicted in **Figure 19A-D** and differences between DR-OVX and DS-OVX are quantified in **Figure 19E**. Compared to ovary intact rats as reported in Chapter 2, the overall carcinogenic response was blunted in ovariectomized rats.

As shown in **Figure 19A**, cancer-free survival was initially reduced in DS-OVX compared to DR-OVX rats at early palpation points but this effect was lost as the study progressed. Cancer incidence was similar between DR-OVX (61.1%) and DS-OVX (64.9%), (**Figure 19B**). In Chapter 2, DS rats had 91% incidence vs. 65% incidence in DR rats. To rephrase, 9% of ovary intact DS rats were tumor free at study termination, compared to 35% of ovary intact DR rats. In the ovariectomy manipulation, a similar percentage (35-40%) of both DR-OVX and DS-OVX rats were tumor-free at the end of the study. However, rats that were tumor free at study termination may have developed tumors at a later point if the study was allowed to progress.

Significantly higher multiplicity (**Figure 19C**) and burden (**Figure 19D**) were observed in DS-OVX compared to DR-OVX (p<0.01 for both analyses). A 1.7-fold increase in cancer multiplicity was observed in DS-OVX vs. DR-OVX rats, in comparison to the 2.5-fold increase in cancer multiplicity observed in ovary intact DS vs. DR rats. Cancer burden was increased 2.6-fold in DS-OVX compared to DR-OVX rats,

in comparison to the 5.4-fold increase observed in ovary intact DS vs. DR rats. Interestingly, per-tumor mass (burden ÷ multiplicity) is approximately 50% larger in DS-OVX compared to DR-OVX. This suggests that the “faster” hypothesis of obesity-related stopwatch programming holds true in tumors that are negative for expression of ER/PR, despite ovarian ablation and absence of high circulating levels of sex hormones.

In summary, obesity did not impact cancer endpoints of latency and incidence, but it did increase cancer endpoints of multiplicity and burden. This data suggests that high levels of circulating estrogen may be permissive for the growth of tumors, as evidenced by reduced overall cancer response in ovariectomized animals, but that high circulating estrogen is not obligatory for the effect of obesity on stimulating growth of mammary cancer cells in this model. Together, these data indicate that obesity maintains a cancer-promoting effect on mammary carcinogenesis in the absence of high circulating estrogen.

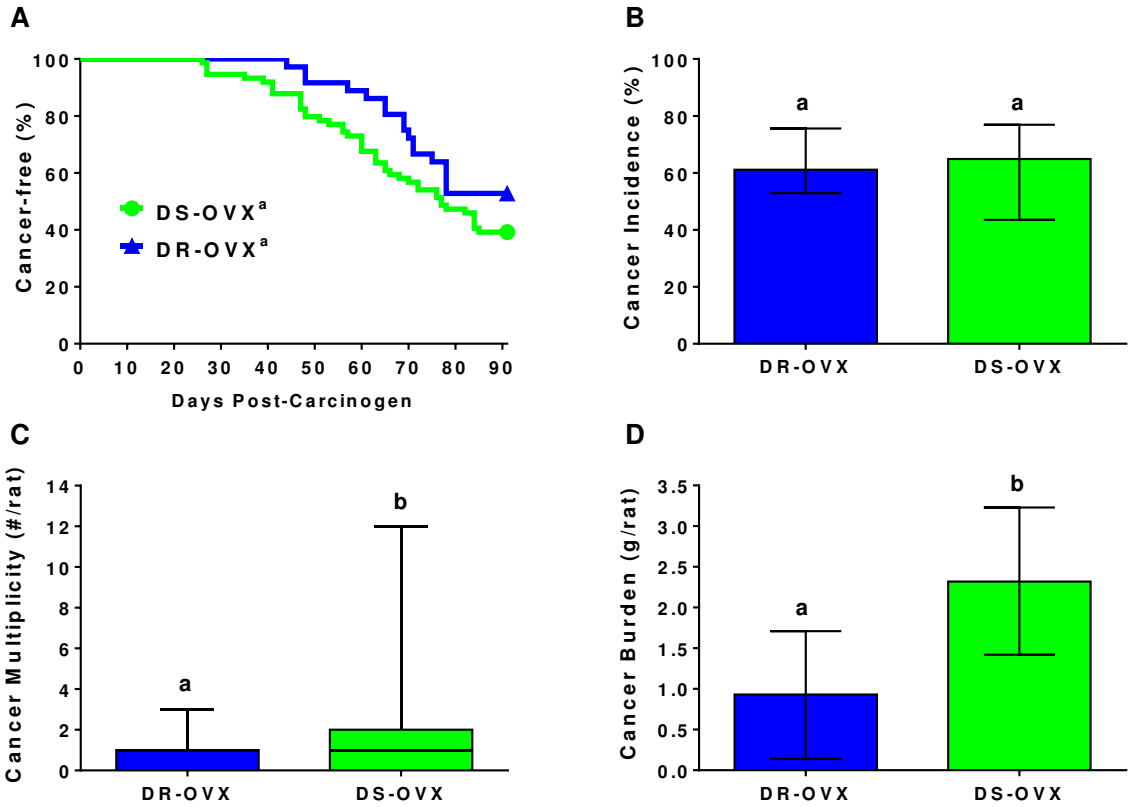

E

Group	N	Latency[1] (days)	Incidence[2] (%)	Multiplicity[3] (#/rat)	Burden[4] (g/rat)
DR-OVX	36	N/A	61.1	0.9	0.93
		(75, N/A)	(52.9, 75.6)	(0.6, 1.4)	(0.14, 1.71)
DS-OVX	74	77	64.9	1.5	2.32
		(65, N/A)	(43.5, 76.9)	(1.2, 1.9)	(1.42, 3.23)

Figure 19

Legend. Obesity accelerates mammary carcinogenesis in ovariectomized DS rats. Mammary carcinogenesis was initiated by injecting rats intraperitoneally with 50 mg/kg MNU at 21 days of age. Study was terminated 91 days (13 weeks) after carcinogen; only palpable confirmed mammary adenocarcinomas were included for analysis. In Panels A-D, groups with different letters significantly differ based on statistical comparisons described in Appendix C. Cancer-free survival (Panel A) and cancer incidence (Panel B) did not differ between DS and DR rats. Cancer multiplicity (Panel C) and cancer burden (Panel D) were elevated in DS compared to DR rats. Panel E) [1]Data corresponds to survival curves in Panel A. Values are point estimates at 50% quartile (95% confidence interval of linear-transformed survivor functions). Censored: DR-OVX N=19, DS-OVX N=29. [2]Values correspond to incidence in Panel B and are percentages (95% CI). [3]Values correspond to multiplicity in Panel C and are means (95% CI). [4]Values correspond to burden in Panel D and are means (95% CI).

4.B.3. Tumors from ovariectomized DS rats do not display higher PR immunoreactivity

Expression of the progesterone receptor was evaluated as a proxy to active estrogen signaling. The random field method of assessing PR status revealed that average PR % immunoreactivity was below 1% for all tumors (**Figure 20**). Given the overall low level of PR immunoreactivity, the hot-spot method (reported in Chapter 2) was not implemented.

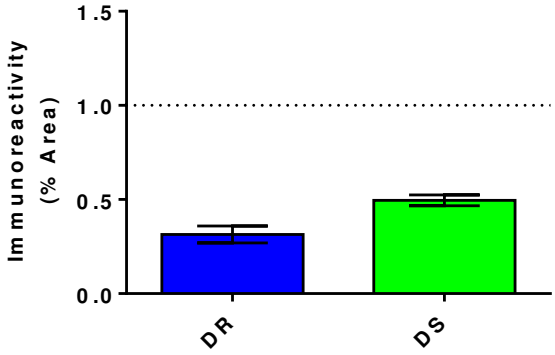

Figure 20
Legend. DS tumors do not display higher PR immunoreactivity than DR tumors. First-palpated tumors (DR-OVX N=21; DS-OVX N=46) were assessed for PR immunoreactivity of random tumor fields. All tumors were considered PR-.

Current histopathological standards for classifying a tumor as hormone receptor positive require ≥1% nuclear immunoreactivity (212). By these standards, all tumors from DR-OVX and DS-OVX animals were classified as PR negative. These data are in agreement with ovarian ablation creating a negative selection pressure environment, which favors growth of cells that can proliferate in very low levels of estrogen. The low percentage of cells expressing PR suggests that estrogen-induced signaling is very low in these tumors.

There was no difference in % PR-expressing cells between DR-OVX and DS-OVX tumors. Most studies report that obesity increases risk of predominantly luminal (ER/PR+) breast cancer subtypes, yet other studies have reported increased risk of ER/PR- breast cancer in obesity (131-133;136). This data provides further evidence against estrogen signaling as an obligatory factor for the cancer-promoting effects of obesity on mammary carcinogenesis.

4.B.4. Evaluation of aromatase mRNA and protein in DS rat mammary gland

In women prior to menopause, the ovaries are the primary sources of endogenous E2, with circulating E2 concentrations ranging from 55-734 fmol/mL (15-200 pg/mL), depending on phase of the menstrual cycle (213). Average levels of E2 in normal breast tissue from premenopausal women were recently reported as 453.0 fmol/g (314.3-652.8) (214). Given the high levels of estrogen produced by the ovaries in premenopausal women, the contribution of peripherally-produced E2 to the total circulating sex hormone pool is probably relatively small.

In contrast, in postmenopausal women following cessation of ovarian function, aromatase activity in peripheral tissues, including adipose tissue, is the primary source of estrogens. Circulating levels of E2 in postmenopausal women are generally 36-73 fmol/mL (10-20 pg/mL), derived almost exclusively from the conversion of adrenal-derived precursors to E2 via the aromatase in peripheral tissues (213). Lønning *et al.* recently reported average local levels of E2 within the breasts of cancer-free postmenopausal women as 29.2 fmol/g (19.3–44.1) (214). Unlike premenopausal women, in which estrogen levels vary with the menstrual cycle, aromatase activity in the breast tissue of postmenopausal women provides the mammary epithelium with continuous, local, direct exposure to estrogen. In clinical populations, fat tissue expresses aromatase, particularly in physiological conditions of adipose tissue inflammation, such as that which may accompany obesity.

To evaluate whether obesity in DS rats was inducing peripheral aromatase activity, we evaluated aromatase at the transcriptional and translational levels through qPCR and Western blot, respectively. To evaluate aromatase at the transcriptional level, real-time PCR was performed on cDNA isolated from cancer-free mammary gland from N=2 each DR-OVX and DS-OVX rats from distal ends of the body weight distribution. To rephrase, we used the leanest DR vs. fattest DS rats to maximize chances of detecting aromatase. While the housekeeping gene *pgk1* was detected in all samples, a signal corresponding to the *cyp19a1* gene product (aromatase) failed to amplify within 45 cycles of PCR (data not shown). As specificity of the primers was confirmed using ovarian cDNA, these data suggest that aromatase expression in these mammary glands is below the limits of detection of qPCR.

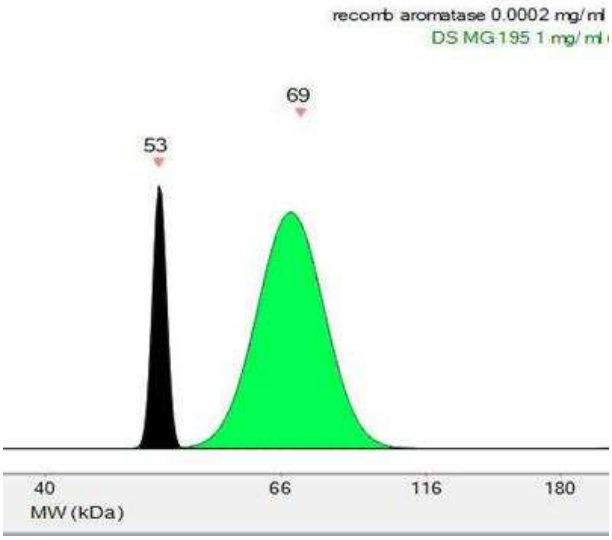

Figure 21
Legend. Rat mammary gland does not yield a signal corresponding to aromatase. Representative chemiluminescent signal from capillary electrophoresis-based detection of aromatase protein in purified recombinant aromatase (black peak) or DS mammary gland lysate (green peak), (1 mg/ml) each. Molecular weight is based on calibration to internal fluorescent standards.

To evaluate aromatase at the translational level, lysate from DR and DS mammary gland was evaluated via capillary electrophoresis using the Protein Simple Wes device. Recombinant aromatase (0.2 µg/ml) yielded a strong peak around 53 kD, similar to the predicted molecular weight of aromatase based on amino acid sequence. As shown in **Figure 21** for a representative DS-OVX sample, rat mammary gland lysate (both DR-OVX and DS-OVX) did not provide a signal corresponding to this molecular weight.

A strong signal from DS-OVX mammary gland lysate was observed at approximately 69 kD. While aromatase does undergo post-translational modifications, including phosphorylation and glycosylation, these modifications seem unlikely to cause the large observed 14 kD shift in molecular weight (215). Therefore, the signal at 69 kD may be due to nonspecific protein interactions with the antibody. These findings are in agreement with those of the MacLean lab at Anschutz Medical Campus at the University of Colorado Hospital, as personal communication with the MacLean lab revealed that their lab was likewise unable to detect aromatase in the mammary gland of ovariectomized obese rats. The failure to detect aromatase mRNA and protein in our ovariectomized rats represents two additional pieces of evidence demonstrating lack of support for an obligatory role for estrogen as a mechanism whereby obesity accelerates carcinogenesis in the rat.

In contrast with our findings and those of the MacLean lab, Zhao *et al.* recently reported that peripheral aromatase increases in fat depots of lean rats over time (216). However, in the Zhao article, aromatase mRNA was only detected in fat pads from 6-month old rats, and aromatase protein was only detected in fat pads from 5-month old rats in the Zhao article (216). Neither aromatase protein nor mRNA were detected in rats younger than 5 months of age. The Levin rats used in the current study were 4 months of age, so it is possible that extragonadal production of estrogen by fat tissue becomes a more biologically relevant process in older rats. However, peripheral aromatase activity does not appear to be a dominant biological process in the current study.

4.B.5. Levels of estrogen metabolites in the mammary gland of lean and obese rats

As a measure of aromatase activity, we evaluated expression of estrogen compounds in N=8 mammary glands from ovary intact and ovariectomized DR and DS rats (N=32 samples total) via ultraperformance liquid chromatography coupled to tandem mass spectrometry (UPLC-MS/MS). This data is presented

and discussed in **Appendix C**. While there is a trend towards higher E2 in mammary gland from DS-OVX compared to DR-OVX rats, the run data, collected from our samples by the West Coast Metabolomics Center at the University of California-Davis, does not make biological sense for reasons discussed in **Appendix C,** and therefore is regarded with skepticism. Moreover, using a separate metabolomics facility, the MacLean lab was unable to detect estrogen within the mammary gland of ovariectomized obese rats via gas chromatography coupled to tandem mass spectrometry (GC-MS/MS). These data provide another piece of evidence in support of our findings that estrogen is not an obligatory mechanism whereby obesity promotes mammary carcinogenesis in the rat.

4.B.6. DS rats do not display evidence of estrogen involvement at the host systemic level

A meta-analysis of prospective studies of breast cancer in postmenopausal women performed by the Endogenous Hormones and Breast Cancer Collaborative Group from the University of Oxford revealed an increased relative risk of breast cancer in overweight women (BMI ≥27.5 kg/m^2) compared to lean women (BMI ≤22.5; RR=1.19 (1.05-1.34)). This relationship was attenuated when free circulating E2 levels were included in risk estimates (adjusted RR= 1.02 (0.89-1.17)) (217). Adjustment for other circulating estrogen metabolites, including total estrogen, estrone (E1), and E1-sulfate, yielded lesser reductions in relative risk, while adjustment for circulating levels of androgens including testosterone had no effect on relative risk in this particular study (217).

To evaluate whether DS-OVX rats display evidence of increased circulating levels of sex hormones (presumably derived from peripheral aromatase activity), plasma from N=10 each DR-OVX and DS-OVX rats was evaluated. For comparison, N=10 each ovary intact DR and DS rats were evaluated at the same time. Values are presented in **Table 5**.

Table 5

Legend. Circulating sex hormones and sex hormone ratios in plasma from DS-OVX (N=10) and DR-OVX (N=10) rats, presented as means ± SD. Animals chosen for analysis of plasma proteins were purposefully chosen from non-overlapping areas of the body weight distribution. Analytes were log-transformed prior to analysis and Welch Satterthwaite method was used as necessary to satisfy statistical assumptions. [1]Analyte concentrations were converted to molarity prior to ratio determination. Abbreviations are defined on page 154.

	DS-OVX	**DR-OVX**	***p***	**DS**	**DR**	***p***
Progesterone (ng/mL)	1.8 ± 1.2	1.3 ± 0.7	0.34	6.3 ± 4.1	5.2 ± 2.4	0.08
E2 (pg/mL)	42.7 ± 8.4	36.0 ± 3.7	0.08	46.1 ± 11.7	39.8 ± 8.6	0.34
E2:progesterone[1]	0.047 ± 0.045	0.046 ± 0.032	0.65	0.012 ± 0.007	0.010 ± 0.004	0.96
SHBG (nmol/L)	9.4 ± 3.5	10.5 ± 6.0	0.96	12.8 ± 4.7	14.5 ± 7.7	0.81
SHBG:E2[1]	66.6 ± 47.3	81.1 ± 49.1	0.56	84.2 ± 47.8	99.3 ± 49.9	0.40
SHBG:progesterone[1]	2.6 ± 2.3	3.5 ± 3.0	0.84	0.9 ± 0.8	1.0 ± 0.5	0.58

There was no difference between progesterone levels in DS-OVX and DR-OVX rats. Compared to ovary intact animals, circulating levels of progesterone were reduced by ≥75% in ovariectomized animals, consistent with ablation of ovarian function (ovary intact: DR 5.2 ± 2.4 pg/mL, DS 6.3 ± 4.1 pg/mL; OVX: DR 1.3 ± 0.7 pg/mL, DS 1.8 ± 1.2 pg/mL). While there was a trend towards elevated E2 in DS-OVX compared to DR-OVX rats, this data is problematic and again subject to skepticism. Specifically, circulating levels of E2 were nearly identical (≤10% reduction) between ovary intact and ovariectomized animals (ovary intact: DR 39.8 ± 8.6 pg/mL, DS 46.1 ± 11.7 pg/mL; OVX: DR 36.0 ± 3.7, DS 42.7 ± 8.4 pg/mL), suggesting that the assay is detecting something other than estradiol.

Direct immunoassays for detection of sex hormones are notoriously nonspecific and widely variable in what is actually being measured, particularly when hormone levels are <50 pg/mL. For example, a study that compared the gold standard GC-MS/MS method of sex hormone measurement with indirect immunoassay (generally radioimmunoassay method with extraction step) and direct immunoassay (no extraction step) found that direct assays from three different vendors systematically overestimated estradiol levels in serum from postmenopausal women by an average of 68% over that reported by GC-MS/MS (218). The routine overestimation of estradiol by direct assay is attributed to a combination of

blindness of the assays to sex hormone metabolites and Phase II conjugates as well as potential matrix interference from components of the mammary gland (219).

Beyond estrogen levels, estrogen signaling is impacted by bioavailability. Sex hormone binding globulin (SHBG) is produced by the liver and binds estrogen and other sex hormones, sequestering it and preventing ligand-mediated activation and downstream activities of the estrogen receptor (220). However, in our ovarian ablation study, there was no difference in SHBG levels in DS-OVX compared to DR-OVX rats. Likewise, ratios of SHBG: E2 and SHBG: progesterone, as an estimate of bioavailability, was not different between DR-OVX and DS-OVX rats.

Cumulatively, these data failed to find evidence in support of the "peripheral estrogen production" mechanism, and suggest that the ovariectomized rat may provide a unique model in which to study the impact of obesity on mammary carcinogenesis in the absence of estrogen effects.

4.C. Clinical Implications

The ovariectomized rat has relevance to the postmenopausal physiological state, including predisposition to rapid weight gain and loss of ovarian-derived sex hormones. Most breast cancer is diagnosed in postmenopausal women, as median age at breast cancer diagnosis between 2002 and 2004 was 61 years of age (2). The World Cancer Research Fund recently reported that the sum of evidence supports a probable link between obesity and postmenopausal breast cancer risk (25). However, the literature is mixed as to which molecular subtypes of breast cancer are associated with increased risk due to obesity.

Most studies report that obesity increases risk of predominantly luminal (ER/PR+) breast cancer subtypes, though this data is mixed, particularly in premenopausal women (131-133). Other studies have reported increased risk of ER/PR- breast cancer in obesity, which may be stratified by menopausal status (reviewed in (136)).

In rats, following ovariectomy, the tumors that develop are predominantly negative for expression of ER and PR, due to negative selection pressure imposed by removal of high levels of sex hormones. This leads to expansion of cell populations whose growth is independent of these receptors. Clinically, ER/PR- tumors are classified into two molecular subtypes of breast cancer. In the first subtype, tumors are ER/PR- but express high levels of the Her2 receptor, due to gene amplification or overexpression. In the second type of ER/PR- breast cancer, tumors that do not express ER, PR, or Her2 are called triple negative breast cancer (TNBC) in the clinical population.

Whereas luminal subtype (ER/PR+) breast tumors have high 5-year survival rates (>90%), Her2+ and TNBC breast cancers are responsible for the majority of breast cancer deaths, with 5-year survival rates of 20-75% and 30-80%, respectively (221). Simply put, ER/PR- breast cancer is the type of breast cancer that kills women. Thus, understanding the involvement of the 4 lines of code in the ER/PR- high mortality breast cancer subtypes of breast cancer has high clinical relevance.

4.D. Conclusions and Future Direction

In Chapter 2, ovary intact rats with susceptibility to diet-induced obesity (DS) had marked acceleration of breast cancer in comparison to lean (DR) counterparts. In Chapter 3, this acceleration was found to be due in part to faster growth rates of DS tumors in ovary intact animals, potentially enabled by accelerated cell cycle transit and reduced apoptotic efficiency. In the current study, we designed a

surgical ovarian ablation manipulation. This served two purposes: 1) to evaluate mammary carcinogenesis in DS and DR rats in the absence of abundant estrogen signaling, and 2) to evaluate whether evidence supports enhanced local production of estrogen by aromatase in the mammary gland of DS rats.

Overall cancer response was blunted in ovariectomized compared to ovary intact animals. Whereas obesity did not affect early cancer outcomes such as cancer incidence or latency, DS-OVX rats displayed higher cancer multiplicity and burden compared to DR-OVX. This suggests that estrogen is not obligatory for cancer-promoting effects of obesity on the carcinogenic process in the breast.

In Chapter 1, we summarized four mechanistic hypotheses that have gained mainstream traction to explain the link between obesity and breast cancer. In the context of the stopwatch analogy, these four hypotheses are referred to as “lines of code” that can program stopwatches (tumors). The first line of code whereby obesity may impact breast carcinogenesis is related to peripheral production of estrogen. In the current study, to determine whether there was evidence in support of this mechanism in our rat model, we examined estrogen using an ovariectomy manipulation. Ovariectomy creates negative selection pressure for expansion of cell populations that can grow in the absence of high levels of estrogen signaling, and tumors that grow in ovariectomized rats are predominantly ER/PR.

We failed to find evidence of estrogen involvement in the accelerated cancer response associated with obesity. Three pieces of evidence, at the level of tumor cells, at the local (mammary gland) level, and at the host systemic level, stand against estrogen as an obligatory mechanism whereby obesity promotes breast carcinogenesis in the current rat model. First, cells in DS-OVX tumors did not display an increase in PR % immunoreactivity, which is a measure of functional estrogen signaling. Indeed, nearly all cells in

tumors from both DS-OVS and DR-OVX rats were negative for expression of PR, suggesting that these tumors have very low levels of estrogen signaling taking place. Secondly, at the local (mammary gland) level, we did not detect aromatase mRNA and protein expression in mammary gland from either DS-OVX or DR-OVX animals, consistent with findings from others in this field. Finally, there was no difference in circulating levels of progesterone as a measure of functional estrogen signaling in DS-OVX compared to DR-OVX rats. Therefore the current study does not support peripheral production of sex hormones by fat tissue as an obligatory mechanism whereby obesity promotes mammary carcinogenesis in the Levin DS rats.

Regarding the relevance of our findings to the clinical population, enhanced aromatase activity has been documented in the breast tissue of clinical obese populations as well as mice (43;222-224). Aromatase inhibitors function well as chemopreventive agents in postmenopausal women, preventing 40-50% of new contralateral ER/PR+ breast tumors (225). Thus, there is a clinical subpopulation in which estrogen does appear to be obligatory for the link between obesity and breast cancer. However, the other side of this coin is that aromatase inhibitors fail to prevent approximately 50% of new contralateral ER/PR+ tumors, in addition to ER/PR- tumors, whose occurrence is largely unaffected by endocrine-based chemoprevention. Thus, clinical subpopulations exist in which estrogen is NOT related to the link between obesity and breast cancer, and our integrated rat model can be used to interrogate obligatory mechanisms for the link between obesity and breast cancer in these distinct subpopulations.

The findings presented herein suggest that the rat represents a model organism in which estrogen is not a key player in the effects of obesity on promoting mammary carcinogenesis. This model thus allows researchers to subtract peripheral production of estrogen from the 4 lines of code related to obesity and breast cancer risk, and focus their investigations on evaluation of the 3 remaining mechanisms. These

investigations are particularly important in the context of ER/PR- tumors, which are responsible for the majority of breast cancer deaths.

To assess the evidence in support of the 3 remaining lines of code whereby obesity may promote mammary carcinogenesis, in Chapter 5 we evaluated a set of analytes corresponding to the mechanisms of chronic inflammation, deregulated insulin signaling, and altered adipokine expression in the plasma of ovary intact and ovariectomized DR and DS rats. Unexpected findings from these hypothesis-generating experiments related to inflammatory cytokines led us to further investigate the evidence in support of the chronic inflammation hypothesis. The final set of experiments in Chapter 5 represents a method that sought to determine whether the combined effects of host systemic and local (mammary gland) factors from DS rats stimulated growth of ER/PR- cells *in vitro.*

CHAPTER 5: HOST SYSTEMIC FACTORS DO NOT EXPLAIN THE CANCER-PROMOTING EFFECTS OF OBESITY[5]

5.A. Rationale

Obesity can influence the development of cancer—the ticking of stopwatches—in a multitude of ways. In Chapter 1, we described four "lines of code" that represent the mechanistic processes that have gained mainstream traction as the link between obesity and breast cancer. These four lines of code can be summarized as follows: 1) peripheral production of sex hormones; 2) chronic inflammation; 3) deregulated insulin signaling; and 4) altered adipokine expression. Each program can be implemented at the cellular level, at the local level within the mammary gland, and at the host systemic level.

In Chapter 2, we reported that mammary carcinogenesis is accelerated in obese DS compared to lean DR rats. In Chapter 3, we determined that the balance of proliferation and apoptosis at the cellular level favored faster tumor growth rates in DS compared to DR. These effects appear to be mediated through accelerated cell cycle transit with concomitant reduced apoptotic efficiency in DS compared to DR. As molecular evidence consistent with this theory, hyperphosphorylation of Rb, lack of suppression of E2F1 signaling, and a struggle for dominance between pro-apoptotic and anti-apoptotic factors was observed in DS tumors.

Proliferation and apoptosis are extremely complex biological processes that are subject to regulation by many pathways, including those that are represented by the 4 lines of code. The experiments in Chapter 4 failed to provide evidence in support of an obligatory role for estrogen signaling in the link between

[5]Chapters 4 and 5 are being combined in a manuscript to be submitted to the journal *Cancer Prevention Research*. Any changes between the version presented herein and that which is published will be minor. Such changes will likely be due to publishing requirements and tone differences between target audiences.

obesity and chemically induced carcinogenesis, although estrogen can influence general tumor growth if it is present (i.e., ovary intact cancer response vs. ovariectomized cancer response).

Therefore, the evidence supports a shift towards evaluation of the remaining 3 lines of code. The first objective of the work reported in the current chapter was to investigate plasma analytes representative of the 3 remaining lines of code (2) chronic inflammation; 3) deregulation of insulin signaling; and 4) altered adipokine expression) to determine which processes were implicated. Next, an *in vitro* model was developed utilizing co-culture of a rat mammary cancer stem cell line and primary DR- or DS-derived mammary gland adipocytes. These experiments were conducted as a means to evaluate whether circulating factors in general or local adipocyte-secreted factors from DS rats would influence cell growth as a cumulative response to a complex set of stimuli. Finally, based on the lack of convincing evidence of the involvement of systemic factors as a link between obesity and mammary carcinogenesis, we further investigated the evidence in support of chronic inflammation (code line 2) at the local (mammary gland) and cellular levels (cancer cells).

Materials and methods for experiments performed in Chapter 5 are provided in **Appendix D**.

5.B. Results and Discussion

Plasma analytes were chosen to represent the components of the mechanistic processes of chronic inflammation, deregulated insulin signaling, and altered adipokine expression, that have been most characterized relative to breast cancer. Values for all analytes are reported in **Table 6.** Fold-change of DS compared to DR is shown for ovary intact rats in **Figure 22** and in ovariectomized rats in **Figure 23**.

5.B.1. Host systemic evidence for code line 2: DS rats do not display elevations in systemic markers associated with chronic inflammation

While a trend towards elevated TNF-α was observed in ovary intact DS vs. DR rats, none of the differences between groups reached statistical significance. In ovariectomized rats, IL-6 and IL-1β displayed a trend towards increased expression in DS-OVX compared to DR-OVX, but again, none of the differences were statistically significant.

5.B.2. Host systemic evidence for code line 3: DS rats display systemic deregulation of insulin signaling

Ovary intact DS rats displayed elevated fasted plasma insulin (3.5-fold increase) and insulin-like growth factor (IGF)-1 (1.2-fold increase). The IGF-1: IGF binding protein (IGFBP)-3 ratio was increased 1.2-fold in ovary intact DS compared to DR. As IGFBP-3 prevents IGF-1 from binding to membrane receptors and inducing signal transduction cascades, these data suggest that DS rats have higher levels of bioavailable IGF-1 ($p<0.05$ for all analyses).

While we did not detect a difference in fasted plasma glucose levels between ovary intact DS and DR, calculated insulin resistance, estimated through homeostasis model assessment-estimated insulin resistance (HOMA-IR), was elevated (2.6-fold increase) in DS versus DR rats. These data are in agreement with Levin's previous characterization of the metabolic abnormalities displayed by DS rats (145;146).

Compared to ovary intact DS rats, DS-OVX rats display a trend towards worsening of parameters associated with insulin resistance, including elevated circulating insulin, glucose, IGF-1, and HOMA-IR. Interestingly, IGFBP-3 increased in both DR-OVX and DS-OVX rats, so the magnitude of IGF-1:IGFBP3 is similar in ovary intact and ovariectomized animals, suggesting that there is no difference in bioavailable

IGF-1. This is consistent with the work of Kalu *et al.*, who reported that both IGF-1 and IGFBP-3 expression increase following ovariectomy in Sprague Dawley rats, potentially due to loss of estrogen-induced repression of IGF-1 expression (226).

5.B.3. Host systemic evidence for code line 4: DS rats display altered adipokine expression

Circulating leptin (6.2-fold increase) and adiponectin (1.8-fold increase) levels were both elevated in ovary intact DS compared to DR rats. While the elevation in adiponectin was unexpected, previous studies utilizing obese (fa/fa) Zucker rats have reported elevated levels of circulating adiponectin with reduced tissue expression of the adiponectin receptor in obese versus lean animals, suggesting that feedback loops may be disrupted in obesity (227). Reduced adiponectin: leptin ratio was observed in ovary intact DS versus DR rats.

In ovariectomized rats, leptin increased in both DR-OVX and DS-OVX rats compared to ovary intact animals. However, adiponectin and the adiponectin: leptin ratio was reduced in both groups of ovariectomized rats. This decrease is particularly evident when comparing ovary intact DR to DR-OVX. This may be due to the additional weight gain that accompanies ovariectomy in all animals, as adipose tissue expansion is associated with reduced adiponectin production (110;228).

Taken together, the investigation of circulating analytes confirmed Levin's previous reports of deregulated insulin signaling and hyperleptinemia in DS rats. Next, we used multivariate modeling of plasma data to evaluate interrelationships between circulating analytes and cancer outcomes.

Table 6

Legend. Circulating analytes in plasma from N=10 each ovary intact and ovariectomized DR and DS rats. Values are means ± SD. Animals chosen for analysis of plasma proteins were purposefully chosen from non-overlapping areas of the body weight distribution. Analytes were log-transformed prior to analysis and Welch Satterthwaite method was used as necessary to satisfy statistical assumptions. [1]Analyte concentrations were converted to molarity prior to ratio determination. Abbreviations are defined on page 154.

Analyte/ Analyte Ratio	**DS**	**DR**	***p***	**DS-OVX**	**DR-OVX**	***p***
INSULIN SIGNALING						
Insulin (pg/mL)	1402.4 ± 851.9	398.9 ± 577.5	**<0.001**	1654.9 ± 1115.4	480.9 ± 452.5	**<0.001**
Glucose (mg/dL)	136.4 ± 78.7	119.1 ± 63.5	0.53	168.6 ± 78.7	95.2 ± 23.3	**<0.001**
HOMA-IR	12.0 ± 6.6	4.6 ± 7.9	**<0.01**	16.9 ± 4.1	2.7 ± 0.7	**<0.001**
IGF-1 (ng/mL)	285.7 ± 28.1	235.3 ± 39.5	**<0.01**	429.4 ± 69.9	289.1 ± 52.3	**<0.001**
IGFBP-3 (ng/mL)	82.7 ± 14.0	80.6 ± 12.9	0.73	137.2 ± 20.0	103.0 ± 18.4	**<0.001**
IGF-1:IGFBP-3[2]	14.6 ± 2.0	12.3 ± 2.3	**<0.05**	13.0 ± 1.2	11.7 ± 1.2	**<0.05**
ADIPOKINES						
Leptin (ng/mL)	5.6 ± 1.4	0.9 ± 0.8	**<0.001**	7.6 ± 1.4	1.5 ± 0.5	**<0.001**
Adiponectin (µg/mL)	31.8 ± 13.3	17.1 ± 4.7	**<0.01**	44.7 ± 18.5	26.8 ± 8.3	**<0.05**
Adiponectin:leptin[2]	0.5 ± 0.3	3.3 ± 2.8	**<0.01**	0.5 ± 0.3	1.7 ± 0.7	**<0.001**
INFLAMMATORY CYTOKINES						
CRP (µg/mL)	695.3 ± 315.0	617.1 ± 200.5	0.52	951.2 ± 205.6	870.2 ± 203.9	0.36
IL-1β (pg/mL)	17.3 ± 25.7	7.8 ± 9.6	0.33	27.4 ± 25.7	6.0 ± 5.5	0.28
IL-6 (pg/mL)	46.3 ± 43.44	111.2 ± 235.6	0.76	871.1 ± 2156.4	132.4 ± 229.6	0.52
TNF-α (pg/mL)	3.3 ± 1.0	2.6 ± 0.9	0.12	8.8 ± 11.6	7.9 ± 6.2	0.78

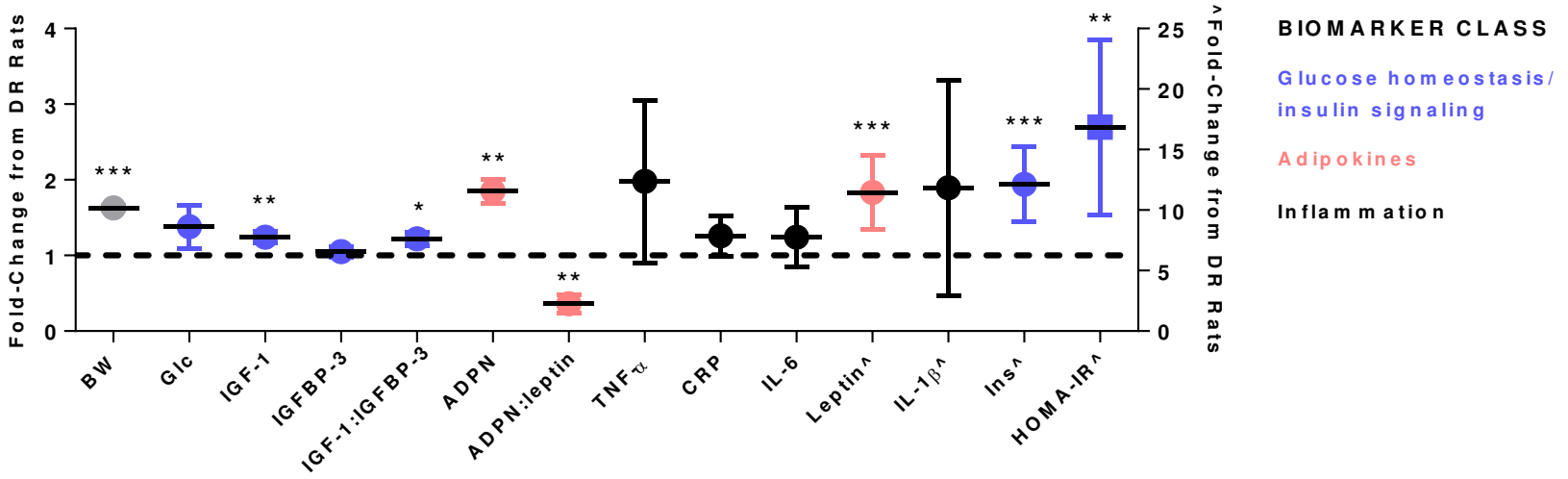

Figure 22

Legend. Ovary intact DS rats display alterations in host systemic analytes involved in insulin signaling and adipokine expression. Values are fold-change levels of circulating analytes in DS compared to DR **ovary intact** rats, sorted by body weight (BW) (i.e., heaviest DS vs. heaviest DR) ± SEM. ^ denotes biomarkers graphed on the right Y-axis to account for differences in magnitude. Values *, **, and *** denotes statistical significance at $p<0.05$, <0.01, and <0.001, respectively, based on t-tests with false discovery rate=1%.

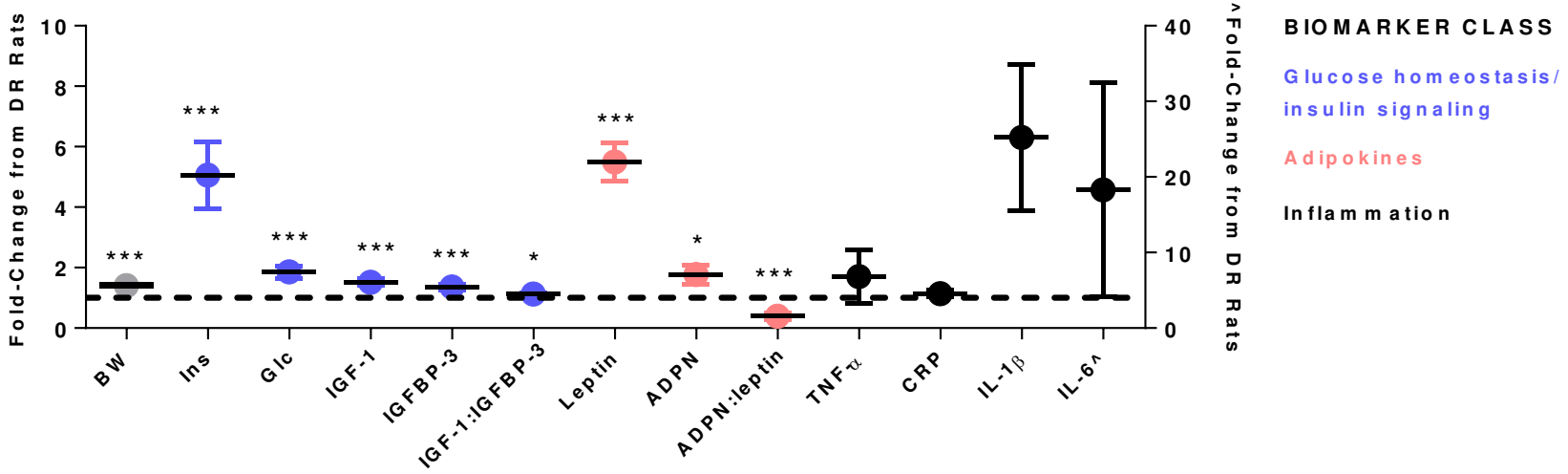

Figure 23

Legend. DS-OVX rats display alterations in host systemic analytes involved in insulin signaling and adipokine expression. Values are fold-change levels of circulating analytes in DS compared to DR **ovariectomized** rats, sorted by body weight (BW) (i.e., heaviest DS vs. heaviest DR) ± SEM. ^ denotes biomarkers graphed on the right Y-axis to account for differences in magnitude. Values *, **, and *** denotes statistical significance at $p<0.05$, <0.01, and <0.001, respectively, based on t-tests with false discovery rate=1%.

5.B.4. Multivariate analysis fails to provide evidence in support of a linkage between plasma analytes and cancer outcomes

Chapter 3 highlighted the utility of using multivariate data analysis tools to visualize high-dimensional datasets with several interrelated, likely co-linear variables. To evaluate the cumulative ability of plasma analytes to predict cancer outcomes, the plasma data reported in sections 5.B.2-4 were used to construct two PLS models using N=13 plasma analytes as X variables with Y (response) variables of cancer multiplicity or burden, which were elevated in obesity in both ovary intact and ovariectomized rats. Circulating estrogen was not included in these analyses due to concern over specificity of the detection method, as reported in Chapter 4. Within these models, whereas positive coefficients are positively correlated with cancer multiplicity and burden, negative coefficients are inversely correlated with cancer outcomes.

The PLS model for cancer multiplicity was fitted by a principal component that explained 58.3% of the variance in X variables (plasma analytes) and 9.4% of the variance in the Y variable (cancer multiplicity). The model cumulatively had very poor ability to predict cancer multiplicity based on cross-validation (Q2 values), as only 0.2% of samples would be predicted correctly based on the plasma data. The PLS model for cancer burden was fitted by a principal component that explained 57.5% of the variance in X variables (plasma analytes) and 8.9% of the variance in Y (cancer burden). The PLS model based on cancer burden had even poorer predictive ability than observed for the cancer multiplicity PLS model, as 0% of samples would be predicted correctly based on the plasma data. Within these models, coefficients for the individual plasma analytes (X variables) are shown with jack-knifed 95% confidence intervals in **Figure 24A** for the cancer multiplicity PLS model and in **Figure 24B** for the cancer burden PLS model. None of the correlation coefficents for the X-variables, other than leptin in the cancer multiplicity PLS

model (**Figure 24A**), reached statistical significance. Thus, little evidence in support of a linkage between the plasma analytes assessed at the host systemic level and cancer outcomes.

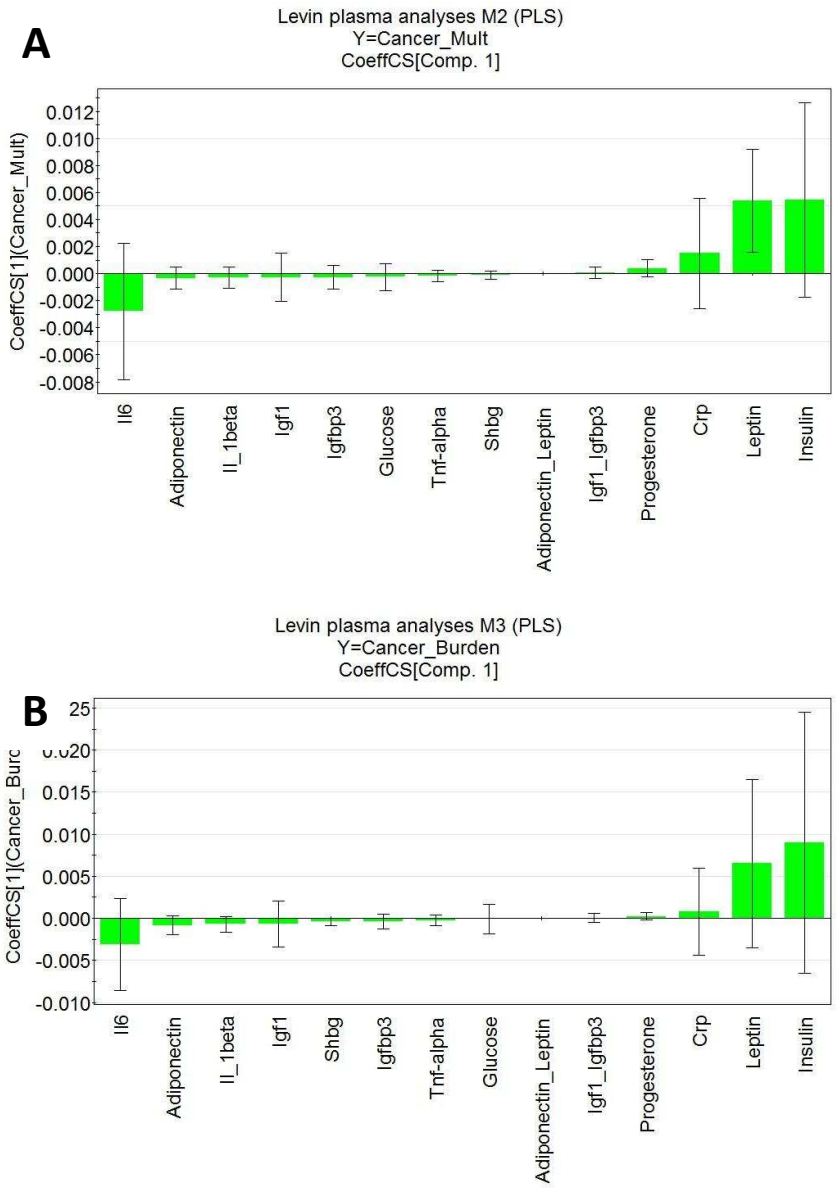

Figure 24
Legend. Host systemic factors have poor correlation with cancer outcomes of multiplicity and burden. Coefficients for partial least squares regression, based on Y= cancer multiplicity (panel A) and Y= cancer burden (panel B) in the first principal component. Plasma values from N=10 each DR ovary-intact, DS ovary-intact, DR-OVX, and DS-OVX rats were included in analysis.

5.B.5. DS serum + adipocyte-secreted factors do not stimulate growth of rat mammary cancer stem cells

The lack of evidence that host systemic factors provide a linkage between obesity and breast cancer was surprising. This finding is also potentially troubling, as much of what is reported clinically is based exclusively on the assessment of circulating factors. Therefore, we decided to use an alternative approach to explore this question. Since increased cancer multiplicity and burden was observed in both ovary intact and ovariectomized DS rats, we conducted a set of *in vitro* experiments designed to model cancer cell growth as a cumulative response to a summation of circulating and local factors. In Chapter 4, we demonstrated that the effect of obesity on promoting mammary carcinogenesis is likely estrogen-independent; therefore, we used the LA7 cancer cell line, which is a rat-derived cancer stem cell line that is negative for expression of ER/PR.

LA7 is a rat mammary cancer stem cell line isolated from a rat mammary tumor induced by the carcinogen DMBA. We hypothesized that serum from DS rats would preferentially stimulate the growth of this cell line over that observed when cells were treated with DR serum. LA7 cells were cultured in 5% fetal bovine serum (standard for cell culture), 5% DR serum, or 5% DS serum for 72 hrs. DS serum did not stimulate the growth of LA7 cells (**Figure 25A**).

To evaluate whether body weight of the DS animal was associated with a linear response in cell growth, LA7 cells were seeded at low density and treated with 5% FBS, DR serum, or DS serum for 168 hrs (7 days, as shown in **Figure 25B**. There was no relationship between growth of LA7 cells and weight of the DS animal, suggesting that circulating factors are not associated with growth of ER/PR- cancer cells in either a cumulative or linear fashion.

Adipose tissue is an endocrine organ whose secretory activity is altered in obesity. To evaluate whether secreted factors from adipocytes impacted the growth of rat cancer stem cells, we co-cultured primary adipocytes with LA7 cells. Adherent LA7 cells were treated with 5% FBS, 500 adipocytes from DR or DS rats, 5% DR or DS serum, or 500 adipocytes + 5% DR/DS rat serum. The addition of adipocytes alone did not independently impact growth of LA7 cells, regardless of whether adipocytes were isolated from DR or DS rats. Interestingly, as shown in **Figure 25C,** the combination of serum + adipocytes slightly suppressed LA7 growth with both DR and DS rats, though the magnitude of this suppression was slightly larger for DS than DR.

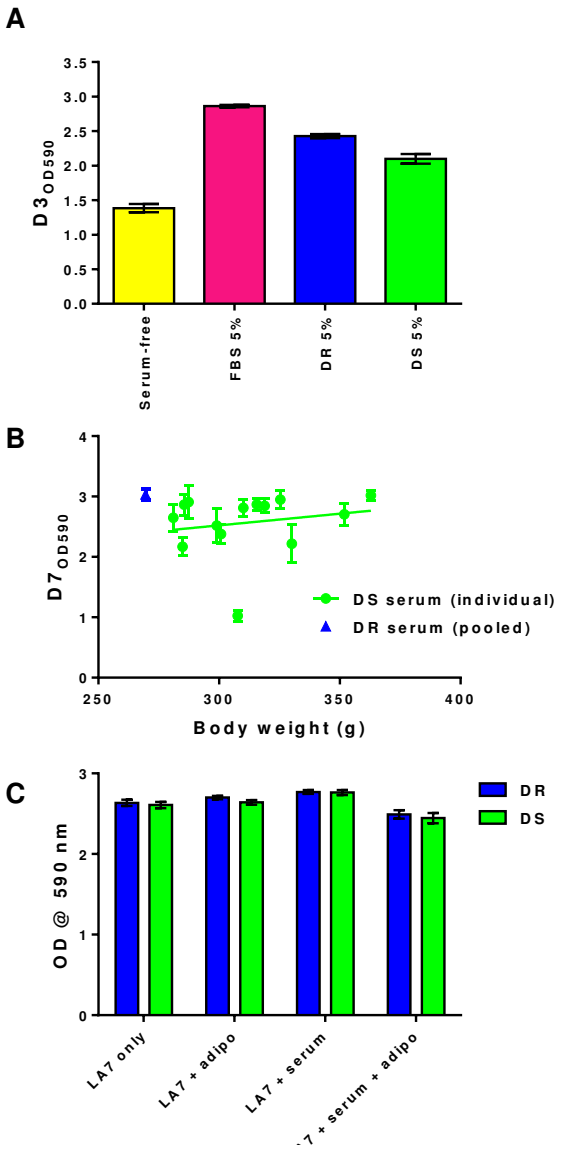

Figure 25
Legend. Neither circulating nor adipose-secreted factors stimulate growth of LA7 cancer stem cells. Cells were seeded into 96 (Panels A and B) or 24 (Panel C) well plates. Following treatment, cells were fixed with 1% glutaraldehyde and stained with 0.02% crystal violet; growth is linear with absorption at 590 nm. Panel A) 3-day treatment with DS serum does not stimulate LA7 growth. Panel B) 7-day treatment with DS serum does not correlate with weight of the DS animal. Panel C) 3-day co-culture of 500 adipocytes/well + DR/DS serum.

Neither DR nor DS serum stimulated the growth of LA7 over that observed with FBS; however, the addition of 5% DS serum caused distinct morphological changes in the growth of the LA7 monolayer. Specifically, LA7 cells rolled up into a mammosphere-like presentation (**Figure 26**). Mammosphere formation by cancer cells is generally associated with reduced differentiation, expression of cancer stem cell markers, the epithelial-to-

mesenchymal cell type transition, tumor aggressiveness, and invasion (229;230). Epithelial cells normally grow in a monolayer in culture, as these cells have impaired mammosphere-forming capacity due to anoikis, or detachment-mediated cell death. Gaining the ability to form mammospheres is associated with independence from adherence and protection from anoikis (230).

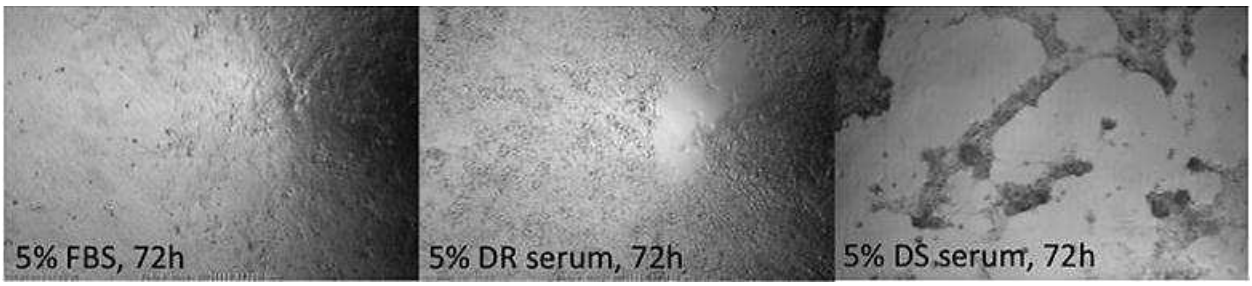

Figure 26
Legend. DS serum treatment induces mammosphere-like changes in morphological growth patterns of LA7 cells, compared to culture with FBS or DR rat serum. Representative fields captured at 40X magnification from 96-well plates treated with indicated serum for 3 consecutive days.

The four "lines of code" discussed throughout this dissertation represent a summary of the four main mechanistic hypotheses whereby obesity may promote the carcinogenic process in the breast. However, there are undoubtedly other lines of code separate from these 4 mechanisms, which may be less well documented or thus far unidentified. Rat plasma potentially contains hundreds of analytes that could be exerting the link between obesity and promotion of breast carcinogenesis. However, these data suggest that neither circulating factors nor adipose-derived factors from DS rats are capable of stimulating the growth of ER/PR- cancer cells in culture. These data do not conclusively rule out a role for insulin and leptin signaling; rather, these data provide evidence in support of shifting focus to interrogate mechanisms that are functioning at the cellular level. With that in mind, we decided to further explore local effects in the model with a focus on the process of chronic inflammation (code line 2).

5.B.6. DS rats display mammary adipocyte hypertrophy

Fat depots have two options with which to store excess energy: hyperplasia (stimulation of preadipocytes differentiating into mature adipocytes) and hypertrophy (expanded volume of existing adipocytes). Compared to smaller adipocytes, hypertrophic adipocytes display increased rates of lipolysis, increased free fatty acid turnover, increased expression of inflammatory cytokines TNF-α and IL-6, and increased risk of adipocyte death (56-60).

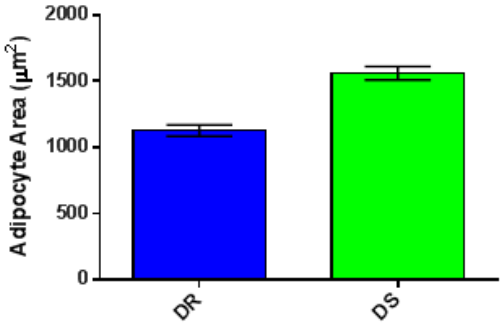

Figure 27
Legend. Adipocytes from DS mammary fat pad are larger than adipocytes from DR. Adipocyte area in H&E stained sections from cancer-free mammary fat pad. Values are means ± SEM.

To evaluate whether DS adipocytes are larger than DR adipocytes, cancer-free mammary fat pad was used to measure adipocyte diameter in DR and DS rats. As shown in **Figure 27,** adipocyte area was significantly larger in DS compared to DR fat pad (DS 1560 ± 83.09 μm^2, DR 1127 ± 30.72 μm^2, $p<0.001$). These data suggest that adipocytes within DS mammary fat pad are hypertrophic compared to DR adipocytes.

Adipocytes are induced to differentiate through action of peroxisome proliferator activated receptor (PPAR)-γ, and clinically obese populations have been previously reported to have impaired ability to stimulate adipocyte differentiation (55). To evaluate whether PPARγ expression was altered in DS vs. DR rats, we evaluated expression of this protein in cancer-free mammary gland. As shown in **Figure 28A**, PPARγ was strongly suppressed in DS mammary gland, suggesting that DS rats may have an impaired ability to stimulate preadipocytes to differentiate into mature adipocytes. Therefore, dealing with chronic positive energy balance in DS rats would be accomplished through hypertrophy of existing adipocytes as opposed to recruitment and differentiation of preadipocytes.

Fatty acid binding protein (FABP)-4 is induced by PPARγ and is frequently used as a marker for mature adipocytes. FABP-4 functions to scavenge fatty acids and thus attenuates PPARγ activity (231). Recently, Queipo-Ortuño *et al.* reported that FABP-4 expression was decreased in subcutaneous fat from obese vs. lean healthy individuals (232). However, as shown in **Figure 28A,** no difference was observed in FABP-4 expression between DR and DS rats.

In the Queipo-Ortuño study, FABP-4 expression in subcutaneous adipose tissue was most strongly correlated with adipose triglyceride lipase expression (232). Thus, this data suggests that although DS rats have larger adipocytes, DS and DR rats may have similar rates of lipolysis. Higher rates of lipolysis generally correspond to an inflammatory adipocyte phenotype.

Several studies have described the presence of crown-like structures (CLS) in obese humans and mice, in which macrophages surround a distressed, dying, or dead adipocyte

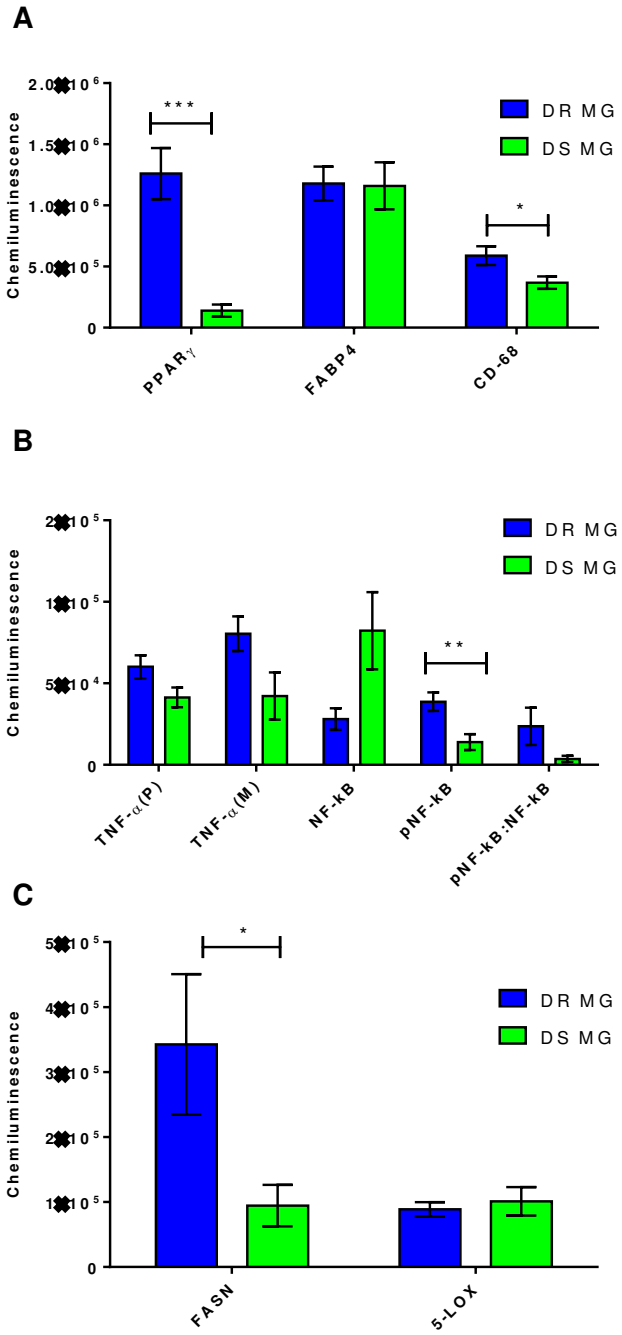

Figure 28
Legend. DS rats do not display evidence of mammary gland inflammation. Lysate from N=6 each DR and DS mammary gland were evaluated for expression of lipid regulatory proteins (Panel A) and inflammatory signaling proteins (Panels B and C) using capillary electrophoresis-based Western blot technology for signal detection. Values are mean chemiluminescence ± SEM, normalized to total protein concentration in lysate.

(222;223;233;234). Quantitation of CLS in rats of the age that were investigated is difficult as these structures occur with very low frequency. As an alternative, expression of the macrophage marker CD-68 was evaluated in mammary gland lysate. Contrary to what would be expected in the presence of chronic inflammation in DS rats, expression of CD-68 was significantly reduced in the mammary gland of DS compared to DR rats as shown in **Figure 28A**, suggesting that DS mammary glands do not have increased macrophage infiltration compared to DR rats.

5.B.7. DS rats do not display elevated inflammatory cytokine expression

Next, expression of several inflammatory markers was evaluated in mammary gland of DR compared to DS rats. The binding of TNF-α binding to its receptor stimulates activity of the inhibitor of kinase kinase (IKK), which activates transcriptional activity of "the central regulator of inflammation", NF-kB (235). As shown in **Figure 28B**, precursor (P) and mature (M) forms of TNF-α were similar between DR and DS rats. Whereas total NF-kB was elevated, expression of phospho-NF-kB and the ratio of phospho: total NF-kB (representing activated NF-kB) was suppressed in the mammary gland of DS compared to DR rats. IL-6 was not detected in mammary gland from ovary intact DR and DS rats. These data suggest that DS rats do not display elevated inflammatory cytokine expression compared to DR rats.

Fatty acid synthase (FASN) and 5-lipoxygenase (LOX) are enzymes that produce lipid species involved in inflammatory signaling cascades. As shown in **Figure 28C**, expression of FASN was significantly reduced in DS compared to DR mammary gland. DS and DR rats displayed similar levels of 5-LOX expression, suggesting that enzymes involved in inflammatory lipid species production did not differ between DR and DS rats.

5.B.8. Tumors from DS rats do not display evidence of IL-6 signaling

IL-6 is associated with increased risk of breast cancer. However, we could not detect a signal corresponding to IL-6 in lysate from DR or DS rat mammary gland. The binding of IL-6 to its membrane receptor causes activation of the signal transducer and activator of transcription (STAT)-3 signaling molecule, which is associated with cancer cell survival and proliferation (63). Nearly all immortalized breast cancer cell lines and approximately 50-60% of primary breast cancers display constitutive activation of STAT3 signaling (236).

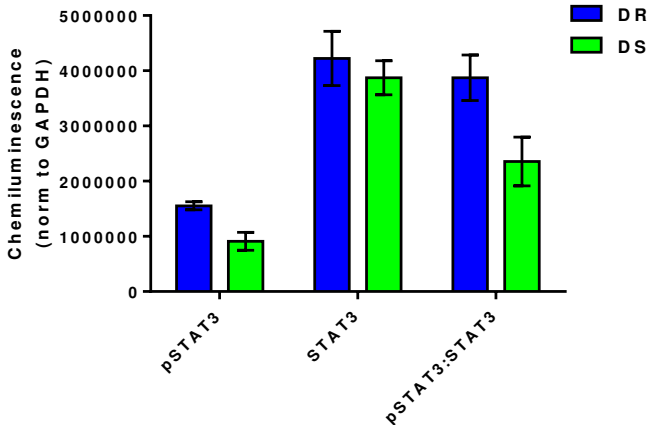

Figure 29
Legend. Lysate from N=6 each DR and DS tumor lysate was evaluated via capillary electrophoresis using the Protein Simple Wes system. Chemiluminescent signal was normalized to GAPDH.

Using STAT3 as a proxy to IL-6 activity, we evaluated expression of total and phospho-STAT-3 in lysate from ovary intact DR and DS tumors. In keeping with results from the mammary gland, as shown in **Figure 29**, DS tumors displayed significantly reduced phospho-STAT-3, suggesting that IL-6 pro-inflammatory activity is not higher in DS tumors.

Taken together, these experiments failed to find evidence in support of the chronic inflammation "line of code" as an obligatory mechanism whereby obesity promotes mammary carcinogenesis in DS rats.

5.C. Conclusions

The data reported in this chapter are consistent with previous findings of Levin that DS rats display alterations in insulin signaling and adipokine expression at the host systemic level; however, little

evidence was found to support host systemic factors in linking the enhanced carcinogenic response to obesity in DS rats. Moreover, while chronic inflammation is reported to be a mechanism whereby obesity increases breast cancer risk, we found no evidence that adipocyte hypertrophy in the mammary gland of DS rats was associated with inflammation in the adipose tissue surrounding the mammary epithelium. To rephrase, chronic inflammation that accompanies obesity may be permissive for breast carcinogenesis, but it does not appear to be obligatory for the heightened cancer response observed in DS rats.

Taken together, the data presented in Chapters 2-5 represent the initial experiments to identify mechanisms whereby obesity promotes mammary carcinogenesis in the DS Levin rat strain. These findings are summarized in Chapter 6, and a clinical corollary to our rat model is considered. Future direction of this research is discussed in two contexts. First, the next logical sets of experiments for the Levin DS project are summarized as specific aims, as an extension of this project in the current laboratory. Next, my research in pursuit of mechanisms that link obesity and breast cancer is discussed in the context of my postdoctoral fellowship. Finally, the impact and utility of our integrated rat model is discussed as a tool for translational preclinical research in the field of obesity and breast cancer research.

CHAPTER 6: SUMMARY, FUTURE DIRECTION, AND CONCLUSIONS

6.A. Summary

6.A.1. Chapter 1: Overview

Breast cancer is a deceptively simple term that encompasses a highly complex, widely heterogeneous disease process that develops decades after the initial transformation of a normal cell to a cell with neoplastic potential. Likewise, most cases of obesity develop as a consequence of chronic consumption of small caloric excesses. In spite of the "magic bullet" mentality that seems pervasive in cancer research, no preclinical tool has been found to be solely sufficient to model the relationship between obesity and breast cancer. Each model has benefits and drawbacks. Rather than searching for a perfect preclinical model, as researchers, our goal should be to utilize the strengths of many models to provide complementary data that can be used to deconstruct the impact of obesity on breast cancer risk and outcomes.

6.A.2. Chapter 2: Obesity accelerates mammary carcinogenesis in DS rats

The initial findings from a novel rat model of obesity and breast cancer are reported, in which the Levin strains of rats, which display different polygenic susceptibility to diet-induced weight gain, are integrated with a polygenic model of mammary carcinogenesis. Acceleration of chemically induced mammary carcinogenesis was observed in obesity resistant (DR) compared to obesity susceptible (DS) rats. Compared to DR rats, DS rats displayed a 16% reduction in cancer latency, a 26% increase in cancer incidence, a 2.5-fold increase in cancer multiplicity, and a 5.4-fold increase in cancer burden. Contrary to our expectations, 34.9% of DS tumors were negative for expression of the progesterone receptor (PR), in comparison to 22.8% of DR tumors (odds ratio =1.78 (0.83–3.81; p=0.134)). This finding has clinical relevance, as hormone receptor negative breast cancers are associated with high cancer aggressiveness

and corresponding poor prognosis. As obese women with breast cancer are more likely to have larger tumors compared to their lean counterparts, we focused on elucidating mechanisms responsible for the increased cancer burden in DS rats.

6.A.3. Chapter 3: DS favors faster tumor growth via accelerated cell cycle transit and reduced apoptotic efficiency

In normal, non-cancerous tissues, size is held in homeostasis through tight regulation of the processes of proliferation and death. Experiments were designed to determine the balance between these processes in cancer cells from DR and DS tumors. DS tumors had higher prevalence of mitotic figures (DR 0.453 ± 0.030; DS 0.581 ± 0.057 mitotic figures per 100 cells; p=0.173), as a marker of proliferation, and higher prevalence of apoptotic bodies (DR 1.877 ± 0.192, N=20; DS 2.549 ± 0.252 apoptotic cells per 100 cells, N=20, p<0.01), as a marker of cell death. Immunohistochemical analyses revealed that DS tumors do not have a higher percentage of cells that express Ki67, a proliferative marker (DR N=20, 9.0% ± 0.7; DS N=20, 9.4% ± 0.9, p=0.41). However, when Ki67 expression was combined with prevalence of mitotic figures, it was observed that more mitotic figures were present than could be accounted for with a 24-hour estimated cell cycle duration. This led to the concept that DS tumors display shorter cell cycle duration, which is consistent with the markedly larger mass of the tumors in DS rats.

To identify cellular machinery that enables the faster growth rate of DS tumors, expression of the proteins that regulate the G1/S transition in the cell cycle was investigated. DS tumors displayed hyperphosphorylation of retinoblastoma protein (Rb) accompanied by release of the E2F1 transcription factor. Free E2F1 induces transcription of proteins required for transition into S phase as evidenced by overexpression of cdc6, a protein required for cell cycle progression that contains an E2F1-binding site in its promoter, in DS compared to DR rat tumors.

To determine whether the increased apoptosis in DS tumors was accomplished through the intrinsic vs. extrinsic pathways of apoptosis induction, the activity of a panel of caspases was assessed, but no differences were observed, leading us to question how increased apoptosis could occur in the absence of increased caspase activity. This puzzle was resolved with the finding that DS tumors had over 5X higher expression of X-linked inhibitor of apoptosis protein (XIAP), which inhibits the activity of the executioner caspases, including caspase 3. This finding informs the trend towards longer apoptotic duration that was identified in DS compared to DR tumors (DR 4.7 ± 0.6 hrs; DS 5.9 ± 1.0 hrs; p=0.306). Thus, the apoptotic process may take longer to accomplish in DS compared to DR tumors due to competition between pro-apoptotic and anti-apoptotic signals; i.e., DS tumors may have impaired apoptotic efficiency.

6.A.4. Chapter 4: obesity in DS rats promotes hormone-receptor negative mammary carcinogenesis in the absence of peripheral estrogen production

One of the dominant mechanisms proposed to link obesity to breast cancer in postmenopausal women centers on peripheral production of sex hormone within adipose tissue. Locally produced estrogen is hypothesized to stimulate the growth of breast cancer cells, due to the proximity of epithelial cells to adipocytes in the breast tissue. Removal of the primary source of sex hormones via ovariectomy in rats selects for a population of cells that can grow in the absence of high levels of estrogen. In ovariectomized (OVX) rats, obesity in DS-OVX rats was associated with a 1.7-fold increase in cancer multiplicity and a 2.6-fold increase in cancer burden compared to DR-OVX rats. These data suggest that obesity can promote mammary carcinogenesis in hormone receptor-negative cell populations.

Several experiments failed to generate evidence in support of peripheral production of estrogens by fat tissue in the female rat. First, <1% of cancer cells in tumors from both DR-OVX and DS-OVX rats were

positive for expression of the progesterone receptor (PR), which is a measure of functional estrogen activity. Obesity in DS-OVX rats did not increase this percentage, as would be expected with expansion of an estrogen-responsive cell population in the presence of abundant peripheral estrogen production. Secondly, no aromatase was detected at the transcriptional (mRNA) or translational (protein) level in mammary gland from either DR-OVX or DS-OVX rats. Finally, there was no difference in concentration of progesterone, a sex hormone whose expression is induced by estrogen signaling, in plasma from DR-OVX vs. DS-OVX rats, suggesting that peripheral estrogen production is not a method whereby a significant amount of estrogen is produced in our rat model. Collectively, the data indicate that estrogen is not obligatory for the effect of obesity on promoting mammary carcinogenesis in DS rats.

6.A.5. Chapter 5: Host systemic factors do not explain the link between obesity and breast carcinogenesis

Experiments were conducted to investigate the obesity-breast cancer link at the host systemic level relative to mechanistic processes of chronic inflammation, deregulated insulin signaling, and altered adipokine expression. Multivariate analyses failed to provide evidence in support of a linkage between these factors and cancer at the host systemic level. Additional experiments were performed to assess the likelihood that circulating factors in DS serum would affect hormone receptor negative disease in a cell culture model. Treatment of LA7 cells, an ER/PR- rat mammary cancer stem cell line derived from a rat mammary adenocarcinoma, with DS serum failed to stimulate the growth of these cells in either a concentration (% serum) or body weight (of the DS rat)-dependent manner. Likewise, co-culture of LA7 cells with primary adipocytes from DS mammary gland did not stimulate cancer cell growth.

Unexpectedly, at the host systemic level, there were no differences between circulating levels of inflammatory cytokines TNF-α, IL-6, IL-1β, or C-reactive protein between DR and DS rats. To pursue this finding at the local (mammary gland) and cellular (tumor) level, the mammary gland of DS rats displayed

adipocyte hypertrophy (DS 1560 ± 83.09 μm^2, DR 1127 ± 30.72 μm^2, $p<0.001$). However, contrary to what is generally reported in the literature, adipocyte hypertrophy was not associated with macrophage infiltration based on expression of macrophage marker CD-68. Evaluation of inflammatory signaling proteins revealed that NF-kB and TNF-α were not increased in DS compared to DR. As IL-6 was not detectable within the mammary gland, we evaluated activity (phosphorylation) of the signal transducer and activator of transcription (STAT)-3 protein. Activation of STAT-3 was significantly reduced in DS tumors compared to DR tumors, consistent with the other evidence that inflammation is not driving the carcinogenic process in DS rats. Collectively, these data failed to support an obligatory role for chronic inflammation as a dominant mechanism whereby obesity promotes mammary carcinogenesis.

6.A.6. Synthesis

The data presented in this dissertation represents the initial set of findings on mechanisms whereby susceptibility to excessive weight gain resulting in obesity increases mammary carcinogenesis in diet-induced obesity susceptible (DS) Levin rats. The evidence in support of or contradictory to the four mainstream hypotheses proposed to link obesity and breast cancer is summarized in Table 7.

Table 7
Legend. Summary of experimental data generated in support or to the contrary of the four mainstream hypothesized to link obesity to breast cancer.

1. Peripheral estrogen production	**Evidence in support**	**Evidence to the contrary**
Host systemic	None	Ch. 4: no difference between circulating levels of progesterone, SHBG: progesterone ratio in DS vs. DR
Local (mammary gland)	None	Ch. 4: aromatase mRNA not detected in DS or DR mammary gland Ch. 4: aromatase protein not detected in DS or DR mammary gland
Cell autonomous	None	Ch. 2: increase in number of tumors classified as PR- in DS rats Ch. 2: % PR-positive cells inversely

		correlated with tumor growth rate Ch. 4: obesity in DS does not increase % PR-expressing cells
2. Chronic inflammation	**Evidence in support**	**Evidence to the contrary**
Host systemic	Ch. 5: trend towards increased IL-6, IL-1β, and	Ch. 5: Plasma pro-inflammatory cytokines unaffected
Local (mammary gland)	Ch. 5: adipocyte hypertrophy	Ch. 5: CD-68 macrophage marker lower in DS compared to DR mammary gland Ch. 5: inflammatory cytokine and lipid production machinery similar in DS rats Ch. 5: co-culture of rat mammary cancer stem cells with primary mammary gland adipocytes does not stimulate cell proliferation
Cell autonomous	None	Ch. 5: STAT3 is not activated as a proxy to IL-6 activity in DS tumors
3. Deregulated insulin signaling	**Evidence in support**	**Evidence to the contrary**
Host systemic	Ch. 5: increased circulating insulin, IGF-1, IGF-1: IGFBP-3	Ch. 5: serum from DS rats does not stimulate proliferation of rat mammary cancer stem cells Ch. 5: circulating insulin, IGF-1 not associated with cancer multiplicity and burden in multivariate model
Local (mammary gland)	N/A	N/A
Cell autonomous	N/A	N/A
4. Altered adipokine expression	**Evidence in support**	**Evidence to the contrary**
Host systemic	Ch. 5: increased leptin, decreased adiponectin: leptin ratio	Ch. 5: serum from DS rats does not stimulate growth of rat mammary cancer stem cells
Local (mammary gland)	N/A	Ch. 5: co-culture of rat mammary cancer stem cells with primary mammary gland adipocytes does not stimulate cell proliferation
Cell autonomous	N/A	N/A

The integrated rat model for obesity and breast cancer appears to be a valuable tool for deconstructing links between these diseases with the potential for unearthing previously unrecognized mechanisms. Our findings do not support a role for peripheral estrogen production or chronic inflammation as key mechanisms underlying the heightened cancer response observed in DS rats; however, this evidence

does not per se mean that those mechanisms are not operative in human disease. Rather, estrogen signaling and chronic inflammation may be permissive, as opposed to obligatory, processes that link obesity to breast cancer. Our findings suggest that mechanisms functioning at the level of tumor cells, as opposed to the host systemic level, are likely involved in linking obesity to breast cancer. Elucidation of these mechanisms at the cellular level will have translational significance in subpopulations of obese women who develop poor prognosis molecular subtypes of breast cancer.

6.A.7. Translational implications

A provocative finding of the experiments reported in this dissertation was that excessive weight gain leading to obesity promoted growth of hormone receptor-negative cancer. This finding is of clinical importance given the mixed clinical literature regarding whether obesity promotes predominantly hormone receptor-positive vs. -negative breast cancer. Hormone receptor-negative breast cancer is less common than luminal, receptor-positive breast cancer. However, hormone receptor-negative breast tumors are more frequently deadly, being associated with increased tumor aggressiveness, higher rates of metastasis, and reduced disease-free and overall survival. These data suggest that our integrated rat model may provide a tool with which to interrogate mechanisms that drive hormone-independent breast carcinogenesis within specific subpopulations of obese women.

6.B. Future Direction

Future studies will focus on determining how obesity-related factors influence pro-carcinogenic signaling processes—to rephrase, how are external factors talking to internal signaling cascades? Hormone receptor-negative tumors can be divided into two subgroups: tumors that overexpress the human epidermal growth factor receptor (Her)-2 (ER/PR-/Her2+) and tumors that are triple negative (ER/PR/Her2-). More than 70% of breast tumors that fall into the triple negative clinical subtype

overexpress Her1 (237), also called epidermal growth factor receptor (EGFR). EGFR and Her2 belong to the same receptor erbB/Her receptor family, and overexpression or constitutive activity of EGFR or Her2 has been associated with cancer aggressiveness, poor prognosis, and reduced overall and disease-free survival (238;239).

EGFR and Her2 function most effectively as heterodimers, as Her2 cannot bind ligand and is dependent on heterodimerization with other growth factor receptors for signal transduction. In addition to heterodimerization between erbB/Her family members, heterodimers can form with insulin-like growth factor receptor (IGF-1R) and the leptin receptor (Ob-R) (240). As obese DS rats were demonstrated to have elevated circulating insulin, IGF-1, and leptin in our studies, crosstalk between Her2/EGFR, insulin, and leptin signaling on the growth of hormone-independent tumors remains an important mechanism to investigate.

6.B.2. ***Specific Aim 1:*** *What growth factor receptors are expressed and actively signaling in tumors from ovariectomized DR and DS rats?*

Specific Aim 1 Approach: Using tumors from Chapter 4's ovariectomized DR and DS rats, expression and activation (phosphorylation) of Her2, EGFR, IGF-1R, the insulin receptor (IR), and ObR will be determined via immunohistochemistry. As ErbB/Her-containing heterodimers signal through the metabolic PI3K/Akt/mTOR pathway and the mitogenic Ras/Raf/MEK/ERK pathway, expression of S6 kinase/eIF-4E and c-myc/CREB will be used as proxies to activity of the metabolic and mitogenic signaling pathways, respectively. To determine whether crosstalk exists between erbB/Her family members and insulin/leptin signaling, Her2 and EGFR will be immunoprecipitated followed by immunoblotting against IGF-1R, IR, and ObR. To confirm the outcomes of these experiments at the histological level, immunofluorescence will be used to visualize co-localization of Her2, EGFR, IGF-1R, and ObR in tumors.

The experiments proposed for Aim 1 will establish whether Her2 and EGFR signaling is active in DS hormone-receptor negative tumors. Moreover, Aim 1 will provide additional evidence on the potential for deregulated insulin signaling and altered adipokine expression as mechanisms driving tumor growth in DS rats, steering future experiments either deeper into these mechanisms, or informing researchers that they should search for additional, less mainstream mechanisms.

6.B.3. ***Specific Aim 2:*** *Does interruption of growth factor receptor signaling impair the ability of obesity to promote estrogen-independent tumor growth?*

Specific Aim 2 Approach: To evaluate whether evasion of growth suppression via inhibition of erbB/Her family signaling is due to plasticity among erbB/Her family members in DS rats, future studies will treat ovariectomized MNU-injected DR and DS rats with monoclonal antibodies against Her2 (trastuzumab) or EGFR (cetuximab). Tumors will be assessed via immunohistochemistry for expression of Her2, EGFR, IGF-1R, and ObR, and via immunoblotting for expression of S6 kinase, EIF4E, c-myc, and CREB.

If targeting erbB/Her signaling with antibody therapy does not significantly reduce tumor growth in conjunction with reduced Her2/EGFR expression, these data would suggest that escape from growth suppression is accomplished via erbB/Her family member plasticity and/or upregulation of IGF-1R or ObR (leptin receptor). Insulin and leptin as escape mechanisms from growth suppression will be further assessed using transgenic mice. Mice selectively bred for polygenic obesity susceptibility, similar to Levin's breeding strategy, will be interbred with the strain Tg(MMTV-Erbb2)^{NK1Mul}/J, modeling the Her2-overexpressing breast tumor subtype, or with the strain Tg(Kras)^{tm4Tyj}/J, modeling the triple negative breast tumor subtype, depending on the findings of Aim 1. Mice with conditional mammary gland deletion of IGF-1R and ObR will be used in combination with the DR-like and DS-like selectively bred mice, allowing for evaluation of whether ablation of these signaling pathways ameliorates the

heightened cancer response. These experiments set the stage for the next set of experiments, in which insulin and leptin signaling will be reduced via weight gain prevention or weight loss. If conditional deletion of IGF-1R or ObR does not halt growth of hormone receptor-negative tumors, but weight gain prevention or weight loss does halt tumor growth, this would suggest that obesity-related factors other than insulin or leptin are promoting tumor growth.

6.B.4. ***Specific Aim 3:*** *Does prevention of weight gain or weight loss protect against the increased cancer response in DS rats, and are these interventions are equally protective?*

DS Levin rats display polygenic susceptibility to development of obesity and heightened cancer response to a chemical carcinogen. Two questions remain unknown: 1) is weight loss sufficient to reverse the epigenetic reprogramming that occurs as a result of chronic positive energy balance?; and 2) is polygenic obesity susceptibility of DS rats sufficient to confer increased cancer response in the absence of actual weight gain? To address these questions, ovariectomized carcinogen-injected rats will be subjected to one of two protocols: 40% energy restriction beginning at 60 days of age, the point at which DR and DS rat body weights significantly diverge; or pair-feeding starting at 21 days of age to maintain similar body weights as DR rats. If obesity susceptibility alone (i.e., prevention of weight gain) does not confer increased cancer response, then the epigenetic changes that occur with progressive weight gain over time are likely responsible for promoting cancer growth.

ELISA will be used determine whether weight loss and weight gain prevention induce equivalent reductions in insulin, IGF-1, and leptin, as both strategies were previously reported by Levin to induce favorable changes in male rats (241;242). Immunohistochemistry will be used to evaluate expression and phosphorylation of Her2 and EGFR, and immunoblotting will be used to evaluate expression of S6 kinase, EIF4E, c-myc, and CREB as proxies to functional activity of erbB/Her signaling. According to Levin,

DS rats display elevated insulin and leptin compared to DR rats prior to becoming obese (243). Therefore, if insulin or leptin signaling are obligatory mechanisms whereby obesity promotes mammary carcinogenesis in DS rats, prevention of weight gain or weight loss will likely not affect cancer response.

Regardless of whether weight loss or weight gain prevention is associated with reduced cancer response in DS rats, these studies can be used to generate hypotheses for additional lines of investigation. Specifically, if weight loss does reduce the cancer response, evaluation of the methylome using comprehensive high-throughput arrays for relative methylation (CHARM) (244) in tumors from DS ad lib-fed animals and DS weight loss will provide a list of genes whose change in methylation status is likely associated with this favorable response. Conversely, if weight loss does not attenuate the increased cancer response in DS rats, genes that differ in methylation status can probably be ruled out as important factors in promoting tumor growth, allowing researchers to focus on genes whose methylation pattern is unchanged in response to weight loss.

The experiments proposed for Aim 3 will reveal whether weight loss or prevention of weight gain in DS rats protects against the increased cancer response. Moreover, these experiments will indicate whether two methods of weight control have equivalent effects on cancer response, metabolic parameters, and expression and activity of growth factor receptors that may be acting to promote growth of hormone receptor-negative mammary tumors. These experiments will pave the way for the next generation of experiments seeking to deconstruct the complex link between obesity and breast cancer in a preclinical model.

6.C. Conclusions

The transformation of a normal cell to a cell with neoplastic potential can be thought of in the context of a stopwatch. In order to start ticking, the stopwatch requires programming. Within the stopwatch analogy, the four most widely accepted mechanisms proposed to link obesity to breast cancer can be thought of as "lines of code" that may be responsible for promoting cancer growth in specific subpopulations of women. These are: 1) peripheral production of estrogen; 2) chronic inflammation; 3) deregulated insulin signaling, and 4) altered adipokine expression.

However, each stopwatch is different. Every tumor can have a unique combination of driver and passenger mutations in addition to epigenetic regulation of the hallmarks that enable cancer growth. Thus, these 4 mechanistic hypotheses are unlikely to explain the link between obesity and breast cancer in all women. Indeed, the experiments conducted herein failed to provide evidence in support of two of these four mechanisms in the increased cancer response conferred by obesity in DS rats and provided only weak evidence for the remaining two mechanisms.

Like most dissertations, these initial experiments, seeking to elucidate mechanisms behind the promotion of breast carcinogenesis by obesity in the Levin rat model, have generated more questions than answers. The core message of this dissertation can be summarized as follows: breast cancer is a heterogeneous disease, and more effort is needed to characterize specific subpopulations of women with breast cancer.

This dissertation highlights the fact that the link between obesity and breast cancer is complex, heterogeneous, and, most importantly, remains poorly understood. More work is required to determine how obesity promotes estrogen-independent cancer cell growth in subpopulations of women with

hormone receptor-negative tumors. To this end, I will be continuing my research in the breast cancer field by studying breast cancer stem cells at the University of Colorado Health Sciences Center in Aurora, working under the mentorship of Dr. Carol Sartorius. My research will focus on the metabolic requirements of breast cancer stem cells.

In summary, this dissertation provides the initial set of experiments interrogating the effects of obesity in a breast cancer model with potential value to a wide range of researchers, from basic scientists to clinicians, in which to study the impact of excess weight and adiposity on mammary carcinogenesis. Given the rapidity of tumor development, this model provides a rapid, cost-effective platform on which to conduct preclinical research into the effects of obesity on malignancies of the breast. Finally, the integrated Levin model represents a preclinical tool that facilitates investigation of unrecognized mechanisms beyond those traditionally accepted to link obesity to carcinogenesis of the breast, in an effort to identify clinical subpopulations at high risk of breast cancer whose disease is not explained via those mechanisms that are commonly cited.

REFERENCE LIST

1. Ferlay J, Soerjomataram I, Dikshit R, Eser S, Mathers C, Rebelo M, Parkin DM, Forman D, Bray F. Cancer incidence and mortality worldwide: sources, methods and major patterns in GLOBOCAN 2012. Int.J Cancer 2015 Mar 1;136(5):E359-E386.

2. American Cancer Society. Cancer Facts and Figures 2012. 2012.

3. Beyond *BRCA*: New hereditary breast cancer susceptibility genes. Cancer Treat.Rev. 2015;41(1):1-8.

4. Easton DF. How many more breast cancer predisposition genes are there? Breast Cancer Res 1999;1:14-7.

5. Shigenaga MK, Ames BN. Oxidants and mitogenesis as causes of mutation and cancer: the influence of diet. Basic.Life.Sci. 1993;61:419-36.

6. Ames BN, Shigenaga MK, Hagen TM. Oxidants, antioxidants, and the degenerative diseases of aging. Proc Natl.Acad.Sci.U.S.A 1993 Sep 1;90(17):7915-22.

7. Cooke MS, Evans MD, Dizdaroglu M, Lunec J. Oxidative DNA damage: mechanisms, mutation, and disease. FASEB J 2003 Jul;17(10):1195-214.

8. Rattan SI. Ageing--a biological perspective. Mol.Aspects.Med 1995;16(5):439-508.

9. Pitot HC. The language of oncology. In Fundamentals of Oncology. 4th ed. New York, NY: Marcel Dekker, Inc.; 2002. p. 27-40.

10. Pitot HC. The etiology of cancer: chemical and physical agents. In Fundamentals of Oncology. 4th ed. New York, NY: Marcel Dekker, Inc.; 2002. p. 41-106.

11. Pitot HC. The natural history of neoplastic development: initiation and promotion. In Fundamentals of Oncology. 4th ed. New York, NY: Marcel Dekker, Inc.; 2002. p. 223-72.

12. Pitot HC. The natural history of neoplastic development: progression. In Fundamentals of Oncology. 4th ed. New York, NY: Marcel Dekker, Inc.; 2002. p. 335-72.

13. Russo J, Russo IH. Atlas and Histologic Classification of Tumors of the Rat Mammary Gland. J.Mammary Gland Biol.Neoplasia 2000;5(2):187-200.

14. Hanahan D, Weinberg RA. The hallmarks of cancer. Cell 2000 Jan 7;100(1):57-70.

15. Hanahan D, Weinberg RA. Hallmarks of cancer: the next generation. Cell 2011 Mar 4;144(5):646-74.

16. Watson IR, Takahashi K, Futreal PA, Chin L. Emerging patterns of somatic mutations in cancer. Nat.Rev.Genet. 2013 Oct;14(10):703-18.

17. Elsheikh SE, Green AR, Rakha EA, Powe DG, Ahmed RA, Collins HM, Soria D, Garibaldi JM, Paish CE, Ammar AA, et al. Global histone modifications in breast cancer correlate with tumor phenotypes, prognostic factors, and patient outcome. Cancer Res 2009 May 1;69(9):3802-9.

18. Holst CR, Nuovo GJ, Esteller M, Chew K, Baylin SB, Herman JG, Tlsty TD. Methylation of p16(INK4a) promoters occurs in vivo in histologically normal human mammary epithelia. Cancer Res 2003 Apr 1;63(7):1596-601.

19. Widschwendter M, Fiegl H, Egle D, Mueller-Holzner E, Spizzo G, Marth C, Weisenberger DJ, Campan M, Young J, Jacobs I, et al. Epigenetic stem cell signature in cancer. Nat.Genetics 2006;39:157-8.

20. Basse C, Arock M. The increasing roles of epigenetics in breast cancer: Implications for pathogenicity, biomarkers, prevention and treatment. Int.J Cancer 2014 Nov 19.

21. Byler S, Goldgar S, Heerboth S, Leary M, Housman G, Moulton K, Sarkar S. Genetic and epigenetic aspects of breast cancer progression and therapy. Anticancer Res 2014 Mar;34(3):1071-7.

22. Breast Cancer in Men. Susan G. Komen; 2013 Jul 1. Report No.: KOMEED007800.

23. Vucenik I, Stains JP. Obesity and cancer risk: evidence, mechanisms, and recommendations. Ann.N.Y.Acad.Sci. 2012 Oct;1271:37-43.

24. World Health Organization. Obesity and overweight. 2011.

25. Wiseman M. The second World Cancer Research Fund/American Institute for Cancer Research expert report. Food, nutrition, physical activity, and the prevention of cancer: a global perspective. Proc Nutr.Soc 2008 Aug;67(3):253-6.

26. Overweight and Obesity Statistics. NIH Publication No. 04-4158 Bethesda, MD: National Institute of Diabetes and Digestive and Kidney Diseases (NIDDK) of the National Institutes of Health (NIH); 2012 Oct 1.

27. Ford ES, Li C, Zhao G, Tsai J. Trends in obesity and abdominal obesity among adults in the United States from 1999-2008. International Journal of Obesity 2011 May;35(5):736-43.

28. Howell A, Anderson AS, Clarke RB, Duffy SW, Evans DG, Garcia-Closas M, Gescher AJ, Key TJ, Saxton JM, Harvie MN. Risk determination and prevention of breast cancer. Breast Cancer Res 2014;16(5):446.

29. Food, Nutrition, Physical Activity, and the Prevention of Cancer: a Global Perspective. Washington, D.C.: World Cancer Research Fund/ American Institute for Cancer Research; 7 A.D. Nov 1.

30. Renehan AG, Tyson M, Egger M, Heller RF, Zwahlen M. Body-mass index and incidence of cancer: a systematic review and meta-analysis of prospective observational studies. Lancet 2008 Feb 16;371(9612):569-78.

31. Berstad P, Coates RJ, Bernstein L, Folger SG, Malone KE, Marchbanks PA, Weiss LK, Liff JM, McDonald JA, Strom BL, et al. A case-control study of body mass index and breast cancer risk in white and African-American women. Cancer Epidemiol Biomarkers.Prev 2010 Jun;19(6):1532-44.

32. Cheraghi Z, Poorolajal J, Hashem T, Esmailnasab N, Irani AD. Effect of Body Mass Index on Breast Cancer during Premenopausal and Postmenopausal Periods: A Meta-Analysis. Plos One 2012 Dec 7;7(12).

33. Anderson GL, Neuhouser ML. Obesity and the Risk for Premenopausal and Postmenopausal Breast Cancer. Cancer Prevention Research 2012 Apr;5(4):515-21.

34. Gail MH, Brinton LA, Byar DP, Corle DK, Green SB, Schairer C, Mulvihill JJ. Projecting individualized probabilities of developing breast cancer for white females who are being examined annually. J Natl.Cancer Inst. 1989 Dec 20;81(24):1879-86.

35. Gail MH, Costantino JP, Pee D, Bondy M, Newman L, Selvan M, Anderson GL, Malone KE, Marchbanks PA, McCaskill-Stevens W, et al. Projecting individualized absolute invasive breast cancer risk in African American women. J Natl.Cancer Inst. 2007 Dec 5;99(23):1782-92.

36. Matsuno RK, Costantino JP, Ziegler RG, Anderson GL, Li H, Pee D, Gail MH. Projecting individualized absolute invasive breast cancer risk in Asian and Pacific Islander American women. J Natl.Cancer Inst. 2011 Jun 22;103(12):951-61.

37. Breast Cancer Risk Assessment Tool National Cancer Institute; 2011.

38. Kelsey JL, Gammon MD, John EM. Reproductive factors and breast cancer. Epidemiol Rev. 1993;15(1):36-47.

39. Warning signs of breast cancer Susan G. Komen; 15 A.D. Mar 24.

40. Cecchini RS, Costantino JP, Cauley JA, Cronin WM, Wickerham DL, Land SR, Weissfeld JL, Wolmark N. Body Mass Index and the Risk for Developing Invasive Breast Cancer among High-Risk Women in NSABP P-1 and STAR Breast Cancer Prevention Trials. Cancer Prevention Research 2012 Apr;5(4):583-92.

41. Cecchini RS, Costantino JP, Cauley JA, Cronin WM, Wickerham DL, Land SR, Weissfeld JL, Wolmark N. Body Mass Index and the Risk for Developing Invasive Breast Cancer among High-Risk Women in NSABP P-1 and STAR Breast Cancer Prevention Trials. Cancer Prevention Research 2012 Apr;5(4):583-92.

42. Cuzick J, Sestak I, Baum M, Buzdar A, Howell A, Dowsett M, Forbes JF. Effect of anastrozole and tamoxifen as adjuvant treatment for early-stage breast cancer: 10-year analysis of the ATAC trial. Lancet.Oncol. 2010 Dec;11(12):1135-41.

43. Sestak I, Distler W, Forbes JF, Dowsett M, Howell A, Cuzick J. Effect of body mass index on recurrences in tamoxifen and anastrozole treated women: an exploratory analysis from the ATAC trial. J Clin.Oncol. 2010 Jul 20;28(21):3411-5.

44. Morimoto LM, White E, Chen Z, Chlebowski RT, Hays J, Kuller L, Lopez AM, Manson J, Margolis KL, Muti PC, et al. Obesity, body size, and risk of postmenopausal breast cancer: the Women's Health Initiative (United States). Cancer Causes Control 2002 Oct;13(8):741-51.

45. Anderson GL, Neuhouser ML. Obesity and the risk for premenopausal and postmenopausal breast cancer. Cancer Prev Res (Phila) 2012 Apr;5(4):515-21.

46. Spencer EA, Appleby PN, Davey GK, Key TJ. Validity of self-reported height and weight in 4808 EPIC-Oxford participants. Public Health Nutr. 2002 Aug;5(4):561-5.

47. Loi S, Milne RL, Friedlander ML, McCredie MRE, Giles GG, Hopper JL, Phillips KA. Obesity and outcomes in premenopausal and postmenopausal breast cancer. Cancer Epidemiology Biomarkers & Prevention 2005 Jul;14(7):1686-91.

48. Carmichael AR. Obesity and prognosis of breast cancer. Obes.Rev. 2006 Nov;7(4):333-40.

49. Protani M, Coory M, Martin JH. Effect of obesity on survival of women with breast cancer: systematic review and meta-analysis. Breast.Cancer Res.Treat. 2010 Oct;123(3):627-35.

50. Ewertz M, Jensen M, Gunnarsdottir KA, Hojris I, Jakobsen EH, Nielsen D, Stenbygaard LE, Tange UB, Cold S. Effect of obesity on prognosis after early-stage breast cancer. J.Clin.Onc. 2011;29(1):25-31.

51. Danaei G, Vander HS, Lopez AD, Murray CJ, Ezzati M. Causes of cancer in the world: comparative risk assessment of nine behavioural and environmental risk factors. Lancet. 2005 Nov 19;366(9499):1784-93.

52. Bradshaw PT, Ibrahim JG, Stevens J, Cleveland R, Abrahamson PE, Satia JA, Teitelbaum SL, Neugut AI, Gammon MD. Postdiagnosis change in bodyweight and survival after breast cancer diagnosis. Epidemiology 2012 Mar;23(2):320-7.

53. Fuentes-Mattei E, Velazquez-Torres G, Phan L, Zhang F, Chou PC, Shin JH, Choi HH, Chen JS, Zhao R, Chen J, et al. Effects of obesity on transcriptomic changes and cancer hallmarks in estrogen receptor-positive breast cancer. J Natl.Cancer Inst. 2014 Jul;106(7).

54. Coussens LM, Werb Z. Inflammation and cancer. Nature 2002 Dec 19;420(6917):860-7.

55. Isakson P, Hammarstedt A, Gustafson B, Smith U. Impaired preadipocyte differentiation in human abdominal obesity: role of Wnt, tumor necrosis factor-alpha, and inflammation. Diabetes 2009 Jul;58(7):1550-7.

56. Cottam DR, Mattar SG, Barinas-Mitchell E, Eid G, Kuller L, Kelley DE, Schauer PR. The chronic inflammatory hypothesis for the morbidity associated with morbid obesity: Implications and effects of weight loss. Obesity Surgery 2004 May;14(5):589-600.

57. Shoelson SE, Herrero L, Naaz A. Obesity, inflammation, and insulin resistance. Gastroenterology 2007 May;132(6):2169-80.

58. Balistreri CR, Caruso C, Candore G. The role of adipose tissue and adipokines in obesity-related inflammatory diseases. Mediators.Inflamm. 2010;2010:802078.

59. Kanda H, Tateya S, Tamori Y, Kotani K, Hiasa K, Kitazawa R, Kitazawa S, Miyachi H, Maeda S, Egashira K, et al. MCP-1 contributes to macrophage infiltration into adipose tissue, insulin resistance, and hepatic steatosis in obesity. J Clin Invest. 2006 Jun;116(6):1494-505.

60. Skurk T, Alberti-Huber C, Herder C, Hauner H. Relationship between Adipocyte Size and Adipokine Expression and Secretion. J Clin Endocrinol.Metab. 2007;92(3):1023-33.

61. Lumeng CN, Bodzin JL, Saltiel AR. Obesity induces a phenotypic switch in adipose tissue macrophage polarization. J Clin Invest. 2007 Jan;117(1):175-84.

62. Hube F, Hauner H. The role of TNF-alpha in human adipose tissue: Prevention of weight gain at the expense of insulin resistance? Hormone and Metabolic Research 1999 Dec;31(12):626-31.

63. Hoene M, Weigert C. The role of interleukin-6 in insulin resistance, body fat distribution and energy balance. Obesity Reviews 2008 Jan;9(1):20-9.

64. Allin KH, Nordestgaard BG. Elevated C-reactive protein in the diagnosis, prognosis, and cause of cancer. Crit.Rev.Clin Lab.Sci. 2011 Jul;48(4):155-70.

65. Bochud M, Marquant F, Marques-Vidal PM, Vollenweider P, Beckmann JS, Mooser V, Paccaud F, Rousson V. Association between C-reactive protein and adiposity in women. J Clin Endocrinol.Metab. 2009 Oct;94(10):3969-77.

66. Nijhuis J, Rensen SS, Slaats Y, van Dielen FM, Buurman WA, Greve JW. Neutrophil activation in morbid obesity, chronic activation of acute inflammation. Obesity (Silver.Spring.) 2009 Nov;17(11):2014-8.

67. Furukawa S, Fujita T, Shimabukuro M, Iwaki M, Yamada Y, Nakajima Y, Nakayama O, Makishima M, Matsuda M, Shimomura I. Increased oxidative stress in obesity and its impact on metabolic syndrome. J Clin Invest. 2004 Dec;114(12):1752-61.

68. Pierce BL, Ballard-Barbash R, Bernstein L, Baumgartner RN, Neuhouser ML, Wener MH, Baumgartner KB, Gilliland FD, Sorensen BE, McTiernan A, et al. Elevated biomarkers of inflammation are associated with reduced survival among breast cancer patients. J Clin Oncol 2009 Jul 20;27(21):3437-44.

69. Sheen-Chen SM, Chen WJ, Eng HL, Chou FF. Serum concentration of tumor necrosis factor in patients with breast cancer. Breast Cancer Res Treat. 1997 May;43(3):211-5.

70. Grivennikov SI, Greten FR, Karin M. Immunity, Inflammation, and Cancer. Cell 2010 Mar 19;140(6):883-99.

71. Jin L, Yuan RQ, Fuchs A, Yao Y, Joseph A, Schwall R, Schnitt SJ, Guida A, Hastings HM, Andres J, et al. Expression of interleukin-1beta in human breast carcinoma. Cancer 1997 Aug 1;80(3):421-34.

72. Grivennikov SI, Greten FR, Karin M. Immunity, inflammation, and cancer. Cell 2010 Mar 19;140(6):883-99.

73. Bromberg J. Stat proteins and oncogenesis. J Clin Invest. 2002 May;109(9):1139-42.

74. Kunigal S, Lakka SS, Sodadasu PK, Estes N, Rao JS. Stat3-siRNA induces Fas-mediated apoptosis in vitro and in vivo in breast cancer. Int.J Oncol 2009 May;34(5):1209-20.

75. Astrup A, Finer N. Redefining type 2 diabetes: 'diabesity' or 'obesity dependent diabetes mellitus'? Obes.Rev. 2000;1(2):57-9.

76. Colditz GA, Willett WC, Rotnitzky A, Manson JE. Weight gain as a risk factor for clinical diabetes mellitus in women. Ann.Intern.Med 1995 Apr 1;122(7):481-6.

77. Clemmons DR. The relative roles of growth hormone and IGF-1 in controlling insulin sensitivity. J Clin Invest. 2004 Jan;113(1):25-7.

78. Savage DB, Petersen KF, Shulman GI. Disordered lipid metabolism and the pathogenesis of insulin resistance. Physiol Rev. 2007 Apr;87(2):507-20.

79. Ruan W, Kleinberg DL. Insulin-like growth factor I is essential for terminal end bud formation and ductal morphogenesis during mammary development. Endocrinology 1999 Nov;140(11):5075-81.

80. Neville MC, McFadden TB, Forsyth I. Hormonal regulation of mammary differentiation and milk secretion. J Mammary Gland Biol Neoplasia 2002 Jan;7(1):49-66.

81. Arcidiacono B, Iiritano S, Nocera A, Possidente K, Nevolo MT, Ventura V, Foti D, Chiefari E, Brunetti A. Insulin Resistance and Cancer Risk: An Overview of the Pathogenetic Mechanisms. Experimental Diabetes Research 2012;2012:1-12.

82. Chappell J, Leitner JW, Solomon S, Golovchenko I, Goalstone ML, Draznin B. Effect of insulin on cell cycle progression in MCF-7 breast cancer cells - Direct and potentiating influence. Journal of Biological Chemistry 2001 Oct 12;276(41):38023-8.

83. Creighton CJ, Casa A, Lazard Z, Huang S, Tsimelzon A, Hilsenbeck SG, Osborne CK, Lee AV. Insulin-like growth factor-I activates gene transcription programs strongly associated with poor breast cancer prognosis. J Clin.Oncol 2008 Sep 1;26(25):4078-85.

84. Gunter MJ, Hoover DR, Yu H, Wassertheil-Smoller S, Rohan TE, Manson JE, Li J, Ho GY, Xue X, Anderson GL, et al. Insulin, insulin-like growth factor-I, and risk of breast cancer in postmenopausal women. J Natl.Cancer Inst. 2009 Jan 7;101(1):48-60.

85. Gupta K, Krishnaswamy G, Karnad A, Peiris AN. Insulin: a novel factor in carcinogenesis. Am J Med.Sci. 2002 Mar;323(3):140-5.

86. Key TJ, Appleby PN, Reeves GK, Roddam AW. Insulin-like growth factor 1 (IGF1), IGF binding protein 3 (IGFBP3), and breast cancer risk: pooled individual data analysis of 17 prospective studies. Lancet.Oncol 2010 Jun;11(6):530-42.

87. Pollak M. Insulin and insulin-like growth factor signalling in neoplasia. Nature Reviews Cancer 2008 Dec;8(12):915-28.

88. Rose DP, Vona-Davis L. The cellular and molecular mechanisms by which insulin influences breast cancer risk and progression. Endocrine-Related Cancer 2012 Dec;19(6):R225-R241.

89. Goodwin PJ, Ennis M, Pritchard KI, Trudeau ME, Koo J, Madarnas Y, Hartwick W, Hoffman B, Hood N. Fasting insulin and outcome in early-stage breast cancer: results of a prospective cohort study. J Clin Oncol 2002 Jan 1;20(1):42-51.

90. Calori G, Lattuada G, Piemonti L, Garancini MP, Ragogna F, Villa M, Mannino S, Crosignani P, Bosi E, Luzi L, et al. Prevalence, metabolic features, and prognosis of metabolically healthy obese Italian individuals: the Cremona Study. Diabetes Care 2011;34(1):210-5.

91. Arita Y, Kihara S, Ouchi N, Takahashi M, Maeda K, Miyagawa J, Hotta K, Shimomura I, Nakamura T, Miyaoka K, et al. Paradoxical decrease of an adipose-specific protein, adiponectin, in obesity. Biochem.Biophys.Res Commun. 1999 Apr 2;257(1):79-83.

92. Maimoun L, Puech AM, Manetta J, Badiou S, Paris F, Ohanna F, Rossi M, Sultan C. Circulating leptin concentrations can be used as a surrogate marker of fat mass in acute spinal cord injury patients. Metabolism 2004 Aug;53(8):989-94.

93. Silha JV, Weiler HA, Murphy LJ. Plasma adipokines and body composition in response to modest dietary manipulations in the mouse. Obesity 2006 Aug;14(8):1320-9.

94. Harris HR, Tworoger SS, Hankinson SE, Rosner BA, Michels KB. Plasma Leptin Levels and Risk of Breast Cancer in Premenopausal Women. Cancer Prevention Research 2011 Sep;4(9):1449-56.

95. Wu MH, Chou YC, Chou WY, Hsu GC, Chu CH, Yu CP, Yu JC, Sun CA. Circulating levels of leptin, adiposity and breast cancer risk. Br.J Cancer 2009 Feb 24;100(4):578-82.

96. Jarde T, Caldefie-Chezet F, Damez M, Mishellany F, Penault-Llorca F, Guillot J, Vasson MP. Leptin and leptin receptor involvement in cancer development: A study on human primary breast carcinoma. Oncology Reports 2008 Apr;19(4):905-11.

97. Caldefie-Chezet F, Damez M, de LM, Konska G, Mishellani F, Fusillier C, Guerry M, Penault-Llorca F, Guillot J, Vasson MP. Leptin: a proliferative factor for breast cancer? Study on human ductal carcinoma. Biochem.Biophys.Res Commun. 2005 Sep 2;334(3):737-41.

98. Miyoshi Y, Funahashi T, Tanaka S, Taguchi T, Tamaki Y, Shimomura I, Noguchi S. High expression of leptin receptor mRNA in breast cancer tissue predicts poor prognosis for patients with high, but not low, serum leptin levels. International Journal of Cancer 2006 Mar 15;118(6):1414-9.

99. Garofalo C, Koda M, Cascio S, Sulkowska M, Kanczuga-Koda L, Golaszewska J, Russo A, Sulkowski S, Surmacz E. Increased expression of leptin and the leptin receptor as a marker of breast cancer progression: Possible role of obesity-related stimuli. Clinical Cancer Research 2006 Mar 1;12(5):1447-53.

100. Dubois V, Jarde T, Delort L, Billard H, Bernard-Gallon D, Berger E, Geloen A, Vasson MP, Caldefie-Chezet F. Leptin induces a proliferative response in breast cancer cells but not in normal breast cells. Nutr.Cancer 2014;66(4):645-55.

101. Yuan H, Sun K, Yu K. Leptin promotes the proliferation and migration of human breast cancer through the extracellular-signal regulated kinase pathway. Mol.Med.Reports 2014;9(1):350-4.

102. Lautenbach A, Budde A, Wrann CD, Teichmann B, Vieten G, Karl T, Nave H. Obesity and the associated mediators leptin, estrogen and IGF-I enhance the cell proliferation and early tumorigenesis of breast cancer cells. Nutr.Cancer 2009;61(4):484-91.

103. Palianopoulou M, Papanikolaou V, Stefanou N, Tsezou A. The activation of leptin-mediated survivin is limited by the inducible suppressor SOCS-3 in MCF-7 cells. Exp.Biol Med (Maywood.) 2011 Jan;236(1):70-6.

104. Knight BB, Oprea-Ilies GM, Nagalingam A, Yang L, Cohen C, Saxena NK, Sharma D. Survivin upregulation, dependent on leptin-EGFR-Notch1 axis, is essential for leptin-induced migration of breast carcinoma cells. Endocr.Relat.Cancer 2011 Aug;18(4):413-28.

105. Macis D, Guerrieri-Gonzaga A, Gandini S. Circulating adiponectin and breast cancer risk: a systematic review and meta-analysis. Int.J Epidemiol 2014 Aug;43(4):1226-36.

106. Miyoshi Y, Funahashi T, Kihara S, Taguchi T, Tamaki Y, Matsuzawa Y, Noguchi S. Association of serum adiponectin levels with breast cancer risk. Clinical Cancer Research 2003 Nov 15;9(15):5699-704.

107. Mantzoros C, Petridou E, Dessypris N, Chavelas C, Dalamaga M, Alexe DM, Papadiamantis Y, Markopoulos C, Spanos E, Chrousos G, et al. Adiponectin and breast cancer risk. Journal of Clinical Endocrinology & Metabolism 2004 Mar;89(3):1102-7.

108. Karaduman M, Bilici A, Ozet A, Sengul A, Musabak U, Alomeroglu M. Tissue levels of adiponectin in breast cancer patients. Medical Oncology 2007;24(4):361-6.

109. Yamauchi T, Kamon J, Minokoshi Y, Ito Y, Waki H, Uchida S, Yamashita S, Noda M, Kita S, Ueki K, et al. Adiponectin stimulates glucose utilization and fatty-acid oxidation by activating AMP-activated protein kinase. Nat.Med. 2002 Nov;8(11):1288-95.

110. Li FY, Cheng KK, Lam KS, Vanhoutte PM, Xu A. Cross-talk between adipose tissue and vasculature: role of adiponectin. Acta Physiol (Oxf) 2010 Nov 10.

111. Cleary MP, Ray A, Rogozina OP, Dogan S, Grossmann ME. Targeting the adiponectin:leptin ratio for postmenopausal breast cancer prevention. Front.Biosci.(Schol.Ed.) 2009;1:329-57.

112. Grossmann ME, Cleary MR. The balance between leptin and adiponectin in the control of carcinogenesis - Focus on mammary tumorigenesis. Biochimie 2012 Oct;94(10):2164-71.

113. Sedlacek SM, Wolfe P, Paul D, Lakoski S, Playdon M, McGinley JN, Matthews SB, Thompson HJ. Impact of Weight Loss and Dietary Pattern on Plasma Leptin and Adiponectin in Overweight-to-Obese Post Menopausal Breast Cancer Survivors. Nutrients 2015;In press.

114. Hair BY, Xu Z, Kirk EL, Harlid S, Sandhu R, Robinson WR, Wu MC, Olshan AF, Conway K, Taylor JA, et al. Body mass index associated with genome-wide methylation in breast tissue. Breast Cancer Res Treat. 2015 May 8.

115. Hair BY, Troester MA, Edmiston SN, Parrish EA, Robinson WR, Wu MC, Olshan AF, Swift-Scanlan T, Conway K. Body mass index is associated with gene methylation in estrogen receptor-positive breast tumors. Cancer Epidemiol Biomarkers.Prev 2015 Mar;24(3):580-6.

116. Xie H, Lim B, Lodish HF. MicroRNAs induced during adipogenesis that accelerate fat cell development are downregulated in obesity. Diabetes 2009 May;58(5):1050-7.

117. Blenkiron C, Goldstein LD, Thorne NP, Spiteri I, Chin SF, Dunning MJ, Barbosa-Morais NL, Teschendorff AE, Green AR, Ellis IO, et al. MicroRNA expression profiling of human breast cancer identifies new markers of tumor subtype. Genome.Biol 2007;8(10):R214.

118. Ali AS, Ali S, Ahmad A, Bao B, Philip PA, Sarkar FH. Expression of microRNAs: potential molecular link between obesity, diabetes and cancer. Obes.Rev. 2011 Dec;12(12):1050-62.

119. Ross SA, Davis CD. MicroRNA, nutrition, and cancer prevention. Adv.Nutr. 2011;2:472-85.

120. Smith WW, Thomas J, Liu J, Li T, Moran TH. From fat fruit fly to human obesity. Physiol.Behav. 2014 Sep;136:15-21.

121. Zheng J, Greenway FL. Caenorhabditis elegans as a model for obesity research. Int.J.Obes. 2012;36(186):194.

122. Farooqi IS, O'Rahilly S. Monogenic obesity in humans. Annu.Rev.Med 2005;56:443-58.

123. Konner AC, Bruning JC. Selective Insulin and Leptin Resistance in Metabolic Disorders. Cell Metabolism 2012 Aug 8;16(2):144-52.

124. Morris DL, Rui LY. Recent advances in understanding leptin signaling and leptin resistance. American Journal of Physiology-Endocrinology and Metabolism 2009 Dec;297(6):E1247-E1259.

125. Cummings DE, Schwartz MW. Genetics and pathophysiology of human obesity. Annu.Rev.Med 2003;54:453-71.

126. Cleary MP, Grande JP, Juneja SC, Maihle NJ. Diet-induced obesity and mammary tumor development in MMTV-neu female mice. Nutrition and Cancer-An International Journal 2004;50(2):174-80.

127. Cleary MP, Grande JP, Maihle NJ. Effect of high fat diet on body weight and mammary tumor latency in MMTV-TGF-alpha mice. International Journal of Obesity 2004 Aug;28(8):956-62.

128. Dogan S, Hu X, Zhang Y, Maihle NJ, Grande JP, Cleary MP. Effects of high-fat diet and/or body weight on mammary tumor leptin and apoptosis signaling pathways in MMTV-TGF-alpha mice. Breast Cancer Research 2007;9(6).

129. Russo J, Ao X, Grill C, Russo IH. Pattern of distribution of cells positive for estrogen receptor alpha and progesterone receptor in relation to proliferating cells in the mammary gland. Breast Cancer Res Treat. 1999 Feb;53(3):217-27.

130. Anderson E, Clarke RB. Steroid receptors and cell cycle in normal mammary epithelium. J Mammary Gland Biol Neoplasia 2004 Jan;9(1):3-13.

131. Althuis MD, Fergenbaum JH, Garcia-Closas M, Brinton LA, Madigan MP, Sherman ME. Etiology of hormone receptor-defined breast cancer: a systematic review of the literature. Cancer Epidemiol Biomarkers.Prev 2004 Oct;13(10):1558-68.

132. Fuhrman BJ, Schairer C, Gail MH, Boyd-Marin J, Xu X, Sue LY, Buys SS, Isaacs C, Keefer LK, Veenstra TD, et al. Estrogen metabolism and risk of breast cancer in postmenopausal women. J Natl.Cancer Inst. 2012;104(4):326-39.

133. Ziegler RG, Fuhrman BJ, Moore SC, Matthews CE. Epidemiologic studies of estrogen metabolism and breast cancer. Steroids. 2015 Feb 26.

134. Medina D, Thompson HJ. A comparison of the salient features of mouse, rat, and human mammary tumorigenesis. In: Ip MM, Asch BB, editors. Methods in Mammary Gland Biology and Breast Cancer Research. New York: Kluwer Academic/Plenum Publishers; 2000. p. 31-5.

135. Wagner KU. Models of breast cancer: quo vadis, animal modeling? Breast Cancer Research 2004;6(1):31-8.

136. Pierobon M, Frankenfeld CL. Obesity as a risk factor for triple-negative breast cancers: a systematic review and meta-analysis. Breast Cancer Res Treat. 2013;137:307-14.

137. Dietary Reference Intakes: Applications in Dietary Planning. National Academy of Sciences; Institute of Medicine; Food and Nutrition Board; 2003.

138. Diet-induced obesity (DIO) diets and phenotypes. The Jackson Laboratory; 2011.

139. Visvader JE. Keeping abreast of the mammary epithelial hierarchy and breast tumorigenesis. Genes.Dev. 2009 Nov 15;23(22):2563-77.

140. Singh M, McGinley JN, Thompson HJ. A comparison of the histopathology of premalignant and malignant mammary gland lesions induced in sexually immature rats with those occurring in the human. Lab.Invest. 2000 Feb;80(2):221-31.

141. MacLean PS, Higgins JA, Johnson GC, Fleming-Elder BK, Peters JC, Hill JO. Metabolic adjustments with the development, treatment, and recurrence of obesity in obesity-prone rats. American Journal of Physiology-Regulatory Integrative and Comparative Physiology 2004 Aug;287(2):R288-R297.

142. MacLean PS, Higgins JA, Jackman MR, Johnson GC, Fleming-Elder BK, Wyatt HR, Melanson EL, Hill JO. Peripheral metabolic responses to prolonged weight reduction that promote rapid, efficient regain in obesity-prone rats. American Journal of Physiology-Regulatory Integrative and Comparative Physiology 2006 Jun;290(6):R1577-R1588.

143. MacLean PS, Giles ED, Johnson GC, McDaniel SM, Fleming-Elder BK, Gilman KA, Andrianakos AG, Jackman MR, Shroyer KR, Schedin PJ. A Surprising Link Between the Energetics of Ovariectomy-induced Weight Gain and Mammary Tumor Progression in Obese Rats. Obesity 2010 Apr;18(4):696-703.

144. Giles ED, Wellberg EA, Astling DP, Anderson SM, Thor AD, Jindal S, Tan AC, Schedin PS, MacLean PS. Obesity and Overfeeding Affecting Both Tumor and Systemic Metabolism Activates the Progesterone Receptor to Contribute to Postmenopausal Breast Cancer. Cancer Research 2012 Dec 15;72(24):6490-501.

145. Levin BE, Dunn-Meynell AA, Balkan B, Keesey RE. Selective breeding for diet-induced obesity and resistance in Sprague-Dawley rats. Am.J Physiol. 1997 Aug;273(2 Pt 2):R725-R730.

146. Madsen AN, Hansen G, Paulsen SJ, Lykkegaard K, Tang-Christensen M, Hansen HS, Levin BE, Larsen PJ, Knudsen LB, Fosgerau K, et al. Long-term characterization of the diet-induced obese and diet-resistant rat model: a polygenetic rat model mimicking the human obesity syndrome. J Endocrinol. 2010 Sep;206(3):287-96.

147. Paulsen SJ, Jelsing J, Madsen AN, Hansen G, Lykkegaard K, Larsen LK, Larsen PJ, Levin BE, Vrang N. Characterization of beta-Cell Mass and Insulin Resistance in Diet-induced Obese and Diet-resistant Rats. Obesity 2010 Feb 10;18(2):266-73.

148. Thompson HJ, McGinley JN, Rothhammer K, Singh M. Rapid induction of mammary intraductal proliferations, ductal carcinoma in situ and carcinomas by the injection of sexually immature female rats with 1-methyl-1-nitrosourea. Carcinogenesis 1995 Oct;16(10):2407-11.

149. Beland FA, Poirier MC. DNA adducts and their consequences. In: Tardiff RG, Lohman PHM, Wogan GN, editors. Methods to Assess DNA Damage and Repair: Interspecies Comparisons. John Wiley & Sons Ltd; 1994. p. 29-55.

150. Sukumar S, McKenzie K, Chen Y. Animal models for breast cancer. Mutat.Res 1995 Dec;333(1-2):37-44.

151. Russo J, Wilgus G, Russo IH. Susceptibility of the Mammary Gland to Carcinogenesis: I. Differentiation of the Mammary Gland as Determinant of Tumor Incidence and Type of Lesion. Am J Pathol. 1992;96(3):721-32.

152. Swann PF, MAGEE PN. Nitrosamine-induced carcinogenesis. The alklylation of nucleic acids of the rat by N-methyl-N-nitrosourea, dimethylnitrosamine, dimethyl sulphate and methyl methanesulphonate. Biochem.J 1968 Nov;110(1):39-47.

153. Swann PF, MAGEE PN. Nitrosamine-induced carcinogenesis. The alkylation of N-7 of guanine of nucleic acids of the rat by diethylnitrosamine, N-ethyl-N-nitrosourea and ethyl methanesulphonate. Biochem.J 1971 Dec;125(3):841-7.

154. Swann PF. The rate of breakdown of methyl methanesulphonate, dimethyl sulphate and N-methyl-N-nitrosourea in the rat. Biochem.J 1968 Nov;110(1):49-52.

155. Macejova D, Brtko J. Chemically induced carcinogenesis: a comparison of 1-methyl-1-nitrosourea, 7,12-dimethylbenzanthracene,diethylnitroso-amine and azoxymethan models (minireview). Endocr.Regul. 2001 Mar;35(1):53-9.

156. Thompson HJ, Adlakha H. Dose-responsive induction of mammary gland carcinomas by the intraperitoneal injection of 1-methyl-1-nitrosourea. Cancer Res. 1991 Jul 1;51(13):3411-5.

157. Thompson HJ, Adlakha H, Singh M. Effect of carcinogen dose and age at administration on induction of mammary carcinogenesis by 1-methyl-1-nitrosourea. Carcinogenesis 1992 Sep;13(9):1535-9.

158. Matthews SB, Zhu Z, Jiang W, McGinley JN, Neil ES, Thompson HJ. Excess weight gain accelerates 1-methyl-1-nitrosourea-induced mammary carcinogenesis in a rat model of premenopausal breast cancer. Cancer Prev Res (Phila) 2014 Mar;7(3):310-8.

159. Trends in Intake of Energy and Macronutrients in Adults from 1999-2000 Through 2007-2008. 2010 Nov 1. Report No.: NCHS Data Brief No. 49.

160. Maimoun L, Puech AM, Manetta J, Badiou S, Paris F, Ohanna F, Rossi M, Sultan C. Circulating leptin concentrations can be used as a surrogate marker of fat mass in acute spinal cord injury patients. Metabolism 2004 Aug;53(8):989-94.

161. Panagopoulou P, Gogas H, Dessypris N, Maniadakis N, Fountzilas G, Petridou ET. Survival from breast cancer in relation to access to tertiary healthcare, body mass index, tumor characteristics and treatment: a Hellenic Cooperative Oncology Group (HeCOG) study. European Journal of Epidemiology 2012 Nov;27(11):857-66.

162. Biglia N, Peano E, Sgandurra P, Moggio G, Pecchio S, Maggiorotto F, Sismondi P. Body mass index (BMI) and breast cancer: impact on tumor histopathologic features, cancer subtypes and recurrence rate in pre and postmenopausal women. Gynecological Endocrinology 2013 Mar;29(3):263-7.

163. Horwitz KB, McGuire WL. Predicting response to endocrine therapy in human breast cancer: a hypothesis. Science 1975 Aug 29;189(4204):726-7.

164. Clarke RB. Steroid receptors and proliferation in the human breast. Steroids. 2003 Nov;68(10-13):789-94.

165. Brenton JD, Carey LA, Ahmed AA, Caldas C. Molecular classification and molecular forecasting of breast cancer: ready for clinical application? J Clin Oncol 2005 Oct 10;23(29):7350-60.

166. Dawood S, Hu R, Homes MD, Collins LC, Schnitt SJ, Connolly J, Colditz GA, Tamimi RM. Defining breast cancer prognosis based on molecular phenotypes: results from a large cohort study. Breast Cancer Res Treat. 2011 Feb;126(1):185-92.

167. Voduc KD, Cheang MC, Tyldesley S, Gelmon K, Nielsen TO, Kennecke H. Breast cancer subtypes and the risk of local and regional relapse. J Clin Oncol 2010 Apr 1;28(10):1684-91.

168. Dent R, Trudeau M, Pritchard KI, Hanna WM, Kahn HK, Sawka CA, Lickley LA, Rawlinson E, Sun P, Narod SA. Triple-negative breast cancer: clinical features and patterns of recurrence. Clin Cancer Res 2007 Aug 1;13(15 Pt 1):4429-34.

169. Steel GG. Cell loss as a factor in the growth rate of human tumours. Eur.J Cancer 1967 Nov;3(4):381-7.

170. Lu J, Jiang C, Mitrenga T, Cutter G, Thompson HJ. Pathogenic characterization of 1-methyl-1-nitrosourea-induced mammary carcinomas in the rat. Carcinogenesis 1998 Jan;19(1):223-7.

171. Steel GG. Growth rate of tumours. In Growth kinetics of tumours: cell population kinetics in relation to the growth and treatment of cancer. Oxford: Oxford University Press; 1977. p. 5-55.

172. Steel GG. Basic theory of growing cell populations. In Growth kinetics of tumours: cell population kinetics in relation to the growth and treatment of cancer. Oxford: Oxford University Press; 1977. p. 56-85.

173. Thompson HJ, Strange R, Schedin PJ. Apoptosis in the genesis and prevention of cancer. Cancer Epidemiol Biomarkers.Prev 1992 Nov;1(7):597-602.

174. Gerdes J, Li L, Schlueter C, Duchrow M, Wohlenberg C, Gerlach C, Stahmer I, Kloth S, Brandt E, Flad HD. Immunobiochemical and molecular biologic characterization of the cell proliferation-associated nuclear antigen that is defined by monoclonal antibody Ki-67. Am J Pathol. 1991 Apr;138(4):867-73.

175. Alberts B, Johnson A, Lewis J, Raff M, Roberts K, Walter P. An overview of the cell cycle. In Molecular Biology of the Cell. 4th ed. New York: Garland Science; 2002.

176. Steel GG. Experimental techniques for cell kinetic studies. In Growth kinetics of tumours: cell population kinetics in relation to the growth and treatment of cancer. Oxford: Oxford University Press; 1977. p. 86-119.

177. Collins JA, Schandi CA, Young KK, Vesely J, Willingham MC. Major DNA fragmentation is a late event in apoptosis. J.Histochem.Cytochem. 1997 Jul;45(7):923-34.

178. Huerta S, Goulet EJ, Huerta-Yepez S, Livingston EH. Screening and detection of apoptosis. J.Surg.Res. 2007 May 1;139(1):143-56.

179. Kanduc D, Mittelman A, Serpico R, Sinigaglia E, Sinha AA, Natale C, Santacroce R, Di Corcia MG, Lucchese A, Dini L, et al. Cell death: apoptosis versus necrosis (review). Int.J Oncol 2002 Jul;21(1):165-70.

180. Kroemer G, Galluzzi L, Vandenabeele P, Abrams J, Alnemri ES, Baehrecke EH, Blagosklonny MV, El-Deiry WS, Golstein P, Green DR, et al. Classification of cell death: recommendations of the Nomenclature Committee on Cell Death 2009. Cell Death and Diff 2009;16:3-11.

181. Braun RJ, Buttner S, Ring J, Kroemer G, Madeo F. Nervous yeast: modeling neurotoxic cell death. Trends.Biochem.Sci. 2010 Mar;35(3):135-44.

182. Madeo F, Carmona-Gutierrez D, Ring J, Buttner S, Eisenberg T, Kroemer G. Caspase-dependent and caspase-independent cell death pathways in yeast. Biochem.Biophys.Res Commun. 2009 May 1;382(2):227-31.

183. Bursch W, Paffe S, Putz B, Barthel G, Schulte-Hermann R. Determination of the length of the histological stages of apoptosis in normal liver and in altered hepatic foci of rats. Carcinogenesis 1990 May;11(5):847-53.

184. Soini Y, Paakko P, Lehto VP. Histopathological evaluation of apoptosis in cancer. Am J Pathol. 1998 Oct;153(4):1041-53.

185. Kerr JF, Wyllie AH, Currie AR. Apoptosis: a basic biological phenomenon with wide-ranging implications in tissue kinetics. Br.J Cancer 1972 Aug;26(4):239-57.

186. Saraste A. Morphologic criteria and detection of apoptosis. Herz. 1999 May;24(3):189-95.

187. Zetterberg A, Larsson O. Kinetic analysis of regulatory events in G1 leading to proliferation or quiescence of Swiss 3T3 cells. Proc Natl.Acad.Sci.U.S.A 1985 Aug;82(16):5365-9.

188. Ohtani K, Tsujimoto A, Ikeda M, Nakamura M. Regulation of cell growth-dependent expression of mammalian CDC6 gene by the cell cycle transcription factor E2F. Oncogene 1998 Oct 8;17(14):1777-85.

189. Hallstrom TC, Mori S, Nevins JR. An E2F1-dependent gene expression program that determines the balance between proliferation and cell death. Cancer Cell 2008 Jan;13(1):11-22.

190. Ginsberg D. E2F1 pathways to apoptosis. FEBS Lett. 2002 Oct 2;529(1):122-5.

191. Ueno T, Toi M, Tominaga T. Circulating soluble Fas concentration in breast cancer patients. Clin Cancer Res 1999 Nov;5(11):3529-33.

192. Wold S, Ruhe A, Wold H, Dunn J. The collinearity problem in linear regression. The partial least squares (PLS) approach to generalized inverses. Siam J Sci Stat Comput 1984;5(3):735-43.

193. Boulesteix A, Strimmer K. Partial least squares: a versatile tool for the analysis of high-dimensional genomic data. Brief Bioinform 2007;8(1):32-44.

194. Wold S, Eriksson L, Trygg J, Kettaneh N. The PLS method -- partial least squares projections to latent structures -- and its applications in industrial RDP (research, development, and production). 2004.

195. Obexer P, Ausserlechner MJ. X-linked inhibitor of apoptosis protein - a critical death resistance regulator and therapeutic target for personalized cancer therapy. Front.Oncol 2014;4:197.

196. Clarke MJ. Ovarian ablation in breast cancer, 1896 to 1998: milestones along hierarchy of evidence from case report to Cochrane review. BMJ. 1998 Oct 31;317(7167):1246-8.

197. Huggins C. Endocrine-induced regression of cancers. 1966 Dec 13. 235-47 p.

198. Bulun SE, Lin Z, Imir G, Amin S, Demura M, Yilmaz B, Martin R, Utsunomiya H, Thung S, Gurates B, et al. Regulation of aromatase expression in estrogen-responsive breast and uterine disease: from bench to treatment. Pharmacol.Rev. 2005 Sep;57(3):359-83.

199. Omoto Y, Iwase H. Clinical significance of estrogen receptor beta in breast and prostate cancer from biological aspects. Cancer Sci. 2015 Apr;106(4):337-43.

200. Prall OW, Rogan EM, Sutherland RL. Estrogen regulation of cell cycle progression in breast cancer cells. J Steroid Biochem.Mol.Biol 1998 Apr;65(1-6):169-74.

201. Cato AC, Nestl A, Mink S. Rapid actions of steroid receptors in cellular signaling pathways. Sci.STKE. 2002 Jun 25;2002(138):re9.

202. Rousseau J, Tetu B, Caron D, Malenfant P, Cattaruzzi P, Audette M, Doillon C, Tremblay JP, Guerette B. RCAS1 is associated with ductal breast cancer progression. Biochem.Biophys.Res Commun. 2002 May 24;293(5):1544-9.

203. O'Lone R, Frith MC, Karlsson EK, Hansen U. Genomic targets of nuclear estrogen receptors. Mol.Endocrinol. 2004 Aug;18(8):1859-75.

204. Stirone C, Duckles SP, Krause DN, Procaccio V. Estrogen increases mitochondrial efficiency and reduces oxidative stress in cerebral blood vessels. Mol.Pharmacol. 2005 Oct;68(4):959-65.

205. Boonyaratanakornkit V, Edwards DP. Receptor mechanisms mediating non-genomic actions of sex steroids. Semin.Reprod.Med 2007 May;25(3):139-53.

206. Li S, Shen D, Shao J, Crowder R, Liu W, Prat A, He X, Liu S, Hoog J, Lu C, et al. Endocrine-therapy-resistant ESR1 variants revealed by genomic characterization of breast-cancer-derived xenografts. Cell Rep. 2013 Sep 26;4(6):1116-30.

207. Fuqua SA, Gu G, Rechoum Y. Estrogen receptor (ER) alpha mutations in breast cancer: hidden in plain sight. Breast Cancer Res Treat. 2014 Feb;144(1):11-9.

208. Rettberg JR, Yao J, Brinton RD. Estrogen: a master regulator of bioenergetic systems in the brain and body. Front.Neuroendocrinol. 2014;35(1):8-30.

209. Boonyaratanakornkit V, Pateetin P. The role of ovarian sex steroids in metabolic homeostasis, obesity, and postmenopausal breast cancer: molecular mechanisms and therapeutic implications. Biomed.Res Int. 2015;2015.

210. McElroy JF, Wade GN. Short- and long-term effects of ovariectomy on food intake, body weight, carcass composition, and brown adipose tissue in rats. Physiol.Behav. 1987;39(3):361-5.

211. MacLean PS, Giles ED, Johnson GC, McDaniel SM, Fleming-Elder BK, Gilman KA, Andrianakos AG, Jackman MR, Shroyer KR, Schedin PJ. A Surprising Link Between the Energetics of Ovariectomy-induced Weight Gain and Mammary Tumor Progression in Obese Rats. Obesity 2010 Apr;18(4):696-703.

212. Hammond ME, Hayes DF, Dowsett M, Allred DC, Hagerty KL, Badve S, Fitzgibbons PL, Francis G, Goldstein NS, Hayes M, et al. American Society of Clinical Oncology/College of American Pathologists guideline recommendations for immunohistochemical testing of estrogen and progesterone receptors in breast cancer (unabridged version). Arch.Pathol.Lab.Med 2010 Jul;134(7):e48-e72.

213. McCormack VA, Dowsett M, Folkerd E, Johnson N, Palles C, Coupland B, Holly JM, Vinnicombe SJ, Perry NM, Dos SS, I. Sex steroids, growth factors and mammographic density: a cross-sectional study of UK postmenopausal Caucasian and Afro-Caribbean women. Breast Cancer Res 2009;11(3):R38.

214. Lonning PE, Helle H, Duong NK, Ekse D, Aas T, Geisler J. Tissue estradiol is selectively elevated in receptor positive breast cancers while tumour estrone is reduced independent of receptor status. J Steroid Biochem.Mol.Biol 2009 Oct;117(1-3):31-41.

215. Harada N. Structure, Regulation, and Polymorphisms of the Aromatase Gene. In: Larionov A, editor. Resistance to Targeted Anti-Cancer Therapies. Springer Science+Business Media; 2015. p. 13-26.

216. Zhao H, Tian Z, Hao J, Chen B. Extragonadal aromatization increases with time after ovariectomy in rats. Reprod.Biol.Endocrinol. 2005;3:6.

217. Endogenous Hormones and Breast Cancer Collaborative Group. Body mass index, serum sex hormones, and breast cancer risk in postmenopausal women. J Natl.Cancer Inst. 2003;95:1218-26.

218. Lee JS, Ettinger B, Stanczyk FZ, Vittinghoff E, Hanes V, Cauley JA, Chandler W, Settlage J, Beattie MS, Folkerd E, et al. Comparison of methods to measure low serum estradiol levels in postmenopausal women. J Clin Endocrinol.Metab. 2006 Oct;91(10):3791-7.

219. Handelsman DJ, Newman JD, Jimenez M, McLachlan R, Sartorius G, Jones GR. Performance of direct estradiol immunoassays with human male serum samples. Clin Chem 2014 Mar;60(3):510-7.

220. Lorincz AM, Sukumar S. Molecular links between obesity and breast cancer. Endocrine-Related Cancer 2006 Jun;13(2):279-92.

221. Phipps AI, Malone KE, Porter PL, Daling JR, Li CI. Body size and risk of luminal, HER2-overexpressing, and triple-negative breast cancer in postmenopausal women. Cancer Epidemiol Biomarkers.Prev 2008 Aug;17(8):2078-86.

222. Morris PG, Hudis CA, Giri D, Morrow M, Falcone DJ, Zhou XK, Du B, Brogi E, Crawford CB, Kopelovich L, et al. Inflammation and increased aromatase expression occur in the breast tissue of obese women with breast cancer. Cancer Prev Res (Phila) 2011 Jul;4(7):1021-9.

223. Subbaramaiah K, Howe LR, Bhardwaj P, Du B, Gravaghi C, Yantiss RK, Zhou XK, Blaho VA, Hla T, Yang P, et al. Obesity is associated with inflammation and elevated aromatase expression in the mouse mammary gland. Cancer Prev Res.(Phila) 2011 Mar;4(3):329-46.

224. Ioannides SJ, Barlow PL, Elwood JM, Porter D. Effect of obesity on aromatase inhibitor efficacy in postmenopausal, hormone receptor-positive breast cancer: a systematic review. Breast Cancer Res Treat. 2014 Sep;147(2):237-48.

225. Cuzick J. Aromatase inhibitors for breast cancer prevention. J Clin Oncol 2005 Mar 10;23(8):1636-43.

226. Kalu DN, Arjmandi BH, Liu CC, Salih MA, Birnbaum RS. Effects of ovariectomy and estrogen on the serum levels of insulin-like growth factor-I and insulin-like growth factor binding protein-3. Bone Miner. 1994 May;25(2):135-48.

227. Oana F, Takeda H, Hayakawa K, Matsuzawa A, Akahane S, Isaji M, Akahane M. Physiological difference between obese (fa/fa) Zucker rats and lean Zucker rats concerning adiponectin. Metabolism-Clinical and Experimental 2005 Aug;54(8):995-1001.

228. Rose DP, Komninou D, Stephenson GD. Obesity, adipocytokines, and insulin resistance in breast cancer. Obes.Rev. 2004 Aug;5(3):153-65.

229. Dontu G, Abdallah WM, Foley JM, Jackson KW, Clarke MF, Kawamura MJ, Wicha MS. In vitro propagation and transcriptional profiling of human mammary stem/progenitor cells. Genes.Dev. 2003 May 15;17(10):1253-70.

230. Dontu G, Al-Hajj M, Abdallah WM, Clarke MF, Wicha MS. Stem cells in normal breast development and breast cancer. Cell Prolif. 2003 Oct;36 Suppl 1:59-72.

231. Makowski L, Hotamisligil GS. Fatty acid binding proteins--the evolutionary crossroads of inflammatory and metabolic responses. J Nutr. 2004 Sep;134(9):2464S-8S.

232. Queipo-Ortuno MI, Escote X, Ceperuelo-Mallafre V, Garrido-Sanchez L, Miranda M, Clemente-Postigo M, Perez-Perez R, Peral B, Cardona F, Fernandez-Real JM, et al. FABP4 dynamics in obesity: discrepancies in adipose tissue and liver expression regarding circulating plasma levels. Plos One 2012;7(11):e48605.

233. Gustafson B, Gogg S, Hedjazifar S, Jenndahl L, Hammarstedt A, Smith U. Inflammation and impaired adipogenesis in hypertrophic obesity in man. Am J Physiol.Endocrinol.Metab. 2009 Nov;297(5):E999-E1003.

234. Cinti S, Mitchell G, Barbatelli G, Murano I, Ceresi E, Faloia E, Wang S, Fortier M, Greenberg AS, Obin MS. Adipocyte death defines macrophage localization and function in adipose tissue of obese mice and humans. J Lipid.Res 2005 Nov;46(11):2347-55.

235. Gudkov AV, Gurova KV, Komarova EA. Inflammation and p53: A Tale of Two Stresses. Genes.Cancer 2011 Apr;2(4):503-16.

236. Berishaj M, Gao SP, Ahmed S, Leslie K, Al-Ahmadie H, Gerald WL, Bornmann W, Bromberg JF. Stat3 is tyrosine-phosphorylated through the interleukin-6/glycoprotein 130/Janus kinase pathway in breast cancer. Breast Cancer Res 2007;9(3):R32.

237. Carey L, Winer E, Viale G, Cameron D, Gianni L. Triple-negative breast cancer: disease entity or title of convenience? Nat.Rev.Clin Oncol 2010 Dec;7(12):683-92.

238. Sainsbury JR, Farndon JR, Needham GK, Malcolm AJ, Harris AL. Epidermal-growth-factor receptor status as predictor of early recurrence of and death from breast cancer. Lancet. 1987 Jun 20;1(8547):1398-402.

239. Masuda H, Zhang D, Bartholomeusz C, Doihara H, Hortobagyi GN, Ueno NT. Role of epidermal growth factor receptor in breast cancer. Breast Cancer Res Treat. 2012 Nov;136(2):331-45.

240. Fiorio E, Mercanti A, Terrasi M, Micciolo R, Remo A, Auriemma A, Molino A, Parolin V, Di SB, Bonetti F, et al. Leptin/HER2 crosstalk in breast cancer: in vitro study and preliminary in vivo analysis. BMC.Cancer 2008;8:305.

241. Levin BE, Dunn-Meynell AA. Defense of body weight depends on dietary composition and palatability in rats with diet-induced obesity. American Journal of Physiology-Regulatory Integrative and Comparative Physiology 2002 Jan;282(1):R46-R54.

242. Patterson CM, Dunn-Meynell AA, Levin BE. Three weeks of early-onset exercise prolongs obesity resistance in DIO rats after exercise cessation. Am J Physiol.Regul.Integr.Comp.Physiol. 2008;294(2):R290-R301.

243. Levin BE, Dunn-Meynell AA, Ricci MR, Cummings DE. Abnormalities of leptin and ghrelin regulation in obesity-prone juvenile rats. American Journal of Physiology-Endocrinology and Metabolism 2003 Nov 1;285(5):E949-E957.

244. Lee RS, Tamashiro KL, Aryee MJ, Murakami P, Seifuddin F, Herb B, Huo Y, Rongione M, Feinberg AP, Moran TH, et al. Adaptation of the CHARM DNA methylation platform for the rat genome reveals novel brain region-specific differences. Epigenetics. 2011 Nov;6(11):1378-90.

APPENDIX A: CHAPTER 2 MATERIALS AND METHODS

Appendix A: Chapter 2 Materials and Methods

A.1. Animal breeding and husbandry

Breeder pairs (approximately 30 pairs each Levin DR and DS) were obtained from Taconic (Taconic, Hudson, NY) at 5-7 weeks of age. These outbred strains of Sprague Dawley rats were originally obtained by Taconic from Barry Levin after 20 generations of selective breeding for rapid weight gain on sucrose and moderate fat (32%) (SUMO32) diet, and are commercially available from the Taconic repository (strain: TacLevin:CD(SD)DIO, stock #DS; TacLevin:CD(SD)DR, stock #DR).

In-house breeding was conducted using a Poiley rotational breeding scheme, in which breeder pairs are systematically rotated in each breeding cycle (245). Pups were weaned at 3 weeks of age and were switched to SUMO32 diet the following day. Post-weaning, rats were housed 3 per cage, maintained on 12 hour light: dark cycle at 24±2°C with 30% relative humidity, and given ad libitum access to SUMO32 diet and distilled water. Animals were weighed weekly. **Figure 4** depicts study design for the studies reported in Chapter 2.

A.2. Diet formulation and composition

Composition of the purified sucrose and moderate (32%) fat (SUMO32) diet is reported in **Table 8**.

Table 8
Legend. SUMO32 purified diet formulation.

Ingredient	g/100g	kcal/100g	%kcal/100g
Anhydrous milk fat	4.2	37.8	8.7
Corn oil	11.3	101.7	23.4
Sucrose	27.8	111.2	25.6
Dextrose	7.2	28.8	6.6
Corn starch	20.6	82.4	19.0
Casein	18.2	72.8	16.7
Solka-Floc	2.9	--	--
DL-methionine	0.3	--	--
Choline bitartrate	0.2	--	--
Calcium carbonate	0.5	--	--
Sodium bicarbonate	0.5	--	--
Potassium citrate monohydrate	1.3	--	--
Mineral mix	3.8	--	--
Vitamin mix	1.1	--	--
Total	100.0	434.7	100.0

The diet provides 4.35 kcal/g (18.2 kJ/g). Anhydrous milk fat and corn oil together provide 32.1% of kcal as fat in the SUMO32 diet, comprised of 29.2% saturated fatty acids (9.4% of total dietary kcal), 28.4% monounsaturated fatty acids (9.1% of total dietary kcal), and 42.4% polyunsaturated fatty acids (13.6% of total dietary kcal) ((246), Mazola nutrition label). The SUMO32 diet provided 16.7% protein and 51.2% carbohydrate by kcal, comparable to the macronutrient composition of the average American woman's diet (247). The SUMO32 rodent diet was mixed on-site at our laboratory's diet mixing facility and stored at -20°C until used.

A.3. N-methyl-N-Nitrosourea-induced mammary carcinogenesis

To initiate mammary carcinogenesis according to the rapid emergence model first developed by our laboratory (148), female ovary intact DR (N=103) and DS (N=101) rats were injected intraperitoneally (50

mg/kg) with N-methyl-N-nitrosourea (MNU) (Ash Stevens, Detroit, MI, prepared fresh in acidified saline) at 21 days of age as previously described (156). In aqueous solutions, MNU rapidly decomposes to diazomethane with a half-life of 1.2 hours at pH 7 and 0.1 hours at pH 8 and is undetectable in the animal after 24 hours (248;249). Bi-weekly palpations for detection of mammary tumors began 24 days post-carcinogen and continued until study termination. All animal studies were performed in accordance with the Colorado State University Institutional Animal Care and Use Committee.

A.4. Necropsy

The study was terminated 63 days post-carcinogen when rats were 84 days of age (DR N=103, DS N=101). At necropsy, fasted rats were euthanized within a 4-hour window via CO_2 inhalation and cervical dislocation. Blood was collected into EDTA VacuTainers (Becton-Dickinson, Franklin Lakes, NJ) and centrifuged to separate plasma. After separation, plasma was kept on ice before freezing at -20°C until use. Rats were skinned and mammary gland chains were examined under translucent light; grossly visible tumors were excised, weighed, and transported for further processing.

A.5. Histopathological characterization of tumors

Our lab has previously described histopathological characterization of MNU-induced lesions in the rat (250). Briefly, formalin fixed paraffin embedded tumors were cut into 4 micron thick sections using a microtome, which is comparable with average nuclear diameter (176) ensuring a single cell-width section, then stained with hematoxylin and eosin (H&E). Briefly, sections are deparaffinized in xylene, hydrated through a series of ethanols, stained in Harris hematoxylin for 4 minutes, rinsed in deionized water, blued in Scott's water for 1 minute, rinsed in deionized water, counterstained with eosin Y for 2 minutes, followed by gradual dehydration in a series of ethanols, cleared in xylene, and allowed to air dry. After mounting and coverslipping, sections were diagnosed according to criteria developed by our

laboratory and others (140;250-252). Only histopathologically confirmed mammary adenocarcinomas were included in statistical analyses of cancer outcomes or in subsequent molecular biology methods. We have previously reported that mammary tumors induced by MNU are histologically similar to human tumors (140).

A.6. Immunohistochemistry for determination of hormone receptor status

Immunohistochemistry was performed as previously described (253) on first-palpated tumors from DR and DS rats. In the event that multiple tumors from the same rat fit first-palpated criteria, both tumors were included in analysis of PR expression (N=65 DR tumors, N=117 DS tumors). Briefly, paraffin-embedded tumor sections were cut into 4 um sections with a microtome, floated onto a tissue flotation bath, placed onto slides, and air dried at room temperature overnight. Sections were deparaffinized in xylene, hydrated in a series of ethanols, and rinsed in deionized (DI) water. Heat-induced epitope retrieval (HIER) was performed for 3 minutes in a pressurized decloaking chamber (Biocare Medical, Concord, CA) using 10mM citrate buffer (Citra Plus, Biogenex, Fremont, CA) and samples were cooled at room temperature for 30 minutes. Sections were rinsed 2X in DI water and endogenous peroxidase activity was quenched by immersing slides in 3% hydrogen peroxide for 5 min. Sections were rinsed 2X in DI water followed by phosphate buffered saline + 0.1% Tween-20 (PBS-T), pH 7.4 2X for 5 minutes each. Sections were blocked with 10% normal donkey serum for 20 minutes.

Blocking serum was drained and PR primary antibody (mouse monoclonal antibody, clone PR88, Biogenex, Fremont, CA; diluted 1:200 in PBS-T + 10% NDS) was applied for 90 minutes followed by 3X 5 minutes rinses in PBS-T. A biotinylated donkey anti-mouse secondary antibody (Jackson Immuno Research, West Grove, PA; diluted 1:1000 in PBS-T + 10% NDS) was applied for 30 minutes followed by 3X 5 minute rinses in PBS-T. Horseradish peroxidase (HRP) conjugated streptavidin (Dako, Carpinteria,

CA; diluted 1:1000) was applied to sections for 30 minutes followed by 3X 5 minute rinses in PBS-T. Sections were rinsed in PBS, 3 rinses X 5 minutes each. Sections were rinsed in DI water, counterstained with Harris hematoxylin (1:10) for 3 minutes, rinsed in DI water, and blued in Scott's water for 1 minute. Sections were dehydrated in a series of ethanols, cleared in xylene, and mounted/ coverslipped.

After drying overnight, N=10 hot-spot (high immunoreactivity) and random (raster pattern) fields per tumor were collected at 100X magnification using a Zeiss AxioCamHR (Zeiss, Thornwood, NY) digital camera mounted on a Zeiss Axioskop II microscope and saved as JPEG files (1300 x 1030 pixels, 24 bit RGB, 150 DPI). PR expression was analyzed using the open source ImmunoRatio plugin for ImageJ image analysis software (NIH), which calculates the percentage of streptavidin- or DAB-stained (brown) nuclei and hematoxylin-stained (blue) nuclei over total nuclear area, giving a labeling index. Thresholding was set using tumors from ovariectomized lean rats, which are considered hormone receptor negative.

A.7. Statistical Analyses

Statistical analyses were performed under the guidance of a biostatistician (P. Wolfe). Analyses were performed on data from palpable mammary adenocarcinomas. Differences were assessed for statistical significance as follows:

- Body weight:
    - Final body weight at study termination was assessed by unpaired t test with Welch-Satterthwaite correction
- Cancer outcomes:
    - Cancer incidence (%) was assessed by chi square test of equal proportions
    - Cancer multiplicity (# carcinomas/ rat) was assessed using Poisson regression

- Carcinoma burden (g/ rat) was assessed using a two-stage model combining chi-square (incidence) and log linear (burden) *p*-values
- Cancer latency was assessed using a log-rank (Mantel-Cox) test in Kaplan-Meier survival analysis, where animals without palpated tumors were right-hand censored at 60 days post-carcinogen, the last day rats were palpated for detectable tumors before study termination (censored: DR N=39, DS N=9).

- Immunohistochemistry:
  - Statistical analysis of PR % immunoreactivity was determined using two-sided Student's t-test with α=.05. Visual thresholding of the frequency analysis of PR immunoreactivity was used to set the cutoff for calling a tumor PR+ for contingency analysis.

APPENDIX B: CHAPTER 3 MATERIALS AND METHODS

Appendix B: Chapter 3 Materials and Methods

B.1. Criteria used to determine tumor subset for evaluation

Nearly 800 histopathologically confirmed adenocarcinomas were obtained from the ovary-intact DS and DR rats reported in Chapter 2, and random choosing of a subset of tumors for further evaluation is arbitrary and can potentially mask causal relationships due to noise. Therefore, we developed a strategy to choose tumors for analysis in a data-driven manner.

As reported in Chapter 3 in **Figure 7**, the slope of the linear regression line for DS tumors was 0.9678 g per week prior to end of study versus 0.5333 g per week for DR rats; this is a fold-change of 1.82 for DS tumors compared to DR tumors. For each week prior to the end of study, 1.82 was used as a multiplier for DR tumors to give a target tumor mass range for matching DS tumors; i.e., if a DR tumor palpated one week prior to the end of study weighed 1 g, the target DS tumor for analysis palpated one week prior to the end of study would weigh 1.82 grams ± 5%. Both DS and DR tumors in a pair were required to have a portion of the tumor frozen for evaluation of protein expression.

Based on these criteria, N=20 DR and DS tumor pairs, or a total of N=40 tumors, were chosen for subsequent evaluation. **These N=20 each DR and DS tumors are referred to as the full tumor set.** As DR and DS tumors display considerable heterogeneity in molecular characteristics, some experiments were performed using only the DR and DS tumors with the highest mitotic index from within the full set of N=20; **this subset of N=9 tumors each DR and DS are referred to as the high mitotic index subset.** Standard practice in histology involves collecting the same number of high powered fields from every tumor (such as used for determination of PR % immunoreactivity). However, tumor size varied widely

within the full subset of N=20 tumors each DR and DS. Counting the same number of fields per tumor regardless of size does not equally characterize the heterogeneity of large and small tumors.

Given the frequency distribution of tumor diameter for 40 tumors (from N=20 each DR and DS rats) in **Figure 30**, we developed a method that bases number of fields to count on the diameter of the tumor at its longest axis rounded to the nearest half millimeter. The implementation of this method, including categories of tumor diameter, corresponding number of fields to image, and the breakdown of the full set of DR and DS tumors into the 4 categories, is depicted in **Table 9**.

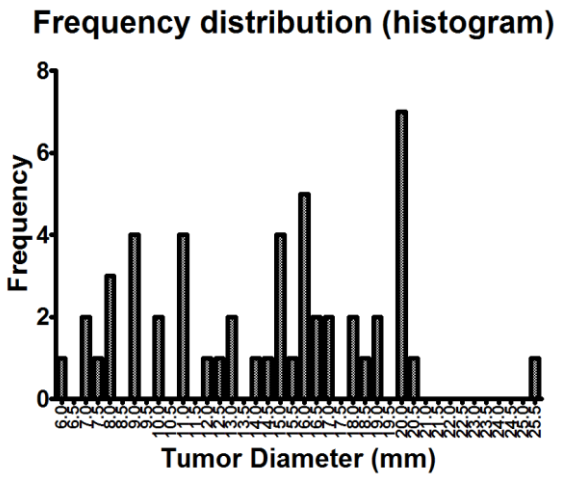

Figure 30
Legend. MNU-induced tumors display high heterogeneity in size. Histogram of DR (N=20) and DS (N=20) formalin-fixed paraffin-embedded tumor section diameter.

Table 9
Legend. Categories of tumor size and corresponding number of fields to capture based on tumor diameter in mm across longest axis.

Category	Diameter range (mm)	Fields to image	DR (% tumors)	DS (% tumors)
1	<9.5	5	34.8	10.3
2	10-14.5	10	21.7	27.6
3	15-19.5	15	30.4	41.3
4	>20	20	13.0	20.7

B.2. Histological evaluation of apoptosis

Using the criteria in Table 9, fields from 4 µm sections of formalin fixed paraffin embedded (FFPE) tumors were collected under 400X magnification. A macro was written by J.N. McGinley in Image Pro Plus v4.5 (Media Cybernetics, Inc. Rockville, MD) to facilitate manual tagging analysis of each image. The macro was designed to load one color JPEG image at a time and assign the complete file path information to a temporary variable. A manual tag parameter file containing all of the necessary class information was then loaded and displayed as a small user interface in a floating window. Three possible tag classes were used; normal (green cross); apoptotic (yellow circle); and mitotic (blue triangle). The macro would then look for a .TAG file with the same file name as the image in the same directory folder. The colored tag points would appear as a non-destructive layer superimposed on the original .TAG image. Necrotic cells were not tagged. The cytological criteria in **Table 10** and **Figure 31** were used as the basis of assigning apoptotic tags.

Table 10

Legend. Cytological characteristics of apoptotic cells. Table developed in collaboration and used with permission from J. N. McGinley, Colorado State University.

	Apoptosis	**Necrosis**
A. Relation to neighboring cells	Pulls away from neighboring cells leaving a vacuolated space.	May or may not pull away from neighboring cells.
B. Nuclear size	Small, pyknotic (condensed)	Pyknotic
C. Nuclear shape	Spherical to crescent shaped. Nuclear material may migrate to one pole.	Irregular
D. Nuclear stain	Hyperchromatic, i.e. indigo to jet black	Hypochromatic
E. Karyorrhexis (nuclear fragmentation)	Yes - small, dark, spherical apoptotic bodies	Yes – fragments into smaller irregular pieces
F. Karyolysis (dissolution of chromatin)	No	Yes
G. Cytoplasm	Hypereosinophilic, i.e. dark red-orange cytoplasm if present	Normal to hypoeosinophilic and may swell prior to lysis.
H. Inflammatory response	Absence of white blood cells.	Increased number of white blood cells, i.e. lymphocytic infiltration.
I. Cell number	Individual cells or small clusters	Groups of cells

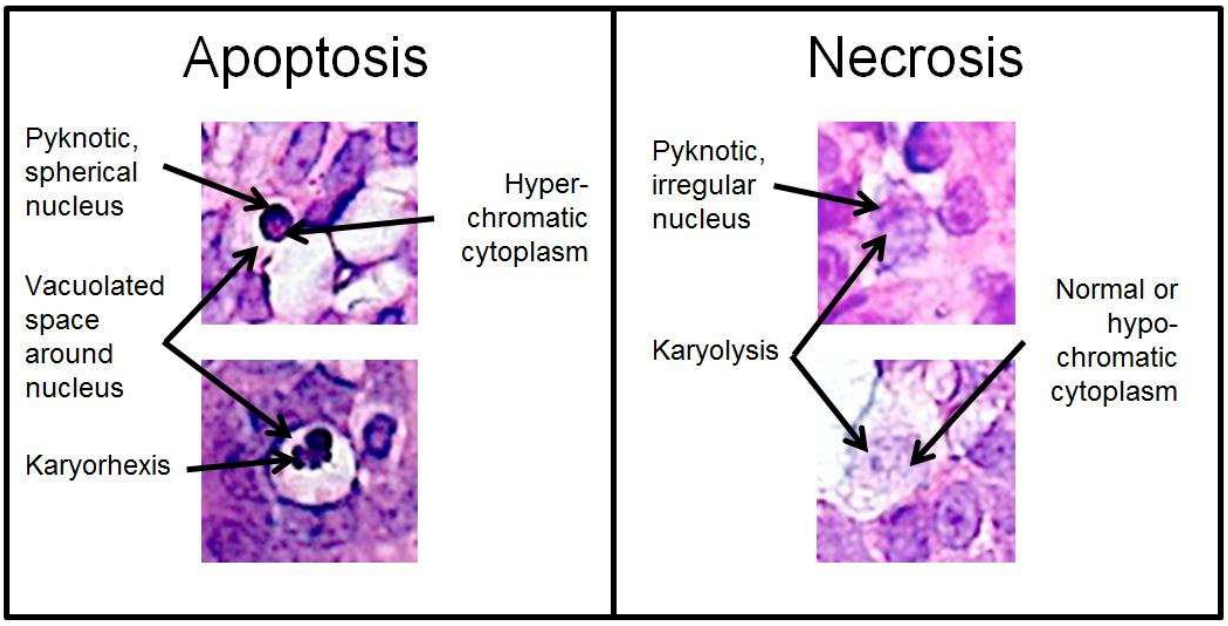

Figure 31
Legend. Examples of cytological characteristics of apoptotic vs. necrotic cells. Images are cropped from H&E stained tumor sections at 400X magnification.

In the event of karyorrhexis, or fragmentation of the nucleus into small spherical bodies, fragments that were touching or in very close proximity to one another were counted as one apoptotic body. Apoptotic index was determined as number of apoptotic bodies per 100 cells in a field. Researchers were blinded as to tumor identity. Each field was tagged by one researcher then checked by another researcher to ensure that all cells were tagged and to align agreement upon tags. A representative tumor field is shown without tags in **Figure 32A** and with tags for normal cells, apoptotic bodies, and mitotic figures in **Figure 32B**.

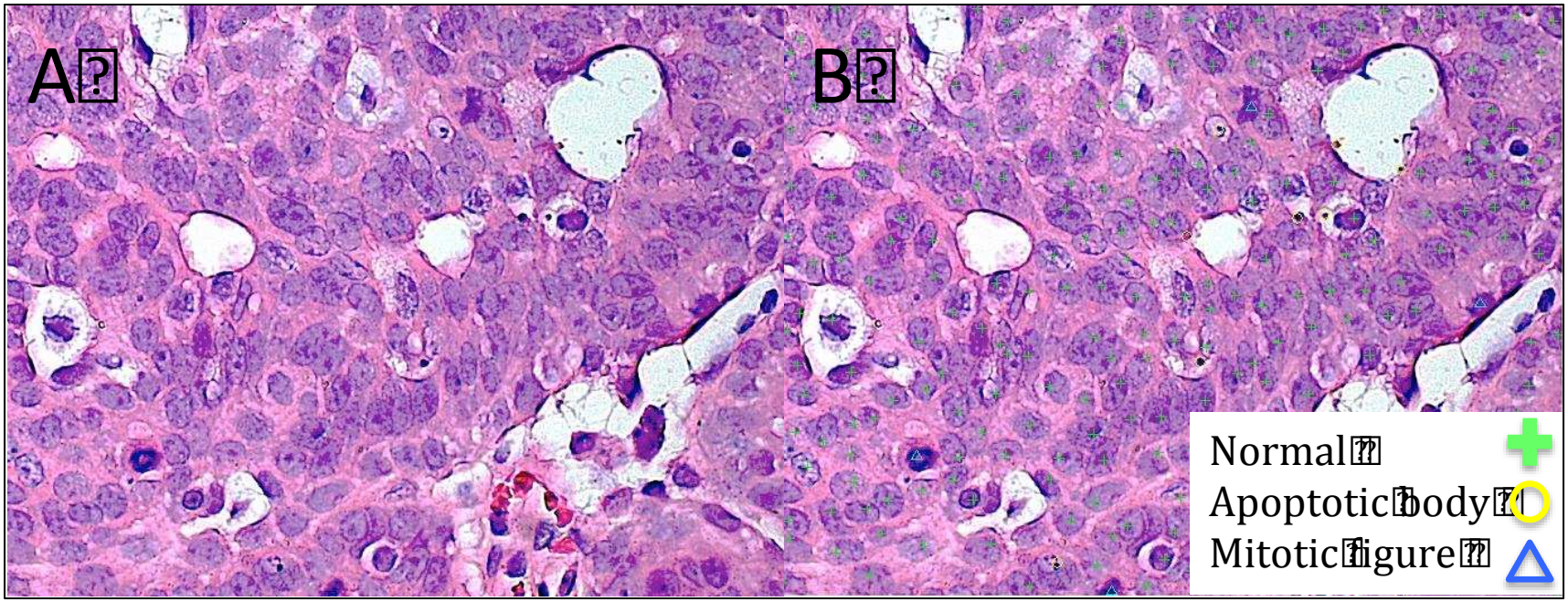

Figure 32
Legend. Example of ImageJ macro for tagging cells in H&E stained tumor fields collected at 400X magnification. Panel A) tumor field prior to tagging with macro. Panel B) same tumor field following tagging, showing presence of normal, apoptotic, and mitotic cells.

B.3. Histological evaluation of proliferation

For a typical rapidly proliferating human cell with a total cycle time of 24 hours, the first gap phase, G1, lasts about 11 hours. DNA synthesis for the daughter cell (S phase) lasts about 8 hours, and the second gap phase G2 lasts about 4 hours. Mitosis, or M phase, in which the newly replicated chromosomes line up along the metaphase plate and divide into daughter cells, lasts about 30 minutes to 1 hour (175). Within M phase, distinct subphases are readily identified in H&E stained tissue sections, with metaphase and anaphase most apparent, as shown in **Figure 33**. According to Steel, the magnitude of the mitotic index is a reliable general estimation of the rate of cell proliferation such that high mitotic index corresponds with a rapid proliferation rate, while low mitotic index corresponds to a slower proliferation rate (176). If tissues excised from animals are fixed promptly, the proportion of cells containing mitotic figures can be assumed to faithfully represent cells which at the time of fixation were undergoing mitosis (176).

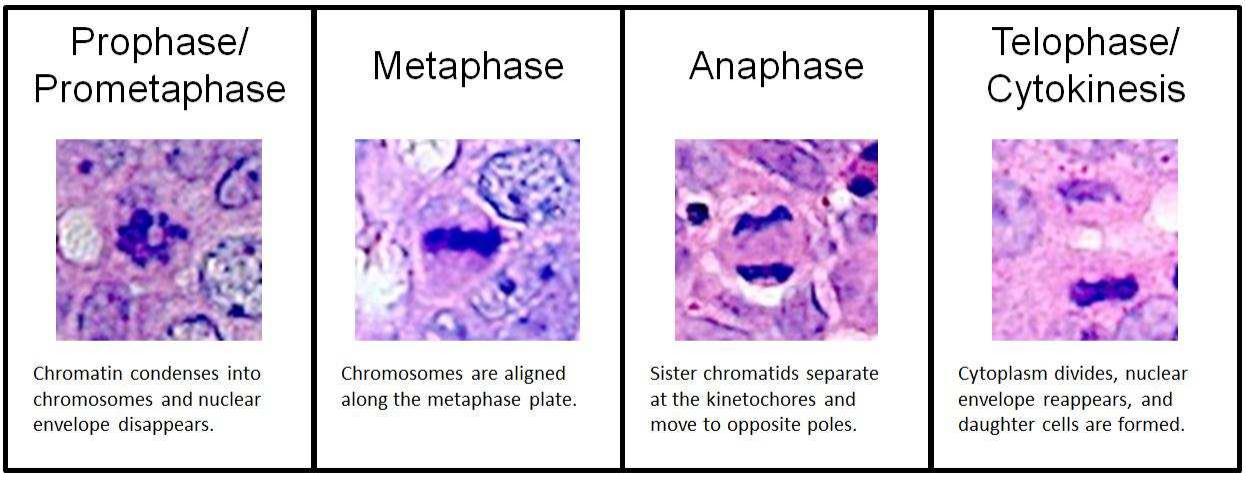

Figure 33
Legend: Representative nuclear characteristics of a cell progressing through phases of mitosis (based on descriptions in (175)). Images are cropped from H&E stained tumor sections at 400X magnification.

B.4. Immunohistochemical evaluation of proliferation (Ki67)

Studies utilizing interfering antibodies or knockout models have demonstrated that the proliferative marker Ki67 is critical for cell division, though the precise role of the protein is still unclear (254). A recent meta-analysis reports that Ki67 positivity of breast tumors is associated with higher probability of relapse and worse survival in all patients (255). To determine the proliferative cell fraction within DR and DS tumors, the full tumor set was assessed for expression of Ki67.

Number of fields collected was based on tumor diameter as described in **Table 9**, and tumors were assessed for Ki67 expression using immunohistochemistry methods as described in Appendix A, section A.6, with the exception of using a Ki67 primary antibody (diluted 1:200 in PBS-T + 10% NDS, clone SP6, rabbit monoclonal antibody, Thermo Scientific, Waltham, MA) for 60 minutes, 3X 5 minute washes in PBS-T, followed by incubation with a biotinylated donkey anti-rabbit secondary antibody (Jackson ImmunoResearch, West Grove, PA; diluted 1:1000 in PBS-T + 10% NDS) applied for 30 minutes followed by 3X 5 minute rinses in PBS-T. Rat cecum tissue was included as a positive control for Ki67 staining. **Figure 34** displays a representative rat tumor section probed for Ki67 and demonstrates the high intratumor heterogeneity commonly found in rat tumors. Random fields from stained sections were collected under 100X magnification. Expression was analyzed using ImmunoRatio plugin for ImageJ image analysis software as described in Appendix A, section A.6.

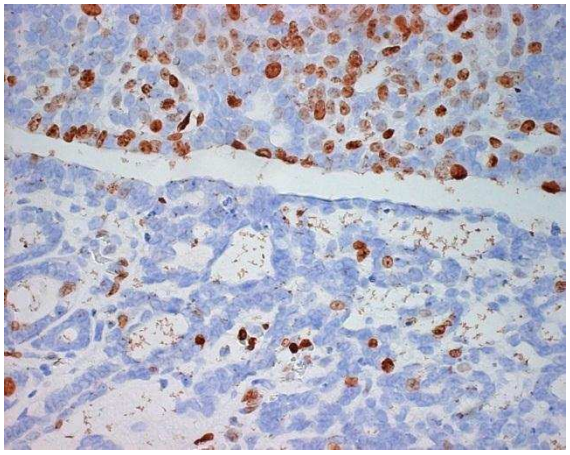

Figure 34
Legend. Representative tumor section for Ki67 staining from fields captured at 100X magnification. Nuclear immunoreactivity for Ki67 results in brown nuclei compared to unreactive nuclei stained blue with hematoxylin.

B.5. Fluorimetric caspase activity assay

To determine if altered activity of apoptotic machinery (intrinsic vs. extrinsic) is responsible for the unexpected heightened apoptosis observed in DS tumors, lysate from the full tumor set of DR and DS tumors was prepared by pulverizing flash-frozen tumors using mortar and pestle, adding ~3 volumes of caspase activity assay lysis buffer (MBL International, Woburn, MA), incubating on ice for 20 minutes, followed by centrifugation at 12,000 *x g* for 20 minutes. The clear supernatant was removed and after determining protein concentration by Bradford assay, samples were further diluted to 1.5 mg protein/ mL lysis buffer. Tumor lysate was first evaluated using the Apo ONE caspase 3/7 Activity Assay Kit from Promega (Madison, WI), which utilizes the consensus peptide sequence DEVD (Asp-Glu-Val-Asp) for caspases 3 and 7, termed executioner caspases for their role in activating proteins including poly-(ADP ribose) polymerase (PARP), DNA-dependent protein kinase (DNA-PK), lamins, and topoisomerases, which are responsible for apoptosome formation and cytological changes associated with apoptosis (179).

Table 11
Legend. Amino acid sequence of consensus caspase target peptides.

Caspase	Type	Peptide Sequence
2	Effector	VDVAD
3/7	Executioner	DEVD
6	Effector	VEID
8/10	Initiator, extrinsic pathway	IETD
9	Initiator, intrinsic pathway	LEHD

In this assay, the consensus sequence for caspases 3/7 (**Table 11**) is conjugated to rhodamine 110 (R110), a profluorophore that becomes intensely fluorescent after cleavage and removal of the DEVD peptide by caspase-3/7 activity. Lysate was diluted 1:1 with ApoOne reagent + caspase substrate in triplicate in black 384-well plates, after which plates were sealed and incubated at 37°C for 1 hour. Evaluation of free R110 was determined by imaging plates with a SpectraMax plate reader (Molecular

Devices, Sunnyvale, CA) at excitation=499 nm/ emission=521 nm. While caspase 8/10 activity was assessed via the colorimetric caspase activity assay (next section, section B.6), due to low colorimetric signal, this caspase was also evaluated with the consensus sequence (**Table 11**) linked to the profluorophore AFC (7-amino-4-trifluoromethyl-coumarin). Evaluation of free AFC as a proxy to caspase activity was evaluating by reading on a SpectraMax plate reader with excitation at 400 nm, excitation=505 nm after incubation at 37°C for 2 hours. Standard curves were constructed using free R110 and AFC standards serially diluted in water to determine caspase activity as nmol free fluorophore released per µg protein (determined by Bradford protein assay) per minute.

B.6. Colorimetric caspase activity assay

Colorimetric activity assays were used to assess the activity of several other caspases. Consensus sequences of caspases 2, 6, 8/10, and 9, displayed in **Table 11**, conjugated to the chromogen para-nitroaniline (pNA), were used to assess caspase activity within tumor lysate. Cleavage of the peptide sequence releases free pNA, a chromogen which absorbs at 405 nm. Lyophilized caspase substrates (Enzo Life Sciences, Farmingdale, NY) were reconstituted at 4 mM in DMSO. Equal volumes of 1.5 mg/ml tumor lysate and 2X caspase activity assay buffer containing 10 mM dithiothreitol (DTT) were combined with 200 µM each caspase substrate-pNA conjugate. Plates were sealed and incubated at 37°C for 2 hours. A standard curve using free pNA serially diluted in water was constructed to determine caspase activity as nmol free pNA released per µg protein (determined by Bradford protein assay) per minute.

B.7. Lysate preparation

To determine cell cycle machinery that could be responsible for the accelerated progression through the cell cycle in DS tumors, protein lysate from the high mitotic subset of DR and DS tumors was prepared using Tissue Protein Extraction Reagent (TPER) from Pierce (Rockford, IL), with all buffers containing 1X

HALT protease and phosphatase inhibitor cocktail (Pierce, Rockford, IL). Briefly, ~200 mg flash-frozen tumor tissue was pulverized using mortar and pestle, then 2 mL TPER was added and incubated with the lysate on ice for 20 minutes. Lysate was centrifuged at 12,000 *x g* for 10 minutes and the clear supernatant containing soluble proteins was transferred to a separate tube and aliquotted; the pellet containing nuclei, membranes, and insoluble material was discarded. Protein concentration was determined by Bradford assay and samples were diluted to equal concentration of protein per mL in ice-cold TPER buffer containing 1X HALT protease/phosphatase inhibitor.

B.8. Western blot-based detection of protein expression

Tumor lysate from the high mitotic index subset was evaluated using sodium dodecyl sulfate-polyacrylamide gel electrophoresis (SDS-PAGE) under denaturing and reducing conditions. Briefly, lysates were prepared to contain final concentration 1X Nu-PAGE LDS sample buffer (Life Technologies, Grand Island, NY) containing a denaturing agent and 0.1M DTT as a reducing agent. Samples were boiled at 95°C for 5 minutes, and 60 µg protein from each sample was loaded into a 4-12% Tris-Glycine gel (Life Technologies, Grand Island, NY) and run at 125V for 90 minutes to separate proteins. Following SDS-PAGE, samples were transferred from the gel to a polyvinylidene fluoride (PVDF) membrane by applying 25V for 2 hours at 4°C. Quality of transfer was evaluated by staining the gel and membrane with Coommassie and Ponceau S stains, respectively (Bio-Rad, Hercules, CA). Membranes were blocked with 5% nonfat dry milk in Tris-buffered saline + 0.1% Tween-20 (TBS-T), and were incubated overnight at 4°C with primary antibodies diluted in 5% bovine serum albumin (BSA) in TBS-T.

For detection, membranes were washed 3X with TBS-T, incubated with appropriate secondary antibodies directed against the host species of the primary antibody, then washed 3X with TBS-T. Membranes were incubated with Clarity Enhanced Chemiluminescence Reagents (ECL) (Bio-Rad,

Hercules, CA) and images were collected within the linear range of detection (below pixel saturation) using a ChemiDoc imager (Bio-Rad, Hercules, CA). Signal specificity was confirmed by comparing observed bands to the Amersham Full-Range Rainbow prestained protein ladder (GE Healthcare, Lafayette, CO).

B.9. Capillary electrophoresis-based detection of protein expression

Mammary gland lysate was evaluated using the Wes system from Protein Simple (San Jose, CA) with the rabbit master kit for proteins sized 12-230 kD. This technology has been previously reported (256;257). Briefly, lysates were diluted to final concentration of 1 mg/ml containing 1X fluorescent master mix (contains SDS and DTT as denaturing and reducing agents, respectively) and boiled at 95°C for 5 minutes. Proteins were separated using a proprietary separation and stacking matrix within a 100-µm diameter glass capillary. Following separation, proteins were irreversibly cross-linked to the capillary wall via UV light, and primary antibodies, secondary antibodies, and chemiluminescent detection reagents were applied via vacuum. Signal specificity was confirmed by comparing signal location to that of a biotinylated protein ladder, detected by streptavidin and by comparing to 3 internal fluorescent standards located at 1, 29, and 230 kD.

B.10. Immunoprecipitation

Immunoprecipitation was performed using the Protein G Dynabeads kit from Novex (Thermo Fisher, Grand Island, NY) according to the manufacturer's protocol. Dynabeads are 2.8 µm magnetic beads covalently linked to protein G (binds Fc region of most antibodies). Briefly, Dynabeads were resuspended and 50 µL was transferred to a tube then placed on the magnet to separate beads from supernatant. Ten µg mouse anti-rat E2F1 antibody (Santa Cruz, Dallas, TX) was incubated with rotation for 10 min at room temperature. Tube was placed back on the magnet and unbound antibody and

supernatant was removed. Beads were washed 1X with PBS-T wash buffer, tube was placed on the magnet, and wash supernatant was removed. Five hundred µL each sample (1 mg/ml) was added to the beads with rotation for 10 minutes at room temperature. The antibody-antigen-Dynabeads complex was washed 3X with wash buffer. After each wash, beads were placed back on the magnet, supernatant was removed, and beads were resuspended in fresh wash buffer.

Immediately prior to running the samples, 21 µL elution buffer and 7 µL 4X LDS sample buffer (Life Technologies, Grand Island, NY) and 0.1 M DTT were added, mixed, and tubes were heated for 10 min at 70°C. Tubes were put on magnet to remove beads and 10 µL supernatant was run via SDS-PAGE as described in section B.8. Blocking and antibody incubation steps were performed as described in section B.8; to prevent detection of antibody heavy and light chains, TrueBlot secondary antibodies were used (detects only native/non-reduced/denatured antibodies (Rockland, Limerick, PA)) and detected via chemiluminescence.

B.10. Statistical methods

- Apoptotic/mitotic indices:
    - While Poisson distributions are commonly used to model tumor data, count data from H&E stained fields was demonstrated to be overdispersed compared to a reference Poisson model. One possible reason for overdispersion, aside from incorrect model usage, is positive correlation among observations (258).
    - Given the overdispersion, probabilities of apoptosis and mitosis were determined using a negative binomial distribution, as recommended by biostatistician J. zumBrunnen at Colorado State University. The negative binomial distribution arises from mixing a

Poisson process with a gamma distribution for the Poisson parameter, resulting in overdispersion compared to a reference Poisson model (259).

  - Count data was averaged across fields and analyzed under a negative binomial distribution using SAS software vs. 9.2.

- Caspase activity assays:
  - Fluorimetric and colorimetric caspase activity assays were analyzed by log-transforming data where necessary to satisfy statistical assumptions of normality and variance, and comparing DR vs. DS groups using a two-sided Student's t-test with α=.05.
- Western blot/CE-based evaluation of protein expression:
  - To quantify Western blot signals, densitometry was performed after correcting for background using the rolling disk method, size 20. Signals are expressed as density/mm^2 normalized to GAPDH as a loading control.
  - To quantify CE-based protein signals, chemiluminescent signal was taken as peak area and normalized to GAPDH as a loading control.
  - Protein expression levels in tumors were separately analyzed using multiple T-tests with false discovery rate (FDR) set at 1%.
- Multivariate statistical modeling[6]
  - Principal components analysis (PCA) is a method to analyze large multivariate dataset which summarizes a set of correlated variables by transforming them, by means of an eigen decomposition, into a new set of uncorrelated variables, reducing the dimensionality of the original high dimensional dataset (261-264).

[6]Interpretation and analysis of metabolomics data was previously published as Matthews SB *et al.* PLoS ONE (2012) 7(8): e44179 (260).

- Partial least squares regression on tumor data was performed using Y=tumor size and Y=cell cycle duration. Coefficients for association of X variables with Y variables are reported with 95% confidence intervals.

APPENDIX C: CHAPTER 4 MATERIALS AND METHODS

Appendix C: Chapter 4 Materials and Methods

C.1. Animal breeding and husbandry

In-house breeding was performed as described in Appendix A, section A.1. Study design for the experiments reported in Chapter 4 is depicted in **Figure 17**.

C.2. Diet formulation and composition

Animals were given ad libitum access to the sucrose and moderate 32% fat (SUMO32) purified diet which is described in **Table 8**, and were provided with distilled water.

C.3. N-methyl-N-Nitrosourea-induced mammary carcinogenesis

MNU was administered to female DR (N=36) and DS (N=72) rats as described in Appendix A, section A.3.

C.4. Ovariectomy procedure

Bilateral ovariectomies (ovex) were performed on rats at 28 days post-carcinogen (49 days of age). Animals were anesthetized to a surgical level via isoflurane inhalation, confirmed via lack of response to toe/skin pinch, and given bilateral eye lubrication followed by subcutaneous administration of a volume of sterile saline solution equivalent to 3-5% of starting body weight. An area from the tail to mid-rib was shaved dorsally on each side of the animal and cleaned. A small horizontal incision (perpendicular to the spine) was made just below the 13th rib. Each ovary was removed and the blood vessels and a small portion of the uterine horn below the ovary were permanently occluded using absorbable suture. The incision into the abdominal cavity was closed using absorbable suture and the skin incision was closed with wound clips, which were removed 7-10 days post-surgery.

Post-surgery, animals were placed under a heating lamp and monitored until recovered from anesthesia. Carprofen was administered subcutaneously at 5 mg/kg, once pre-operatively and then every 24 hours for three days post-operatively.

C.5. Necropsy

The study was terminated 91 days post-carcinogen when rats were 112 days of age (DR-OVX N=36, DS-OVX N=74). Gross necropsy and blood, tissue, and tumor collection and processing were performed as described in Appendix A, section A.4. Tumors were stained with hematoxylin and eosin and diagnosed according to histopathological criteria as described in Appendix A, section A.5.

C.6. Immunohistochemistry for determination of hormone receptor expression

PR expression was used as proxy to functional estrogen signaling. PR expression was assessed via immunohistochemistry as described in Appendix A, section A.6, for first palpated tumors from DR-OVX and DS-OVX rats, resulting in analysis of N=21 DR-OVX and N=46 DS-OVX tumors.

C.7. Real-time PCR

RNA was isolated from approximately 100 mg DR and DS mammary gland from the gland 4 anatomical position (N=2 each) using the RNeasy Lipid Mini Kit from Qiagen (Valencia, CA) according to the manufacturer's instructions. RNA was reverse-transcribed to cDNA using the High Capacity cDNA Reverse Transcription Kit from Applied Biosystems (Thermo Fisher, Grand Island, NY) with random priming. The primers used are listed in **Table 12.**

Table 12
Legend. Primers used for quantitative real-time PCR.

Gene Name	Protein Name	Forward Primer	Reverse Primer	Amplicon Length
cyp19a1	aromatase	CACTGTTGTTGGTGACAGAGA	AGTCCACGACAGGCTGAT	104
pgk1	phospho-glycerate kinase 1	GTGATGAGGGTGGACTTCAAT	CAGAATTTGATGCTTGGGACA	92

Real-time polymerase chain reaction (PCR) was performed with 10 µL iQ Sybr Green Supermix (Bio-Rad Laboratories, Hercules, CA) containing the hot start iTaq polymerase, $MgCl_2$, dNTPs, 0.2 µm forward and reverse primers, and 3 µl cDNA with ultrapure water used to bring final volume to 20 µL. Polymerase was activated by hot-start at 95°C for 3 minutes, following by 45 cycles of 95°C for 15 seconds followed by 65°C for 45 seconds. Final extension was performed at 55°C for 1 minute. Melt-curve analysis was then performed by increasing temperature 0.5°C every 10 seconds. Efficiency of primer sets was evaluated by using serially diluted rat ovarian cDNA, and both primer sets gave efficiency between 90-110%. Calculated threshold (Ct) values were based on the maximum correlation coefficient method; however, no signal corresponding to cyp19a1/aromatase cDNA crossed the amplification threshold within 45 cycles.

C.8. Capillary electrophoresis-based protein evaluation

Lysate from ovariectomized DR and DS rats was prepared as described in Appendix B, section B.8 and analyzed via the Protein Simple Wes device as described in section 3.B.10. Recombinant aromatase protein from Novus Biologicals (Littleton, CO) was used at 0.0002 mg/ml as a positive control for a rabbit anti-cyp19a1 antibody from Novus Biologicals (Littleton, CO).

C.9. UPLC-MS/MS detection of estrogen

Samples from N=8 each DR and DS, ovary intact and ovariectomized female rats (N=32 samples total) were evaluated. Approximately 500 mg of flash-frozen mammary fat pad was diced and put into 2 ml cryovials with exact weight recorded separately. Samples were shipped to the University of California-Davis West Coast Metabolomics Center on dry ice. Mammary gland samples were ground and suspended in 4 mL of a 1:1 water/ methanol mixture. The suspension was homogenized, and the resulting homogenate was cooled on ice. The precipitated material was removed by centrifuging at high speed for 5 min, and the supernatant was removed and evaporated in a SpeedVac (Labconco Inc.) followed by lyophilizer (Labconco Inc.). The residue was suspended in 150 µL of water/methanol (1:1), filtered through a 0.2 µm ultracentrifuge filter (Millipore Inc.) and run in duplicate for UPLC-MS/MS analysis. Prior to analysis, samples were held in an Acquity sample manager at 5°C to preserve the analytes.

Sex steroids were determined by the Gaikwad lab at the West Coast Metabolomics Center using ultra-performance liquid chromatography coupled to tandem mass spectrometry (UPLC-MS/MS) as previously described (265). Briefly, 1 mg/ml stock solutions of pure steroid standards were prepared in a methanol/water (1:1 v/v) mixture and stored at −80°C until use. Stock solutions of steroid standards were diluted to working concentrations of 0.02 mg/ml by diluting 1:50 in methanol/ water (1:1 v/v) and were used to optimize run conditions prior to sample analysis. Analytical separations were conducted using an Acquity UPLC HSS T3 1.8 µm 1×150 mm analytical column held at 50 °C with a flow rate of 0.15 mL/min. The gradient started with 100% A (0.1% formic acid in H2O) and 0% B (0.1% formic acid in CH_3CN) for 2 min, changed to 80% A/20% B over 2 min, then changed to 45% A/55% B over 5 min, followed by 20% A/80% B for 2 min. Finally, over 1 min, it was restored to the original 100% A, resulting in a total separation time of 12 min.

The elutions from the UPLC column were introduced to a Xevo-TQ triple quadruple mass spectrometer (Waters, Milford, MA, USA) with electrospray ionization (ESI) in positive ion (PI) and negative ion (NI) mode, capillary voltage of 3.0 kV, extractor cone voltage of 3 V, and detector voltage of 650 V. Cone gas flow was set at 50 L/h, and desolvation gas flow was maintained at 600 L/h. Source temperature and desolvation temperatures were set at 150 and 350°C, respectively. The collision energy was varied to optimize daughter ions and the acquisition range was 20−500 Da.

Samples were introduced to the column at a flow rate of 5 µL/min by using acetonitrile/water (1:1) and 0.1% formic acid as the carrier solution, and mass spectra were recorded. The masses of parent ion and daughter ions were obtained in the MS and MS/MS operations. MS/MS parameters were further used in the multiple reaction monitoring (MRM) method for UPLC/MS/MS operation and resulting data were analyzed and processed using MassLynx 4.1 software.

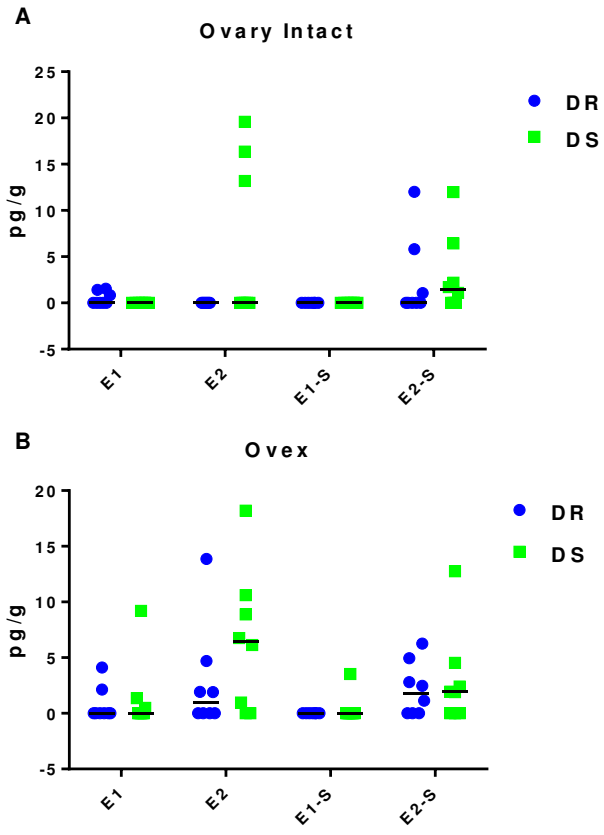

Figure 35
Legend. UPLC-MS/MS analysis of estrogen metabolites in mammary gland from N=8 each DR and DS rats, ovary intact and ovariectomized rats. E1=estrone; E2=estradiol; E1-S=estrone sulfate; E2-S=estradiol sulfate. Bar represents data median.

Raw values for estrogen metabolites in the mammary glands of ovary intact and ovariectomized DR and DS rats are shown in **Figure 35**. While UPLC-MS/MS detection of estrogen is one of the most reliable methods for detecting sex hormones, the data (shown in **Figure 35**) gave us cause for concern for

several reasons. First, regardless of whether rats were DR, DS, ovary intact, or ovariectomized, nearly a third (10 out of 32 total) mammary gland samples had a signal corresponding to sulfated estrogen metabolites when there was no corresponding signal for either of the free estrogens. Conjugation of 100% of the available E1 or E2 seems unlikely—a percentage of estrogens, even a small percentage, should be detected as the unconjugated/ bioavailable form, particularly in ovary intact rats.

As another way to look at the data, we created contingency tables (shown in **Figure 36**) for estradiol/E2, based on E2 signal=0 (no signal detected) vs. E2>0 (any signal detected). The lack of any E2 signal in mammary gland of ovary intact animals was unexpected (**Figure 36**). As these animals are cycling, they should have some estrogen present in the mammary gland, regardless of phase of the estrus cycle.

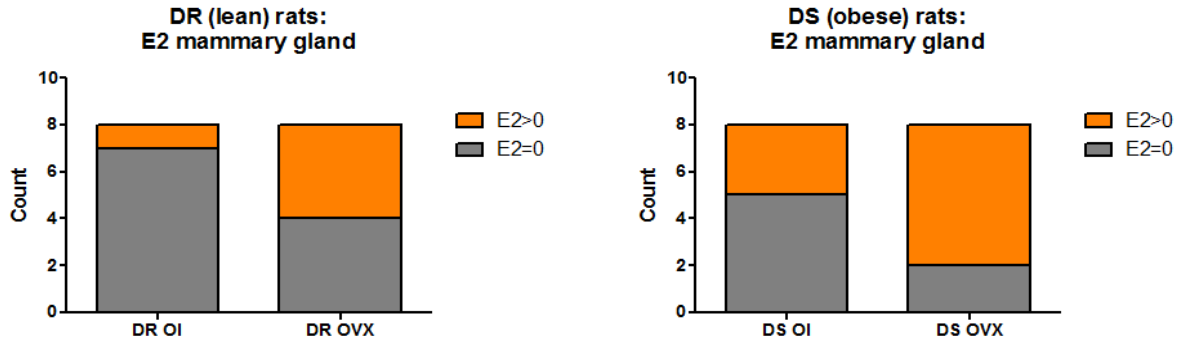

Figure 36
Legend. Contingency analysis for estradiol (E2) in DR and DS ovary intact and ovariectomized rates. Contingency was based on E2=0 or E2>0. Left panel, DR ovary intact vs. DR ovariectomized mammary gland E2 levels. Right panel, DS ovary intact vs. ovariectomized mammary gland E2 levels.

In the contingency graphs, DR ovary intact vs. DR ovariectomized (left graph) is compared to DS ovary intact vs. DS ovariectomized mammary glands (right graph). It seems biologically implausible that there are more zeros (i.e., samples with no estrogen detected) in ovary intact rats than in ovariectomized rats.

On the contrary, we would have expected zeros more often in ovariectomized rats since in the absence of the ovaries, estrogen levels are extremely low.

C.10. Plasma analyses

Body weights of both DR and DS strains are normally distributed; therefore to maximize statistical power, animals chosen for plasma analysis were purposely sampled from non-overlapping areas of the distributions, e.g. lean DR and heavy DS. All systemic analytes were determined using commercial ELISA kits according to manufacturer's specifications. Estradiol (E2), progesterone, and sex hormone-binding globulin (SHBG) were determined using commercial ELISAs from GenWay Biotech (San Diego, CA).

C.11. Statistical analyses

Statistical analyses were performed on data from palpable mammary adenocarcinomas. Differences were assessed for statistical significance as follows:

- Body weight:
    - Final body weight at study termination was assessed by unpaired T-test with Welch-Satterthwaite correction
- Cancer outcomes
    - Cancer incidence (%) was assessed by chi square test of equal proportions
    - Cancer multiplicity (# carcinomas/ rat) was assessed using Poisson regression
    - Carcinoma burden (g/ rat) was assessed using a two-stage model combining chi-square (incidence) and log linear (burden) *p*-values
    - Cancer latency was assessed using a log-rank (Mantel-Cox) test in Kaplan-Meier survival analysis, where animals without palpated tumors were right-hand censored at 90 days

post-carcinogen, the last day rats were palpated for detectable tumors before study termination (censored: DR-OVX N=19, DS-OVX N=29).

- Plasma analyses:
    - Between-group differences in plasma analytes were assessed by unpaired t test with Welch-Satterthwaite correction and $\log_{10}$-data transformation as needed to satisfy statistical assumptions.

APPENDIX D: CHAPTER 5 MATERIALS AND METHODS

Appendix D: Chapter 5 Materials and Methods

D.1. Plasma analyses

Animals were chosen for analyses as described in Appendix C, section C.10. ELISAs were used to evaluate circulating levels of analytes in rat plasma according the manufacturer's specifications. Specifically, glucose was determined using a kit obtained from Thermo Fisher (Waltham, MA). Insulin, leptin, IL-6, IL-1β, and TNF-α were determined using a multiplex kit, while adiponectin and IGF-1 were separately quantified using commercial single-plex kits from Millipore (Billerica, MA). IGF-1 binding protein (IGFBP)-3 kit was from BioVendor (Asheville, CA). C-reactive protein (CRP) was determined using a commercial rat ELISA from Helica Biosystems Inc. (Fullerton, CA). Homeostasis model assessment-estimated insulin resistance (HOMA-IR) was calculated from fasted insulin and glucose levels as shown in **Equation 6** (266).

Equation 6

$$HOMA - IR = \frac{fasting\ plasma\ insulin\ \left(\frac{mU}{L}\right)\ x\ fasting\ plasma\ glucose\ \left(\frac{mmol}{L}\right)}{22.5}$$

D.2. Adipocyte area

Formalin-fixed paraffin embedded (FFPE) mammary fat pads from N=5 each DR and DS rats were used to determine adipocyte area. Random fields (N=5-10 fields per fat pad) from 4 µm sections of hematoxylin and eosin (H&E) stained mammary fat pad were captured at 100x magnification. For analysis, a macro was written by J.N. McGinley in Image Pro Plus v4.5 (Media Cybernetics, Inc., Rockville, MD) to facilitate analysis of each image. The macro was designed to load a previously defined calibration data file used for 100X magnification images and convert one color JPEG image at a time to 8-bit grayscale. Once converted, the macro applied a predefined look up table to enhance image brightness

and contrast. Morphological filters were applied to enhance adipocyte borders. Specifically, one pass of a 2x2 square erode filter (erodes edges of bright objects while enlarging dark objects) and 2 passes of a 2x2 square open filter (allows smoothing of object contours, separates narrowly connected objects and removes small dark holes) were used in quantifying adipocyte diameter.

This pre-processing resulted in a black and white image suitable for analysis, with segmentation range set 10-255, ensuring that black adipocyte borders (range 0-9) were excluded and only the white vacuolated spaces (adipocytes) were included in the count. Partially visible adipocytes at the periphery of the image were excluded. The minimum area was set to 131 μm^2 to eliminate any small objects that were not adipocytes. Objects filled with red (shown in **Figure 37**) allowed the user to visualize the objects (adipocytes) chosen by the software, and to toggle any of these objects on or off prior to counting; e.g. toggling off a large white space created as a result of cutting artifact. Obvious artifacts (i.e. large irregular white spaces, flattened oblong shape of adipocytes) due to cutting or poor penetrance of fixative were excluded.

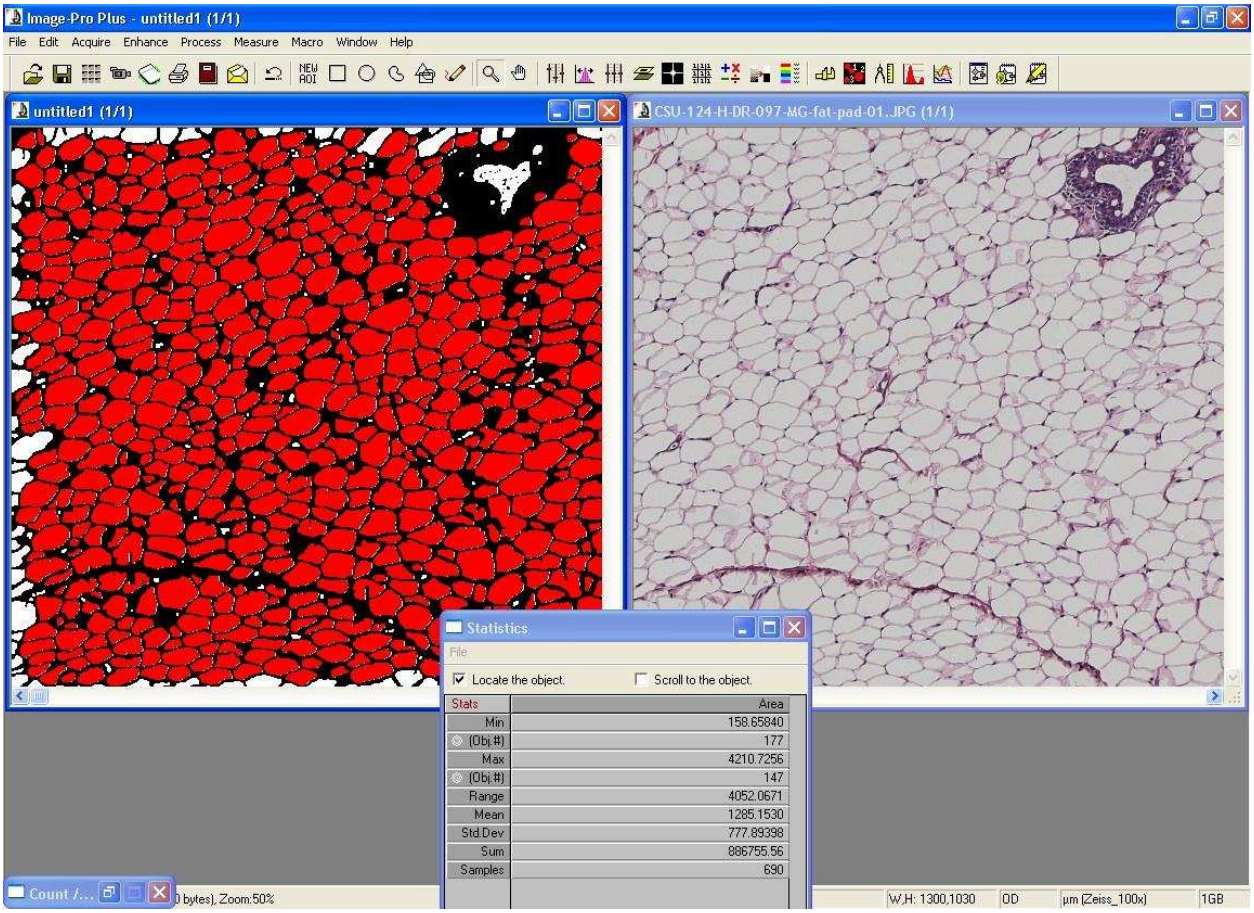

Figure 37
Legend. Representative H&E stained fat pad sections from rat adipose tissue. Original image is on the right; image after running through the macro is on the left. Red areas indicate areas which meet criteria and are counted as adipocytes.

D.3. Capillary electrophoresis-based evaluation of protein expression

Mammary gland lysate was evaluated using the Wes system from Protein Simple (San Jose, CA) with the rabbit master kit for proteins sized 12-230 kD. This technology has been previously reported (256;257). Briefly, lysates were diluted to final concentration of 1 mg/ml containing 1X fluorescent master mix (contains SDS and DTT as denaturing and reducing agents, respectively) and boiled at 95°C for 5 minutes. Proteins were separated using a proprietary separation and stacking matrix within a 100-µm diameter glass capillary. Following separation, proteins were irreversibly cross-linked to the capillary wall via UV light, and primary antibodies, secondary antibodies, and chemiluminescent detection

reagents were applied via vacuum. Signal specificity was confirmed by comparing signal location to that of a biotinylated protein ladder, detected by streptavidin and by comparing to 3 internal fluorescent standards located at 1, 29, and 230 kD.

D.4. Cell culture

The LA7 cell line was derived from a carcinogen-induced rat mammary tumor and has been demonstrated to display cancer stem cell properties (267;268). Cells were obtained from American Type Culture Collection (ATCC) (Manassas, VA). Cells were cultured at 37°C with 5% CO_2 in Dulbecco's Modified Eagle's Medium (DMEM) culture medium (ATCC, Manassas, VA) containing high glucose (4.5 mM), L-glutamine, phenol red, 20 mM HEPES buffer, 5 µg/ml insulin, and 50 nM hydrocortisone. Cells were seeded at $3e^3$ or $2e^4$ cells/well in 96- or 24-well plates, respectively.

To prepare rat serum for use in cell culture experiments, DR and DS rats were anesthetized with isoflurane and whole blood was collected via cardiac puncture, followed by cervical dislocation. Blood was allowed to coagulate for 15-30 minutes at room temperature followed by centrifugation at 1000 *x g* for 10 minutes. Serum was separated and 0.2 µm sterile-filtered. Cells were incubated with 5% v/v fetal bovine serum, DR serum, or DS serum.

For adipocyte co-culture, 1-2 g mammary fat pad from DR and DS rats was digested in a collagenase solution (2 mg/ml collagenase Type IV, 4% w/w BSA in culture medium) for 1 hour, followed by coarse shredding through a syringe, centrifugation at 150 *x g* for 5 minutes, then aspiration of solution below the floating adipocyte layer. Adipocytes were counted via hemacytometer and approximately 500 adipocytes were added to each well of a 24-well plate containing adherent LA7 cells. Following treatment, the medium was removed, and LA7 cells were fixed with 1% glutaraldehyde for 15 minutes,

rinsed with 1X PBS, then stained with 0.02% crystal violet (w/w) in distilled water for 30 minutes. Following staining, wells were thoroughly rinsed 3X with running distilled water to remove unbound crystal violet, then cells were destained in equal volumes of 70% ethanol for 2 hours with gentle agitation. Absorbance at 590 is linear with cell number using this method, and plates were read using a SpectraMax plate reader (Molecular Devices, Sunnyvale, CA).

D.5. Statistical analyses

- Plasma analyses
    - Between-group differences in plasma analytes were assessed by unpaired t test with Welch-Satterthwaite correction and $\log_{10}$-data transformation as needed to satisfy statistical assumptions.
- CE-based protein expression
    - For CE, signal quantitation was taken as peak area and normalized to total protein content in lysate:
        - Expression of GAPDH in adipose tissue has been reported to vary widely between subjects of varying adiposity as well as between different fat depots
        - β-actin shows relatively consistent expression across adipose tissue depots (269); however, it makes a poor loading control for mammary gland, as tissues with predominantly epithelial cells express higher levels of β-actin than do adipocyte-dominant tissues, such as mammary gland (270). Thus, mammary gland from a leaner animal will have a higher ratio of epithelial-derived protein: adipocyte-derived protein than an obese animal, which could skew results.
    - Protein expression in mammary gland was normalized to total protein in the lysate determined by Bradford assay.

    - Compiled protein expression levels in tumors and mammary gland were separately analyzed using multiple T-tests with false discovery rate (FDR) set at 1%.

- Cell culture studies
    - Experiments utilizing cells cultured with rat serum and co-cultured with serum +/- adipocytes were analyzed using ANOVA.
    - Cell growth over time was analyzed using linear regression. Absorbance at 405 nm as a proxy to cell number was regressed on DS rat body weight at study termination.

APPENDIX REFERENCE LIST

1. Poiley SM. A systematic method of breeder rotation for non-inbred laboratory animal colonies. Proc Anim Care Panel 1960;10(10):159-66.

2. Deffense E. Milk Fat Fractionation Today: A Review. J Amer Oil Seed Chem Soc 1993;70(12):1193-201.

3. Trends in Intake of Energy and Macronutrients in Adults From 1999-2000. Centers for Disease Control; 2010 Nov 1. Report No.: NCHS Data Brief No. 49.

4. Thompson HJ, McGinley JN, Rothhammer K, Singh M. Rapid induction of mammary intraductal proliferations, ductal carcinoma in situ and carcinomas by the injection of sexually immature female rats with 1-methyl-1-nitrosourea. Carcinogenesis 1995 Oct;16(10):2407-11.

5. Thompson HJ, Adlakha H. Dose-responsive induction of mammary gland carcinomas by the intraperitoneal injection of 1-methyl-1-nitrosourea. Cancer Res. 1991 Jul 1;51(13):3411-5.

6. de Boer THJ, Backer HJ. A new method for the preparation of diazomethane. Recueil des Travaux Chimiques des Pays-Bas 1954;73(3):229-34.

7. Druckrey H, Preussmann R, Ivankovic S, Schmahl D. [Organotropic carcinogenic effects of 65 various N-nitroso- compounds on BD rats]. Z.Krebsforsch. 1967;69(2):103-201.

8. Thompson HJ, McGinley JN, Wolfe P, Singh M, Steele VE, Kelloff GJ. Temporal sequence of mammary intraductal proliferations, ductal carcinomas in situ and adenocarcinomas induced by 1-methyl-1-nitrosourea in rats. Carcinogenesis 1998 Dec;19(12):2181-5.

9. Steel GG. Experimental techniques for cell kinetic studies. In Growth kinetics of tumours: cell population kinetics in relation to the growth and treatment of cancer. Oxford: Oxford University Press; 1977. p. 86-119.

10. Thompson HJ, Singh M, McGinley JN. Classification of premalignant and malignant lesions developing in the rat mammary gland after injection of sexually immature rats with 1-methyl-1-nitrosourea. J Mamm Gland Biol Neoplasia 2000;5(2):201-10.

11. Singh M, McGinley JN, Thompson HJ. A comparison of the histopathology of premalignant and malignant mammary gland lesions induced in sexually immature rats with those occurring in the human. Lab.Invest. 2000 Feb;80(2):221-31.

12. Russo J, Russo IH, Rogers AE, van Zwieten MJ, Gusterson B. Pathology of tumours in laboratory animals. Tumours of the rat. Tumours of the mammary gland. IARC.Sci.Publ. 1990;(99):47-78.

13. Knott KK, McGinley JN, Lubet RA, Steele VE, Thompson HJ. Effect of the aromatase inhibitor vorozole on estrogen and progesterone receptor content of rat mammary carcinomas induced by 1-methyl-1-nitrosourea. Breast Cancer Res.Treat. 2001 Dec;70(3):171-83.

14. Alberts B, Johnson A, Lewis J, Raff M, Roberts K, Walter P. An overview of the cell cycle. In Molecular Biology of the Cell. 4th ed. New York: Garland Science; 2002.

15. Urruticoechea A, Smith IE, Dowsett M. Proliferation marker Ki-67 in early breast cancer. J Clin Oncol 2005 Oct 1;23(28):7212-20.

16. de AE, Cardoso F, de CG, Jr., Colozza M, Mano MS, Durbecq V, Sotiriou C, Larsimont D, Piccart-Gebhart MJ, Paesmans M. Ki-67 as prognostic marker in early breast cancer: a meta-analysis of published studies involving 12,155 patients. Br.J Cancer 2007 May 21;96(10):1504-13.

17. Kanduc D, Mittelman A, Serpico R, Sinigaglia E, Sinha AA, Natale C, Santacroce R, Di Corcia MG, Lucchese A, Dini L, et al. Cell death: apoptosis versus necrosis (review). Int.J Oncol 2002 Jul;21(1):165-70.

18. Anderson GJ, Cipolla M, Kennedy RT. Western blotting using capillary electrophoresis. Anal.Chem 2011 Feb 15;83(4):1350-5.

19. Liu S, Sardi S, Sonom B, Zocco D, McSweeney R, Fraser AD, Halleck AE, Li H, Smejkal GB, Munevar S, et al. The Application of a Novel Nanovolume Capillary Electrophoresis Based Protein Analysis System in Personalized & Translational Medicine Research. J Bioanal Biomed 2013;2013(S3).

20. Example 38.14 Generalized Poisson mixed model for overdispersed count data. In: SAS Institute Inc., editor. SAS/STAT(R) 9.2 User's Guide. 2nd ed. 2015.

21. zumBrunnen J. Personal communication, 2014 Aug 27.

22. Matthews SB, Santra M, Mensack MM, Wolfe P, Byrne PF, Thompson HJ. Metabolite profiling of a diverse collection of wheat lines using ultraperformance liquid chromatography coupled with time-of-flight mass spectrometry. Plos One 2012;7(8):e44179.

23. Morrison DF. Multivariate Statistical Methods. 3rd ed. New York City: McGraw-Hill Publishing Co.; 1990.

24. Trygg J, Wold S. Orthogonal projections to latent structures (O-PLS). Journal of Chemometrics 2002 Mar;16(3):119-28.

25. Wiklund S, Johansson E, Sjostrom L, Mellerowicz EJ, Edlund U, Shockcor JP, Gottfries J, Moritz T, Trygg J. Visualization of GC/TOF-MS-based metabolomics data for identification of biochemically interesting compounds using OPLS class models. Anal.Chem. 2008 Jan 1;80(1):115-22.

26. Wiklund S. Multivariate Data Analysis and Modeling in "omics". In Umetrics, Umea, Sweden; 2008.

27. Gaikwad NW. Ultra performance liquid chromatography-tandem mass spectrometry method for profiling of steroid metabolome in human tissue. Anal.Chem 2013 May 21;85(10):4951-60.

28. Wallace TM, Levy JC, Matthews DR. Use and abuse of HOMA modeling. Diabetes Care 2004 Jun;27(6):1487-95.

29. Dulbecco R, Bologna M, Unger M. Differentiation of a rat mammary cell line in vitro. Proc Natl.Acad.Sci.U.S.A 1979 Mar;76(3):1256-60.

30. Zucchi I, Sanzone S, Astigiano S, Pelucchi P, Scotti M, Valsecchi V, Barbieri O, Bertoli G, Albertini A, Reinbold RA, et al. The properties of a mammary gland cancer stem cell. Proc Natl.Acad.Sci.U.S.A 2007 Jun 19;104(25):10476-81.

31. Perez-Perez R, Lopez JA, Garcia-Santos E, Camafeita E, Gomez-Serrano M, Ortega-Delgado FJ, Ricart W, Fernandez-Real JM, Peral B. Uncovering suitable reference proteins for expression studies in human adipose tissue with relevance to obesity. Plos One 2012;7(1):e30326.

32. Kouadjo KE, Nishida Y, Cadrin-Girard JF, Yoshioka M, St-Amand J. Housekeeping and tissue-specific genes in mouse tissues. BMC.Genomics. 2007;8:127.

LIST OF ABBREVIATIONS

ANIMAL MODELS:
DOA: days of age
DPC: days post-carcinogen injection
DR: diet-induced obesity resistant
DS: diet-induced obesity susceptible
OI: ovary-intact rats
OVX: ovariectomized rats
SUMO32: sucrose and moderate fat (32%) purified diet formulation

EXPERIMENTAL METHODS:
AFC: 7-amino-4-trifluoromethyl-coumarin, fluorophore
BSA: bovine serum albumin
CE: capillary electrophoresis; alternative to traditional Western blotting
DI: deionized water
DTT: dithiothreitol, reducing agent for disulfide bonds
ECL: enhanced chemiluminescence based on activity of horseradish peroxidase
ELISA: enzyme-linked immunosorbent assay
FBS: fetal bovine serum
FFPE: formalin-fixed paraffin embedded; method of tissue processing
DMEM: Dulbecco's modified Eagle's cell culture medium
GC-MS/MS: gas chromatography coupled to tandem mass spectrometry
H&E: hematoxylin and eosin method of staining tissue sections; by this method nuclei are stained blue, whereas proteins in cytoplasm and extracellular matrix are stained pink
IHC: immunohistochemistry
UPLC-MS/MS: ultraperformance liquid chromatography coupled to tandem mass spectrometry
MNU: N-methyl-N-nitrosourea, carcinogen and DNA alkylating agent
NDS: normal donkey serum
PBS-T: phosphate-buffered saline + 0.1% Tween-20 (detergent)
pNA: para-nitroaniline, chromogen
PVDF: polyvinylidene fluoride membrane
R110: rhodamine 110, fluorophore
SDS-PAGE: sodium dodecyl sulfate-polyacrylamide gel electrophoresis
TBS-T: Tris-buffered saline + 0.1% Tween-20

GENES:
BRCA1/2: breast cancer early onset gene
CDH1: E-cadherin 1
Cyp19a1: aromatase
Erbb2: encodes Her2 protein; can be used to drive tumor growth in animal models
PIK3CA: phosphatidylinositol 3-kinase, catalytic subunit alpha
PTEN: phosphatase and tensin homolog
SKT11: serine threonine kinase 11 gene
TP53: tumor protein 53 gene

MMTV: mouse mammary tumor virus; long-terminal repeat (LTR) of the promoter generally used to direct expression of transgenes to the mammary gland in transgenic mouse strains
ObR: leptin receptor

PROTEINS:
AMPK: adenosine monophosphate-activated protein kinase
AP-1: activator protein 1
Cdc6: cell division cycle 6
Cdk: cyclin dependent kinase
CRP: C-reactive protein
E2F1: E2F transcription factor 1
EGF: epidermal growth factor
EGFR: epidermal growth factor receptor, also called Her1
EIF4E: eukaryotic initiation factor 4E
ER: estrogen receptor
FABP-4: fatty acid binding protein 4/ activator protein (AP)-2
FASN: fatty acid synthase
GnRH: gonadotropin-releasing hormone
Her: human epidermal growth factor receptor, also called erbB
IL: interleukins, i.e., IL-6, IL-1β
IGF-1: insulin-like growth factor-1
IGF-1R: IGF-1 receptor
IGFBP-3: IGF binding protein-3
IR: insulin receptor
LOX: lipoxygenase
MAPK: mitogen activated protein kinase
mTOR: mammalian target of rapamycin
NF-kB: nuclear factor kB transcription factor
PC-1: prohormone convertase-1
POMC: pro-opiomelanocortin
ObR: leptin receptor
PPAR: peroxisome proliferator-activated receptor
PR: progesterone receptor
Rb: retinoblastoma protein
S6K: s6 kinase
SHBG: sex hormone binding globulin
TNFα: tumor necrosis factor α
TGFβ: transforming growth factor β

STATISTICS:
ASR: age-standardized rates; expressed as cases per 100,000 individuals
HOMA-IR: homeostasis model assessment-estimated insulin resistance; mathematical representation of fasted insulin and glucose levels
HR: hazard ratio; ratio of hazard functions of survival analysis of at-risk population to reference population
PLS: partial least squares regression
RR: relative risk; ratio of risk in at-risk population to reference population

MISCELLANEOUS:
AI: aromatase inhibitor; i.e. letrozole or vorozole
BMI: body mass index
E1: estrone
E2: estradiol
miR: microRNA
MMR: DNA mismatch repair processes
NIH: National Institutes of Health
P-1: Breast Cancer Prevention Trial
SERM: selective estrogen receptor mimetic; i.e. tamoxifen, raloxifene
STAR: Study of Tamoxifen and Raloxifene/ P-2 Trial
SWAN: Study of Women's Health Across the Nation
V_0: tumor volume at point of cancer cell initiation
V_{max}: maximal tumor volume